Physicochemical Problems of Mineral Processing 45 (2010)

www.minproc.pwr.wroc.pl/journal

WROCŁAW 2010

The papers published in the Physicochemical Problems of Mineral Processing journal are abstracted in
Chemical Abstracts, Thomson Reuters (Science Citation Index Expanded, Materials Science Citation Index, Journal Citation Reports), Coal Abstracts, Google Scholar and other sources

This publication was supported by
European Economic Area and Norwegian Financial Mechanisms and
Polish Ministry of Science and Higher Education through the grant EEA PL0084

ISSN 1643-1049
OFICYNA WYDAWNICZA POLITECHNIKI WROCŁAWSKIEJ
WYBRZEŻE WYSPIAŃSKIEGO 27, 50-370 WROCŁAW, POLAND

CONTENTS

Physicochem. Probl. Miner. Process. 45(2010) 5-14

journal homepage
www.minproc.pwr.wroc.pl/journal/

Physicochemical Problems of Mineral Processing

Index No. 32213X ISSN 1643-1049

Ewa ADAMEK *, Justyna ZIEMIAŃSKA **, Ilona LIPSKA *,
Andrzej MAKOWSKI *, Andrzej SOBCZAK *,**, Wojciech BARAN *

ASSESSMENT OF RADIANT FLUX ABSORPTION BY IRRADIATED PHASE ON THE KINETICS OF PHOTOCATALYTIC REACTIONS

Received March 16, 2010; reviewed; accepted May 12, 2010

In this study, the kinetics equation describing heterogeneous photocatalytic process in relation with the absorption of radiation by inactive photochemically reagents was presented. The proposed expression was verified based on the results of degradation process of selected azo-dyes. The experiments were carried out in one- and two component solutions in the presence of TiO_2 (anatase) during UV-a irradiation.

keywords: photocatalysis, kinetics, radiant flux, Langmuir-Hinshelwood, absorption

1. INTRODUCTION

In the last decade, there have been high hopes for the use of a photocatalytic process as an effective method for the degradation of toxic and biologically persistent substances. Usually, this process is carried out under heterogeneous conditions in the presence of TiO_2 [1-5]. Its photocatalytic properties have been known since the end of the 1930s [5]. This substance may be used in the form of particles suspended in an

* Medical University of Silesia, Department of General and Inorganic Chemistry, 4 Jagiellońska Str., 41-200 Sosnowiec, bw-xxl@wp.pl (W. Baran)
** Institute of Occupational Medicine and Environmental Health, 13 Kościelna Str., 41-200 Sosnowiec

aqueous solution/ medium or may be applied on the surfaces of different materials. Moreover, a modification of TiO_2 surface by doping with various metals having positive reduction potential (e.g., Ag, Au, Pt, Cu), lanthanides dopants, Fe(III) and nonmetal such as boron, carbon and nitrogen have been studied [3,6-8].

Among the factors having the significant effect on the efficiency of the photocatalytic process are [1,3-5,9,10]:

- crystal structure of TiO_2
- way of the preparation and application of the photocatalyst surface
- photocatalyst concentration
- useful spectrum of UV-VIS light absorbed by photocatalyst
- sorption properties of photocatalyst
- concentration of degraded compounds
- ability of degraded substances to the adsorption onto TiO_2 surface
- presence of other substances such as strong oxidants or reducing agents in the irradiated samples
- ability of degraded compounds to photolysis
- oxygen saturation of the irradiated samples.

Moreover, important parameters of the photocatalytic process are:

- intensity and wavelength of the used radiation
- thickness of the layer of the irradiated samples
- temperature and pH of medium.

The limiting step of photocatalytic processes carried out in the presence of TiO_2 may be the adsorption of substrates onto the photocatalyst surface and the absorption of radiation having energy sufficient for generation of electron-hole pairs (h^+,e^-) [3-5,9,10]:

$$TiO_2 + h\nu \rightarrow TiO_2(h^+,e^-) \quad (1)$$

These pairs can react with water and dissolved oxygen molecules:

$$h^+ + H_2O \rightarrow HO^\bullet + H^+ \quad (2)$$

$$e^- + O_2 \rightarrow O_2^{-\bullet} \quad (3)$$

Moreover, the photogenerated pairs can participate directly in the redox reactions with photochemically inactive substances:

$$h^+ + RH \rightarrow R^\bullet + H^+ \quad (4)$$

$$ne + Me^{m+} \rightarrow Me^{(m-n)+} \quad (5)$$

The kinetics of photochemical process is usually described by the Langmuir-Hinshelwood's theory [1-5]:

$$r_i = -\frac{dC_i}{dt} = k_i\Theta_i = k_i\frac{K_iC_i}{1+\sum_i K_iC_i} \quad (6)$$

where: r_i is the reaction rate (i-th substrate), C_i is the molar concentration of

substrate, t is the irradiation time, k_i is the reaction rate constant, Θ is the degree of coverage of photocatalyst surface, and K_i is the adsorption coefficient for the adsorption of substrate on TiO_2.

In very diluted solutions, Eq.6 can be simplified to the following form:

$$r_i = -\frac{dC_i}{dt} = k_i K_i C_i \tag{7}$$

Experimental data show that in the wide range of the radiation intensity, the reaction rate is directly proportional to its value [1,3,4,11]. Therefore the following equation is correct:

$$r_i = -\frac{dC_i}{dt} = \Phi_i I_A \tag{8}$$

where: φ is the quantum yield and I_A is the intensity of radiation absorbed by photocatalyst.

If we assume that the quantum yield of photochemical reaction is the product of k_i and Θ, the relationship can be expressed as follows:

$$r_i = -\frac{dC_i}{dt} = k_i \Theta_i I_A \tag{9}$$

Therefore, the I_A value may depend on the absorption of radiation by solution containing suspended TiO_2 particles.

We supposed that the important factor that limited the photocatalytic process rate can be the absorption of part of the radiation by solution containing degraded substrates. This effect causes the decrease in the radiation intensity reaching the photocatalyst surface. In previous studies we have found the correlation between the absorbance of dyes solutions and their photocatalytic degradation rate [12]. According to the Lambert-Beer law the intensity of radiation absorbed by photocatalyst should by exponentially proportional to the sum of the product of the molar extinction coefficients for the used radiation *(ε),* concentrations of all components in solution (C) and the thickness of the layer of irradiated samples absorbing radiation *(l):*

$$I_A = I_o^{-l\sum_i \varepsilon_i C_i} \tag{10}$$

where: I_o is the radiation intensity that reaches directly the surface of exposed sample.

Based on Eqs.6, 9 and 10, we propose the following equation to describe the kinetics of photocatalytic process:

$$r_i = -\frac{dC_i}{dt} = k_i \frac{K_i C_i}{1 + \sum_i K_i C_i} I_o e^{-l\sum_i \varepsilon_i C_i} \tag{11}$$

The mathematical model concerning the use of electromagnetic radiation energy in photocatalytic processes was presented by Brandi et al. [13,14]. It can be useful for the determination of the effective radiation flux reaching the reactor mixture in the closed flow reactor with an external source of radiation; however, the authors did not analyze the effect of distribution of radiant flux between the various components within the reaction mixture. Thus, they omitted the fact of absorption of radiation by photochemically inactive components of this mixture.

The aim of the work was to verify experimentally the kinetics equation, taking into account that the radiation absorption by irradiated solution effects on the photocatalytic reaction rate.

2. EXPERIMENTAL

2.1. Reagents

The experiments were carried out with the use of two azo-dyes as model compounds. Acid Orange 7 obtained from Fluka and Acid Black 1 purchased from POCH were of analytical grade. None of the investigated dyes underwent photolysis under the experimental conditions. The titanium dioxide powder (TiO_2, anatase, pH of isoelectric point was 3, the surface area was 9-11 m^2g^{-1}, residues on filter >40μm after dispersion in water was <0,02%) used as the photocatalyst was purchased from Riedel-de Haën. In all experiments amount of photocatalyst was 2.5 g l^{-1}. Doubly distilled water was used throughout experiments.

2.2. Irradiation

Before irradiation of aqueous dyes solutions with TiO_2, the samples were magnetically stirred in the dark for 30 min in order to reach the adsorption/desorption equilibrium among the dyes, photocatalyst and the dissolved oxygen. The stirring was continued throughout the whole process. Since the pH values in the irradiated samples were in the range of 5.8 - 6.8, the influence of changes of pH on the obtained results was eliminated (the adsorption of azo-dyes onto TiO_2 surface was very low at this pH value). In all cases during the experiments, the samples at volume 100 ml containing TiO_2 and dyes were irradiated in glass crystallizer (500 ml) by means of four UV lamps (Philips TL-40 W/05) emitting radiation with a maximum energy at λ 366 nm. The surface intensity of the radiation determined by Parker's actinometer [15] was $8.76 \cdot 10^{-5}$

Einstein $s^{-1}m^{-2}$. The exposed samples surface was 102 cm^2. The reaction temperature was kept at 21 ± 2ºC. During irradiation the solutions had a free contact with atmospheric air but, additionally, were not aerated.

2.3. Analysis

The samples of the investigated suspensions (2 ml) were taken at the appropriate irradiation time, when the degree of degradation of each dye was <80%. In order to separate the photocatalyst from the suspension, samples were centrifuged for 30 min at 4000 rpm.

In samples before and after irradiation the concentration of azo-dyes were determined according to *abs* measurement at 480 and 618 nm for Acid Orange 7 and Acid Black 1, respectively, using UV-VIS spectrophotometer Secomam S 750. During the preliminary studies it was found that the dyes solutions follow the Lambert –Beer's law in the used concentration range. In these ranges, the determination coefficients (R^2) of the calibration curves obtained for Acid Orange 7 and Acid Black 1 were 0.9952 and 0.9989, respectively. Moreover, results obtained in mixtures of dyes were also validated using HPLC methods (HPLC Merck Hitachi, detector UV L 7400, λ 254 nm; column SEPARON SGX 7 μm, C-18, 250×4 mm; mobile phase – MeOH:H_2O in the ratio 3:7). Additionally, in all investigated mixtures before the irradiation the *abs* was measured at λ 366nm.

2.4. Calculations

According to Eq. 7, the photocatalytic process carried out in very diluted solutions is a pseudo-first order reaction. This fact is supported by experimental literature data [1-4]. Therefore, the values of observed reaction rate constant *(k)* were determined as a slope of linear relationship (Eq.12).

$$\ln \frac{C}{C_o} = -k\ t \tag{12}$$

In all cases, the initial reaction rate *(r_o)* was calculated as follows:

$$r_o = k\ C_o \tag{13}$$

3. RESULTS AND DISCUSSION

3.1. One-component samples

In the case of low adsorption efficiency and low concentration of substrates the

following approximation is used:

$$1 + \sum_i K_i C_i \cong 1 \tag{14}$$

Taking into account Eq. 14, the kinetics equation for photocatalytic process carried out in solution containing only one substrate (dye) and TiO_2 suspension can be simplified to the form:

$$r_i = k_i K_i C_i I_o e^{-l\varepsilon_i C_i} \tag{15}$$

According to Eqs.13 and 15 the k value can be expressed as follows:

$$k = k_i K_i I_o e^{-l\varepsilon_i C_i} \tag{16}$$

Since under the investigated conditions the k_i, K_i I_o, l and ε_i values are constant, the following relationship is obtained:

$$C_o \sim ln\, k \tag{17}$$

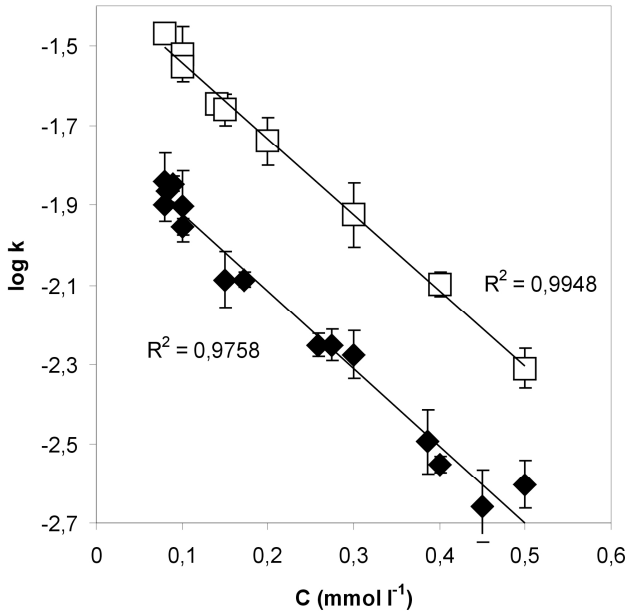

Fig. 1. The effect of initial dyes concentrations on the logarithm value of the photodegradation rate constant of Acid Orange 7 (□) and Acid Black 1 (◆)

Fig.1 presents the effect of initial dyes concentrations on the logarithm value of the photodegradation rate constant of Acid Orange7 or Acid Black1 in solutions with only one dye.

A course of the function was comparable in dyes solutions at the concentration in the range of 0.08-0.5 mmol l^{-1}. In these ranges, the coefficient of determination (R^2) of the straight line function obtained for Acid Orange 7 and Acid Black 1 were 0.9948 and 0.9758, respectively. A very good fit to a linear regression (Fig.1) indicates that it can be treated as a confirmation of the hypothesis presented in Eq. 16. However, when concentrations of dyes in solutions were < 0.08 mmol l^{-1}, a linear dependence was not observed. In the experiments performed in the presence of TiO_2 (the *l* value is also very low) at very low concentration of dye, the approximation of expression $e^{-l\varepsilon C} \cong 1$ is correct. In this case, in one-component solutions (C_o< 0.08 mmol l^{-1}) the effect of absorption of radiation by dye molecules can be treated as a negligible.

3.2. Two - component samples

In mixtures containing constant concentration of one of the compounds (dye A), the degree absorption of radiation can be changed by other compounds, for example by other dye (B). For example, in the case of Acid Orange 7 (AO7, dye A) if the expression (14) is fulfilled, the kinetics equation can be described as follows:

$$r_{oAO7} = k_{AO7} K_{AO7} C_{AO7} I_o e^{-l(\varepsilon_{AO7} C_{AO7} + \varepsilon_{AB1} C_{AB1})} \tag{18}$$

In this case, the $ln\ r_i$ value for dye A should be inversely proportional to the relationship:

$$\varepsilon_A C_A + \varepsilon_B C_B = \Sigma \varepsilon_i C_i \tag{19}$$

Table 1. The composition of the irradiated dyes mixtures and the fitting of linear function

$$\log r_o = f(\sum_i \varepsilon_i C_i)$$

Mixture		Initial dye concentration (mmol l^{-1})		Function	R^2
		Acid Black1	Acid Orange7		
I	Fig. 2	0-0.0487	0.0143	$log\ r_o = -4.6406x^a - 2.5711$	0.9955
II		0-0.024	0.0057	$log\ r_o = -10.819x^a - 2.6973$	0.9969
III		0.0162	0-0.0571	$log\ r_o = -3.3474x^a - 2.7355$	0.9811
IV	Fig. 3	0.00812	0-0.0857	$log\ r_o = -3.717x^a - 3.0408$	0.9870
V		0.00325	0-0.0429	$log\ r_o = -8.5405x^a - 3.2529$	0.9884

[a)] $x = \sum_i \varepsilon_i C_i$; ε at 366 nm $\varepsilon_{\text{Acid Black1}}$ = 4031 l mol^{-1} cm^{-1}; $\varepsilon_{\text{Acid Orange7}}$ = 3093 l mol^{-1} cm^{-1}

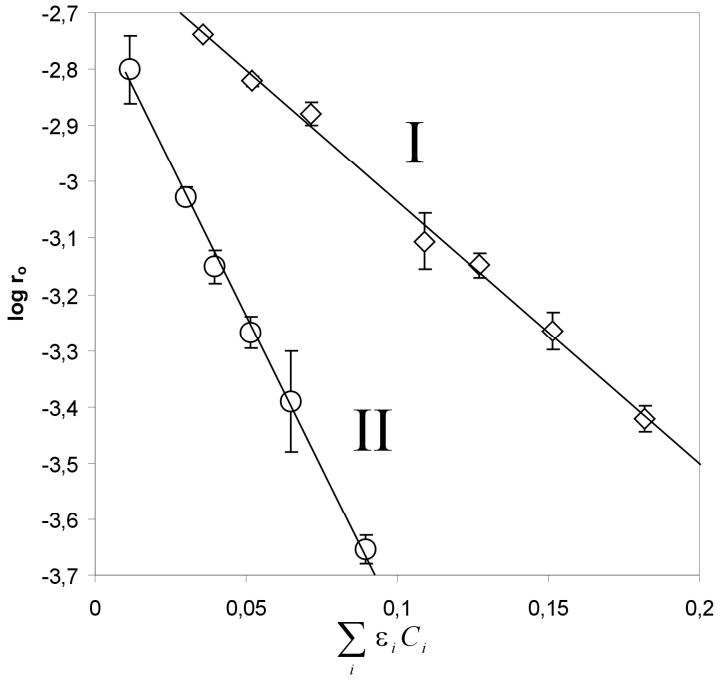

Fig. 2. The effect of $\sum_i \varepsilon_i C_i$ value in samples containing mixture of Acid Orange 7 and Acid Black 1 on the logarithm value of the initial photodegradation rate of Acid Orange 7, (◇) C_{AO7}=0.0143, C_{AB1}=0-0.0487 mmol l^{-1}; (○) C_{AO7}=0.0057, C_{AB1}=0-0.0244 mmol l^{-1}

The ε_A and ε_B values (for Acid Orange 7 and Acid Black 1, respectively) were determined experimentally at λ 366 nm. Table 1 presents the range of concentrations of both dyes and the fitting of the experimental data to the linear function. The values of ε are showed below Table 1. Figures 2 and 3 show the relationships between $ln\ r_i$ and $\varepsilon\Sigma_i C_i$.

A good fit to a linear regression in the range studied (Figs. 2 and 3) indicates that it can be treated as a confirmation of the hypothesis presented in Eq. 11.

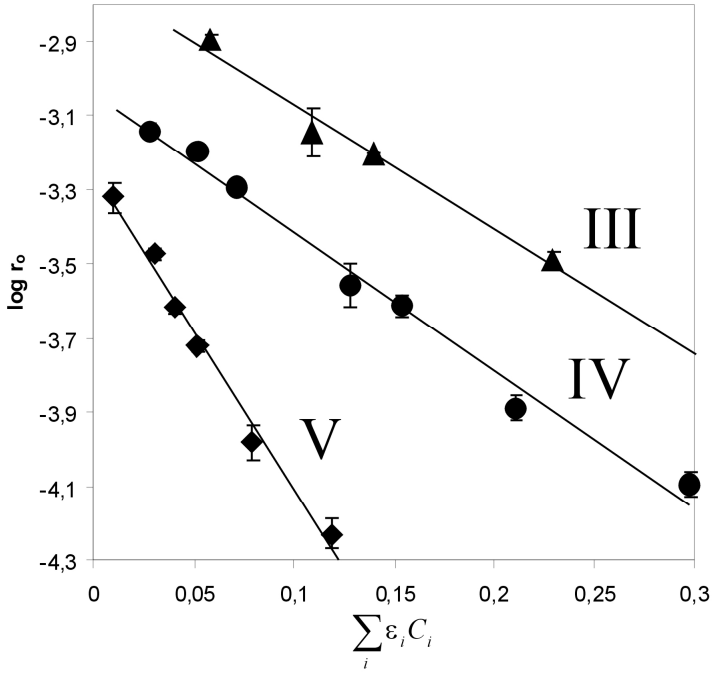

Fig. 3. The effect of $\sum_i \varepsilon_i C_i$ value in samples containing mixture of Acid Orange 7 and Acid Black 1 on the logarithm value of the initial photodegradation rate of Acid Black 1, (▲) C_{AB1} = 0.0162, C_{AO7} = 0-0.0571 mmol l^{-1}; (●) C_{AB1} = 0.00812, C_{AO7} = 0-0.0857 mmol l^{-1}; (◆) C_{AB1} = 0.00325, C_{AO7} = 0-0.0429 mmol l^{-1}

4. CONCLUSION

The obtained results point out to the correctness of own hypothesis that the photocatalytic reaction rate depends on the radiant flux absorbed by the irradiated solution (i.e., depends on the thickness of solution layer over the photocatalyst surface) and on the sum of the products of concentrations and molar extinction coefficients. In the case of reaction carried out in clear water in the presence of TiO_2, this influence will be negligible. However, during the design engineering degradation processes of real wastewater having high level of radiation absorption and containing high concentration of substrates this effect can be significant. More particularly, in the cases of the use of photocatalyst applied onto the surface of other materials.

REFERENCES

[1] HERRMANN J.M., 1999, *Heterogeneous photocatalysis: fundamentals and applications*, Catal. Today, 53, 115-129.

[2] BLAKE D.M., 2001, *Bibliography of work on the heterogeneous photocatalytic removal of hazardous compounds from water and air*, Technical Report of National Renewable Energy Laboratory, U.S. Department of Energy Laboratory, USA, Update Number 4.

[3] CARP O., HUISMANC.L., RELLER A., 2004, *Photoinduced reactivity of titanium dioxide*, Prog. Solid. State. Chem., 32, 33–177.

[4] HERRMANN J.M. 2005, *Heterogeneous photocatalysis: state of the art and present applications*, Top. Catal., 34, 49-65.

[5] FUJISHIMA A., ZANG X., TRYK D.A., 2008, *TiO_2 photocatalysis and related surface phenomena*, Surf. Sci. Rep., 63, 515-582.

[6] BARAN W., MAKOWSKI A., WARDAS W., 2003, *The influence of inorganic ions on the photocatalytic degradation of Orange II in aqueous solutions*, Eng. Protect. Environ., 6, 75-85.

[7] GÓRSKA P., ZALESKA A., HUPKA J., 2009, *Photodegradation of phenol by UV/TiO_2 and Vis/N,C-TiO_2 processes: Comparative mechanistic and kinetic studies*, Sep. Purif. Technol., 68, 90-96.

[8] TRYBA B., PISZCZ M., GRZMIL B., PATTEK-JANCZYK A., MORAWSKI A.W., 2009, *Photodecomposition of dyes on Fe-C-TiO_2 photocatalysts under UV radiation supported by photo-Fenton process*, J. Hazard. Mater., 162, 111-119.

[9] BIZANI E., FYTIANOS K., POULIOS I., TSIRIDIS V., 2006, *Photocatalytic decolorization and degradation of dye solutions and wastewaters in the presence of titanium dioxide*, J. Hazard. Mater. 136, 85-94.

[10] WU R-J., CHEN CH-CH., LU CH-S., HSU P-Y., CHEN M-H., 2010*, Phorate degradation by TiO_2 photocatalysis: Parameter and reaction pathway investigations*, Desalination 250, 869–875.

[11] FEITZ A.J., BOYDEN B.H., WAITE T.D., 2000*, Evaluation of two solar pilot scale fixed-bed photocatalytic reactors*, Water Res. 34, 3927-3932.

[12] BARAN W., MAKOWSKI A., WARDAS W., 2008, *The effect of UV radiation absorption of cationic and anionic dye solutions on their photocatalytic degradation in the presence TiO_2*, Dyes Pigments 76 (2008) 226-230.

[13] BRANDI R.J., ALFANO O.M,. CASSANO A.E., 2000, *Evaluation of Radiation Absorption in Slurry Photocatalytic Reactors. 1*. Assessment of Methods in Use and New Proposal, Environ. Sci. Technol., 34, 2623-2630.

[14] BRANDI R.J., ALFANO O.M,. CASSANO A.E., 2000, *Evaluation of Radiation Absorption in Slurry Photocatalytic Reactors. 2*. Experimental Verification of the Poposed Method, Environ. Sci. Technol.,34, 2631-2639.

[15] HATCHARD C., PARKER C, 1956, *A new sensitive chemical actinometer. II. Potassium ferrioxalate as a standard chemical actinometer*, Proc. Roy. Soc. A 235, 518-36.

Physicochem. Probl. Miner. Process. 45(2010) 15-28

journal homepage
www.minproc.pwr.wroc.pl/journal/

Physicochemical Problems of Mineral Processing

Index No. 32213X ISSN 1643-1049

Justyna DZIEDZIC *, Dawid WODKA *, Paweł NOWAK*, Piotr WARSZYŃSKI *, Christian SIMON **, Izumi KUMAKIRI **

PHOTOCATALYTIC DEGRADATION OF THE HUMIC SPECIES AS A METHOD OF THEIR REMOVAL FROM WATER – COMPARISON OF UV AND ARTIFICIAL SUNLIGHT IRRADIATION

Received May 10, 2010; reviewed; accepted May 25, 2010

The possibility of application of the process of photocatalytic decomposition of humic substances (humic acid – HA) to their removal from water was investigated. Commercial TiO_2 (Evonic-Degussa P-25) and the periodic reactor were used in the experiments. The decomposition under artificial sunlight (ASL) and UV irradiation was tested. It was stated that ASL irradiation is not sufficient to cause significant decomposition of HA whereas TiO_2 appeared to be very effective under the UV irradiation. Strong adsorption of HA on the surface of TiO_2 was observed.

keywords: humic substances, photocatalysis, photodegradation, TiO_2, water purification

1. INTRODUCTION

Severe requirements regarding the quality of drinking water result in the necessity to elaborate the innovative methods of water treatment. So far applicable disinfection methods secured only neutralization of microorganisms but remaining problem are

* Institute of Catalysis and Surface Chemistry, Polish Academy of Sciences, Niezapominajek 8, 30-239 Kraków, Poland, ncdziedz@cyf-kr.edu.pl (J. Dziedzic)
** SINTEF , Materials and Chemistry, P.O. Box 124 Blindern, 0314, Oslo, Norway

hardly – degradable organic compounds present in water which cannot be remove by simple filtration or coagulation processes.

Humic substances represent a major fraction of natural organic matter (NOM) in ground and surface waters that are known to be a complex class of biogenic polyanionic weak electrolytes with varying molecular sizes [1]. These substances have not as yet been properly chemically defined. Only average molecular weight can be determined [2] in the case of humic substances. They are formed during the degradation of plants and animal material, and both microbiological and abiotic processes contribute to their production [3]. Humic substances (HS) can be further separated into three classes, according to solubility, as humic acids, fulvic acids and humins [2]. Macromolecules of humic acid contain conjugated olefinic, aromatic, phenolic–semiquinone–quinone structures of a wide spectrum with different functional groups (–CO, –COOH, –OH, –NH–, $–NH_2$, –N) and chromophores [1]. They are capable of absorbing UV radiation. In many publications authors stated that the short – wave UV range of solar radiation (UV – B, $\lambda < 320$ nm) is the most important mineralizer of humic species [4]. What else, humic substances react with chlorine species (OCl^-/HOCl) and produce trihalomethanes (THMs), haloacetic acids (HAAs) and other halogenated disinfection byproducts (DBPs) in chlorinated water [5]. Trihalomethanes have been known to cause cancer and other toxic effects in human beings [6]. In addition, humic substances can form strong complexes with both inorganic and organic contaminants and mineral surfaces and they have been known as photoreactive contaminants. [7] From these reasons HAs are considered as highly reactive species in the environment and their removal from water during the water treatment is necessary.

Recently TiO_2 based photocatalysis of humic acids (HAs) has been extensively investigated [9–17]. It has been known that solar radiation alone has not enough energy for sufficient degradation of humic substances, but in combination with heterogeneous photocatalyst - titanium dioxide (TiO_2), with or without other chemicals, the degradation rate could increase [8].

The main photochemical phenomenon in the UV/TiO_2 process is the formation of an electron/hole pair through the absorption of light with the energy equal or greater than the band gap of TiO_2 (E_{bg} = 3.2 eV). Energized electrons and holes can either recombine, dissipating energy or be available for redox reactions with electron donor or electron acceptor species adsorbed on the semiconductor surface [18]. In aqueous environment at the presence of oxygen highly reactive oxygen species ($OH^{\bullet}$, $O_2^{\bullet -}$) are formed in the photocatalytic process. The oxidation/reduction processes involving those species may lead to complete degradation of organic compounds to CO_2 and to the formation of low-molecular-weight carboxylic acids (oxalic, succinic, formic, acetic, etc.) [3].

The aim of this study was to test the applicability of the photocatalytic process with the use of titanium dioxide to the removal of humic acids from water and to establish

the optimum conditions for the application of this process. In this work the photocatalytic removal of humic acid (HA) under UV and artificial sunlight (ASL) irradiation was examined by monitoring changes in the UV absorbance at the wavelength of 254 nm (A_{254}). The absorbance value measured at 254 nm is widely accepted as a parameter which shows the degradation rate of humic acids and a parameter replacing total organic carbon (TOC) – usually used to measure photodegradation rate of HAs [18]. TiO_2 Degussa P – 25 is commercially available form of TiO_2 and has been used in many studies because of its chemical stability, availability and photocatalytic activity for oxidative destruction of organics [9,16,17].

2. EXPERIMENTAL

2.1. Materials

Deionized water for the preparation of the solutions was obtained from the Millipore Direct Q UV apparatus. TiO_2 powder Degussa P – 25 Aeroxide (SPECIFIC surface area - 50 $m^2 g^{-1}$) was kindly supplied by Evonic-Degussa and used as a photocatalyst for the degradation of humic acid without any modification. Humic acid sodium salt (technical grade) was supplied by Sigma – Aldrich. HA working solution of 40 mg dm^{-3} for photocatalytic degradation experiments was always freshly prepared by dilution of the stock solution (500 mg l^{-1}) with water. Stock solution was prepared in a following way. 500 mg of the HA sodium salt was dispersed in deionized water and sonificated 60 minutes in order to accelerate the dissolution of the HA. Then, the suspension was filtered through the 0.45 μm filter (Sartorius Membrane Filters) with the use of Sartorius filtration apparatus. Next, filtered solution was centrifugated at the rate of 15000 rpm for 60 minutes. Such prepared solution was stable for weeks.

2.2. Photodegradation experiments

The photooxidation experiments were performed in two quartz flat bottomed batch reactors of the volume 40 ml. In one of the reactors halogen lamp (150 W, Philips) was used as the artificial sunlight (ASL) source, in the other one, dedicated for ultraviolet (UV) region, the high pressure xenon arc lamp (250 W, Optel) was applied. Both lamps were used without any cut-off filters, except the layer of cooling water flowing below the bottom of the cell. The cell illumination was monitored by the radiometer Radiometer RD 0.2/2/100 (Optel). In those measurements sensor was placed at the top of the empty reactor. The distance between the source and the sensor was about 25 cm for ASL and 15 cm for UV light and the illumination area was 16.3 cm^2. The irradiation intensity was 68.8 mW cm^{-2} for ASL and 48.8 mW cm^{-2} for UV source. The

photocatalyst suspension was stirred during the experiments in both reactors with a mechanical stirrer at a constant rate of 300 rpm. Mechanical stirrer, with the stirring rod positioned a few millimeters above the bottom of the cell was used instead of a magnetic stirrer to avoid "milling" of the TiO_2 grains during the experiment. The temperature was stabilized at 25±0.5°C (Fig. 1). Together with the sample used in a photocatalytic experiment an identical reference sample was always prepared and kept in the dark during the same period of time. After the experiment three portions of both suspension and reference samples were taken, subjected to 25 min of centrifugation at 15000 rpm to separate TiO_2 and then analyzed for the contaminant concentration. In that way the influence of adsorption on the TiO_2 surface on the uptake of the contaminant from the solution was eliminated.

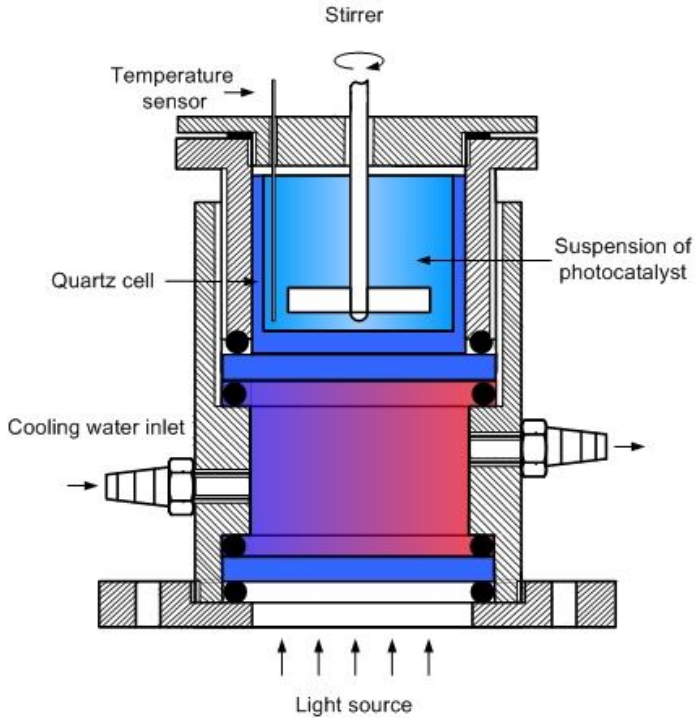

Fig. 1. The scheme of the quartz flat bottomed photoreactor

Samples were irradiated with halogen or xenon lamp for the time period from 10 min to 9 hours depending on the aim of the experiment. After irradiation the investigated solution was transferred to the Eppendorf vessel of the 2 ml volume and centrifugated at the rate of 15000 rpm for 25 minutes before spectrophotometric analysis. The absorption of the supernatant at the wavelength of 254 nm was measured using Specord

40 (Analytic Jena) single beam spectrophotometer.

The photooxidation experiment in this study included a few sets of tests for different objectives. The first set of experiments was carried in order to determine the degree of HA degradation under UV and ASL irradiation in the absence of photocatalyst. Initial HA concentration in that series of experiments was always 40 mg dm^{-3}, the duration of the experiment was extended to 9 h. The next step was the investigation of adsorption and desorption processes of humic acid on TiO_2 surface. Again the same initial HA concentration of 40 mg dm^{-3} was used. The third set of tests was performed with different experimental conditions including UV/ASL irradiation and TiO_2 catalyst in order to determine the best experimental conditions. The fourth set of tests was carried out with different TiO_2 loadings (100, 200, 500, 1000, 2000 mg dm^{-3}) to determine the effects of TiO_2 loading during the photodegradation reaction of HA. Finally the set of tests was carried out to determine the photodegradation rate of humic acid as a function of initial concentrations of HA (20, 40, 60 and 80 mg dm^{-3}).

3. RESULTS AND DISCUSSION

3.1. Decomposition of HA during UV/ASL irradiation in the absence of a photocatalyst

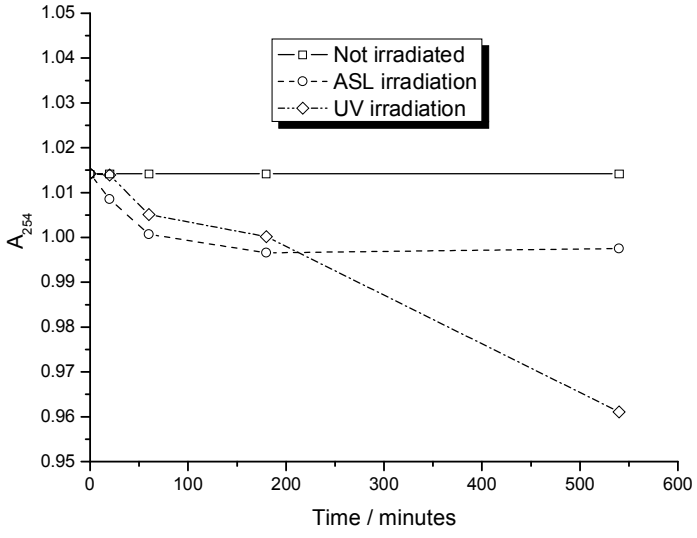

Fig. 2. Change of absorbance of the solution of humic acid (concentration 40 mg dm^{-3}) at the wavelength 254 nm under UV and ASL irradiation.

In the preliminary investigations humic acid degradation in the absence of photocatalyst was followed. Parallel blank experiment (without the irradiation of the samples) was performed too. The changes in the absorbance at 254 nm during the 9 h of reaction are showed in Fig. 2.

The changes in A_{254} even during the prolonged reaction periods were found to be negligible. Absorbance decreased only by 5.3 % after 9 h of irradiation by UV lamp, the decrease in absorbance caused by ASL was of the order of 2% only. It means that the irradiation by either ASL or ultraviolet light is not enough to attain significant degradation of humic acid without a photocatalyst. So the simultaneous action of irradiation and the photocatalyst – TiO_2 - was investigated in further work.

3.2. Adsorption of humic acid on TiO_2 surface

In order to investigate the effectiveness of the HAs removal in a photocatalytic process the influence of the adsorption of HAs on titania surface on the abstraction of HA from the solution should be determined. Tested catalyst – titanium dioxide Degussa P – 25 has high specific surface area (50 $m^2 g^{-1}$) and can adsorb quite a lot of HA. So, the experiment was performed to test adsorption of HA on TiO_2 in order to conclude which portion of HA, that disappeared from the solution, was degraded in a photocatalytic reaction and which part was simply adsorbed on the surface.

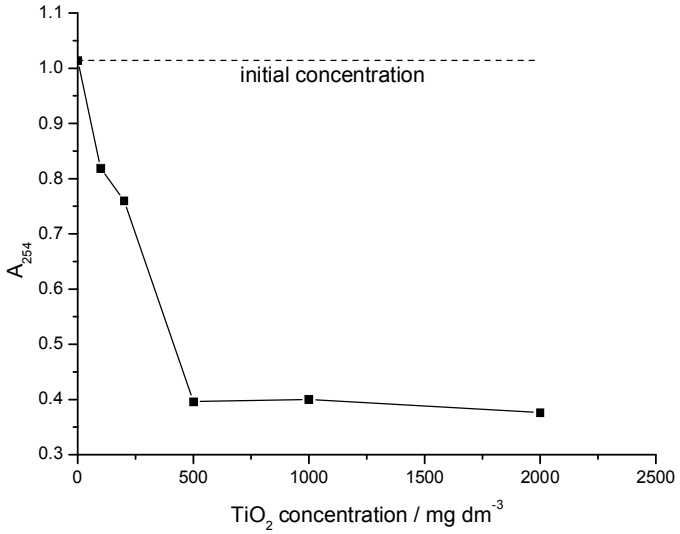

Fig. 3. Changes of absorbance of the HA solution (concentration 40 mg dm^{-3}) at the wavelength 254 nm in the dark due to the adsorption of humic acid on TiO_2 surface.

The suspensions of P – 25 TiO_2 (100, 200, 500, 1000, 2000 mg dm^{-3}) in solution of HA sodium salt (40 mg dm^{-3}) were prepared and kept in the dark for 1 hour, then the absorbance value of the samples was measured. The results are presented in Fig. 3.

The results presented in Fig. 3 indicate that TiO_2 adsorbs strongly HA – more than 60% of HA was adsorbed on TiO_2 surface for the suspension concentration higher than 500 mg dm^{-3}. For that reason rather low concentration of TiO_2 was used in the experiments (usually 100 mg dm^{-3}) and the results of the experiments were always compared with the results obtained for samples of the same composition, kept in dark during the same time. Another conclusion which may be drawn from the experiment presented in Fig. 3 is that HA is composed of at least two components, one adsorbing easily at the TiO_2 surface, the other one that does not adsorb at all or adsorbs to a very limited extent.

Photodegradation reaction of such complicated compounds, as undoubtedly humic substances are, is not possible to occur in one stage. Intermediate species formed during degradation may desorb from the surface with some delay. So, the experiment to verify the occurrence of desorption of HA decomposition byproducts was performed. A HA solution of the concentration 40 mg dm^{-3} with the addition of TiO_2 (100 mg dm^{-3}) was UV and ASL irradiated through the 60 min, then for the next 3 hours stirred at the absence of light. Absorbance of the solution was measured just after the irradiation period and after 1, 2 and 3 hours of stirring. Results of experiments are showed in Figs 4 and 5.

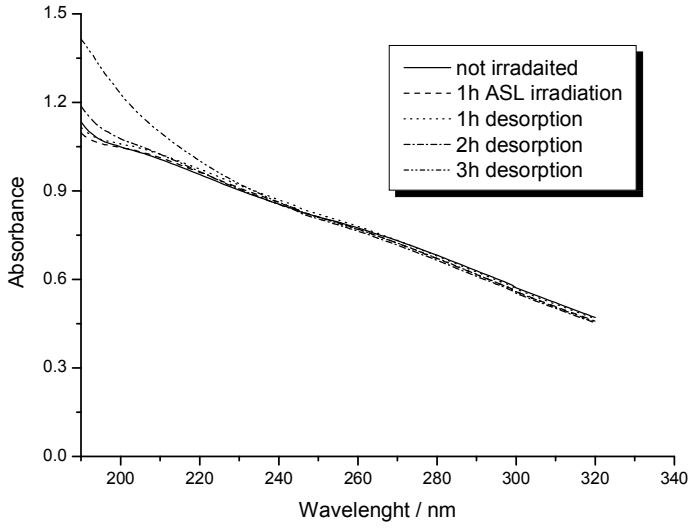

Fig. 4. UV spectra of humic acid solution (initial concentration 40 mg dm^{-3}) after 1 h of ASL irradiation and subsequent 3 hours in the dark.

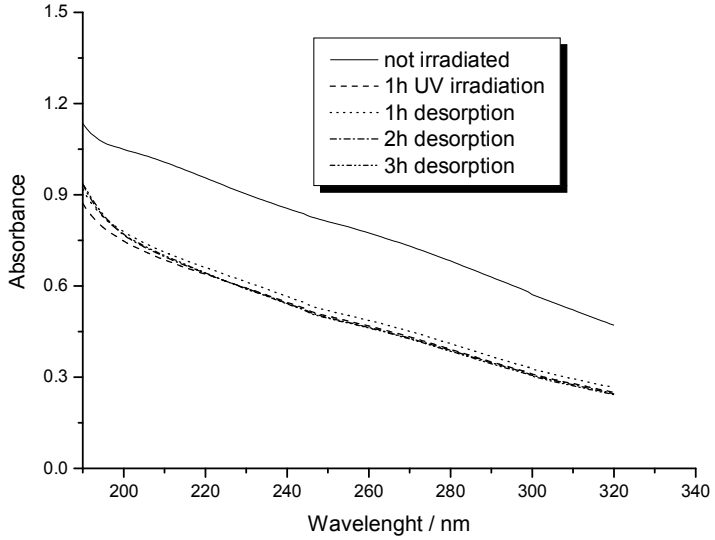

Fig. 5. UV spectra of humic acid solution (initial concentration 40 mg dm^{-3}) after 1 h of UV irradiation and subsequent 3 hours in the dark.

Fig. 4 and 5 showed that desorption of probable intermediate products of HA degradation from TiO_2 occurred to a very low degree. After ASL irradiation the spectra differed from each other to some extent in the wavelength range of 190 – 220 nm, however in the case of UV irradiation no desorption might have been observed. Note that in both cases (UV and ASL) no changes in the absorption at the wavelength 254 nm were observed.

3.3. Degradation of HA at the TiO_2 surface

The suspension consisting of 40 mg dm^{-3} of HA sodium salt and 100 mg dm^{-3} of TiO_2 was UV and ASL irradiated. The parallel blank test was conducted too. The samples were irradiated 10 min, 20 min, 40 min, 60 min, 120 min and 180 min. Fig 6 shows the results of photocatalytic experiment.

After 20 min of UV irradiation 15 % decrease of A_{254} was observed whereas 1 – hour UV irradiation of HA in TiO_2 suspension caused nearly 50 % drop of HA concentration. So 60 min irradiation time was selected as optimal to investigate the degradation rate of humic acid during the photocatalytic process. The results of ASL irradiation of the samples showed much lower decrease of absorbance - only about 18 % after 3 hour exposure to ASL. Note that almost linear dependence of absorbance

on time was observed in the initial period of reaction. It may suggest that the rate of decomposition reaction was controlled by the rate of the generation of reactive radicals, not by the rate of humic acid reaction with these radicals.

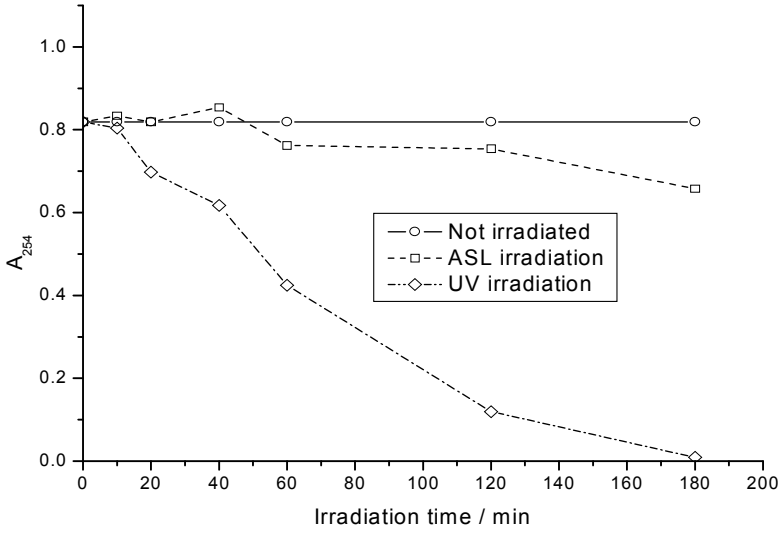

Fig. 6. Changes of absorbance at 254 nm of humic acid solution under UV and ASL irradiation at the presence of TiO_2. Concentration of photocatalyst: 100 mg dm^{-3}, concentration of HA: 40 mg dm^{-3}.

3.4. The effect of TiO_2 loading on the photodegradation of HA.

To begin with the study of optimal TiO_2 dosage it is necessary to remember that the decrease of HA concentration in solution might be caused not only by photodegradation reaction but also by the adsorption of HA on TiO_2 surface. Further, the presence of TiO_2 particles in suspension causes the dispersion of radiation. At the high TiO_2 concentration the penetration depth of radiation into the layer of suspension may be limited, leaving part of the solution not irradiated. The last effect undoubtedly depends on the cell geometry. Te decrease of the radiation intensity due to (mainly) dispersion of light on TiO_2 particles is presented in table 1. So, the growth of TiO_2 concentration in suspension caused not only the enhancement of degradation rate due to the increase of the available catalyst surface area but also the increase of the HA amount adsorbed at the TiO_2 surface as well as the decrease in degradation rate due to the increase in light dispersion.

The effect of TiO_2 dosage on the degradation of HA was investigated for the same initial HA concentration (40 mg dm^{-3}) and different TiO_2 concentrations (100, 200, 500, 1000 and 2000 mg dm^{-3}). The time of the experiment was 1 h. The results were

compared with the absorbance values of the samples kept in the dark for 1 h and are depicted in Fig. 7.

Table 1. Impact of TiO_2 presence in the cell on radiation intensity.

Conditions of the experiment	Radiation	
	ASL	UV
Empty cell, measurement above the top of the cell	68.8 mW cm^{-2}	48.8 mW cm^{-2}
1000 mg dm^{-3} TiO_2, 40 ml of solution, measurement above the surface of reaction suspension	10 mW cm^{-2}	4 mW cm^{-2}

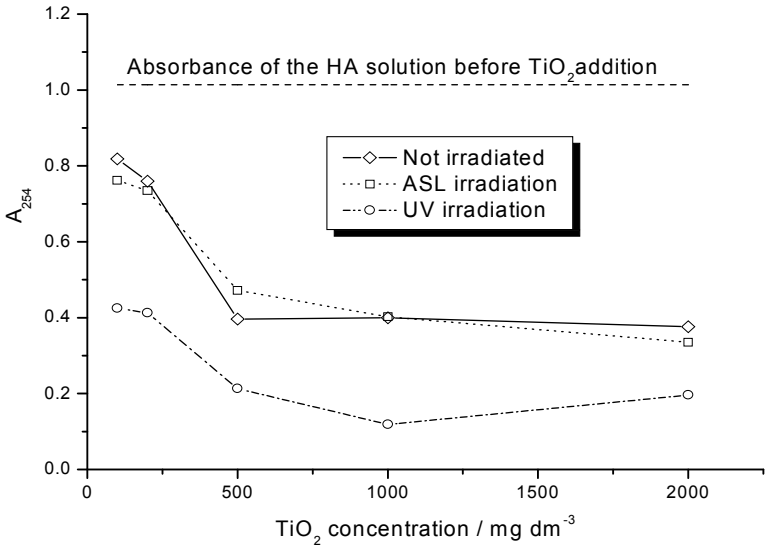

Fig. 7. Decrease of the absorbance of HA solution at 254 nm under the influence of UV and ASL irradiation, depending on TiO_2 concentration in investigated suspension. Irradiation time 60 min, initial HA concentration 40 mg dm^{-3}.

From the course of the curve recorded for UV irradiated samples it have to be concluded that 100 and 200 mg dm^{-3} TiO_2 additions gave similar results (about 45 % conversion of HA). Dramatic increase in absorbance was noticed when the dosage of TiO_2 was increased to 500 mg dm^{-3}. Significant differences were also recorded between 500 mg dm^{-3} and 1000 mg dm^{-3} TiO_2 dosages however no further decrease of

absorbance value was observed when the TiO_2 dosage was increased from 1000 mg dm^{-3} to 2000 mg dm^{-3}, contrary some increase of absorbance was noticed. As the difference between 200 mg dm^{-3} and 500 mg dm^{-3} may be ascribed to the increased adsorption, the increase in absorbance observed for the loading 2000 mg dm^{-3} may probably be ascribed to very strong dispersion of radiation by the suspension of high concentration.

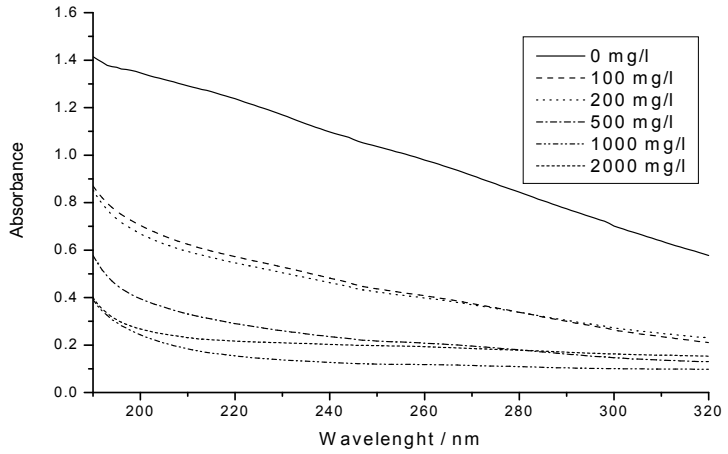

Fig. 8. UV spectra of the reaction mixture after 60 min of irradiation by UV light for different TiO_2 concentrations (marked in the figure). Initial concentration of HA 40 mg dm^{-3}.

The UV spectra of the reaction mixture after 1 hour of UV irradiation are presented in Fig. 8. The character of the spectrum changes, depending on the dosage of TiO_2, however it is impossible to draw clear conclusions because of the mutual influence of adsorption and degradation reaction on the spectrum.

3.5. The influence of the initial HA concentration on the photodegradation rate of HA

The series of solution consisted of 20, 40, 60 and 80 mg dm^{-3} of HA and 100 mg dm^{-3} of TiO_2 was prepared. Samples were UV and ASL irradiated for 60 min. The results are depicted in Fig. 9 and 10. The experimental results, presented in Figs 9 and 10 again suggest that the reaction rate is limited by the rate of reactive oxygen radicals, not by the process of their reaction with HA. Note that the amount of HA removed from the solution was almost independent on initial concentration of HA, except the first point, for the initial concentration of 20 mg dm^{-3} where the absorbance after reaction dropped down to zero. So, it may be stated that the reaction of the decomposition of humic acid in our case did not followed the Langmuir – Hinshelwood

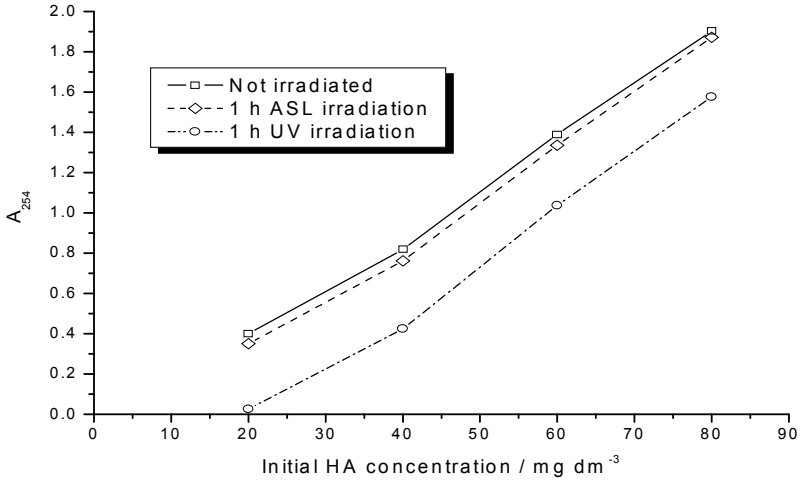

Fig. 9. Influence of initial concentration of HA on the absorbance at 254 of HA solution, depending on TiO_2 concentration in suspension. Irradiation time: 60 min.

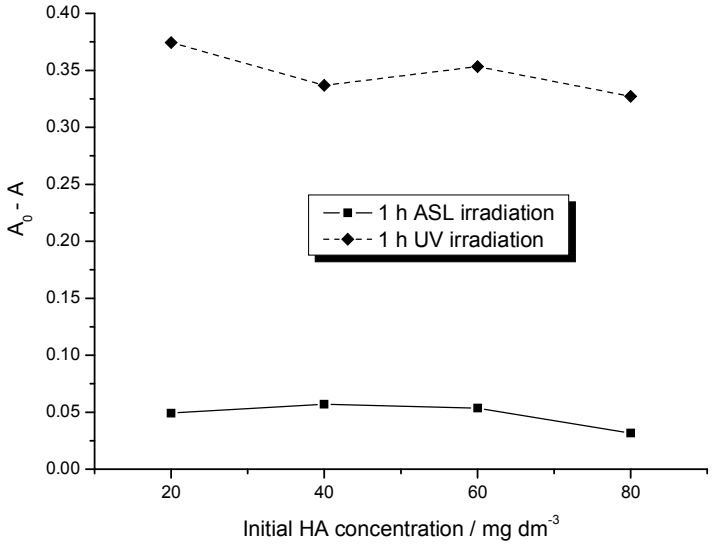

Fig. 10. Decreases of absorbance values of HA at 254 nm in TiO_2 suspension under the influence of ASL and UV irradiation, depending on initial HA concentration (A_0 – absorbance of not irradiated HA solution, A – absorbance of irradiated HA solution). Irradiation time 60 min.

(LH) kinetics which is usually observed in the case of many other contaminants. Looking for the most probable explanation of that fact the very strong adsorption of HA on the TiO_2 surface must be invoked in the first instance. In the derivation of the kinetic equation based on LH kinetics one assumes that the reaction rate is proportional to the surface coverage of the (photo)catalyst by the substrate of the reaction. However the results of the adsorption studies and the results of the other experiments strongly suggest that even at rather low concentration of HA in solution the surface is covered by the substrate in almost 100%. On the other hand it should be stated that humic acids are composed also by the substances that do not adsorb at the TiO_2 surface (see Fig. 3). The results of the experiment presented in Figs 9 and 10 suggest that those substances are also decomposed in the photocatalytic process.

4. CONCLUSIONS

Humic substances adsorb strongly at the surface of TiO_2. More than 50% of humic acid may be removed from the solution simply by adsorption on the surface if the concentration of TiO_2 in suspension is high enough. The presence of at least two types of humic species with diverse tendency to adsorption on TiO_2 surface was observed. Some part of HA does not adsorb at the TiO_2 surface in a measurable extent, however both the strongly adsorbing part of humic acid as well as that part which adsorb to only very limited extent may be removed from the solution by the photocatalytic process using UV radiation. The energy of the artificial sunlight appeared not to be high enough to cause the degradation of humic substances in a photocatalytic process at the TiO_2 surface – at all conditions applied the rate of degradation of HA by ASL was very low. 100% removal of HA substances may be achieved even at relatively low dosage of TiO_2 (100 mg dm^{-3}) if UV radiation and sufficiently long time of irradiation is applied. However time required for the complete removal of HA from water with the use of the photocatalyst only is relatively long. Three hours of irradiation was necessary at the 100 mg dm^{-3} TiO_2 concentration in the suspension to attain almost 100% removal of HA from solution at rather high UV irradiation intensity (48.8 mW cm^{-2}). Because rather high yield is required in the potable water treatment it is rather doubtful if the photocatalytic process alone may lead to the required efficiency.

The results of the experiments suggests that the process that HA decomposition does not follow the Langmuir – Hisnshelwood kinetics and is controlled rather by the rate of the generation of the reactive radicals in the photoexcitation process. If so, it means that either more active photocatalyst or additional destructive component (oxidant) is needed in the system, to speed up the process of HA decomposition. The works in both directions are being conducted now in our laboratory.

REFERENCES

[1] UYGUNER C.S., BEKBOLET M., *Evaluation of humic acid photocatalytic degradation by UV/VIS and fluorescence spectroscopy*, Catalysis Today 101 (2005) 267–274.

[2] MCDONALD S., BISHOP A.G., PRENZLER P.D., ROBARDS K., *Analytical chemistry of freshwater humic substances,* Analytica Chimica Acta 527 (2004) 105–124.

[3] CORIN N., BACKLUND P., KULOVAARA M., *Degradation products formed during UVradiation of humic waters*, Chemosphere 33 (2), (1996) 245 – 255.

[4] KULOVAARA M., CORIN N., *Impact of UV- radiation on aquatic humic substances*, Chemosphere 33 (5), (1996) 783 – 790.

[5] BEKBOLET M., UYGUNER C.S., SELCUK H., RIZZO L., NIKOLAU A.D., MERI S., *Application of oxidative removal of NOM to drinking water and formation of disinfection by-products***,** Desalination 176 (2005), 155-166.

[6] MOSTEO R., MIGUEL N., MARTIN – MUNIESA S., ORMAD M.P., OVELLEIRO J.L., *Evaluation of trihalomethane formation potential in function of oxidation processes used during the drinking water production process,* Journal of Hazardous Materials 172 (2009), 661–666.

[7] MYNENI S. C. B., WARWICK T. A., MARTINEZ G. A., MEIGS G., *C-Functional Group Chemistry of Humic Substances and Their Spatial Variation in Soils,*

[8] LJUBAS D., *Solar photocatalysis—a possible step in drinking water treatment,* Energy 30 (2005), 1699–1710.

[9] BEKBOLET M., OZKOSEMEN G., *A preliminary investigation on the photocatalytic degradation of a model humic acid*, Water Science Technology 33 (6), (1996) 189 – 194.

[10] BEKBOLET M., BALCIOGLU I., *Photocatalytic degradation kinetics of humic acid in aqueous TiO2 dispersions: The influence of Hydrogen Peroxide and bicarbonate ion*, Water Science Technology 34 (9), (1996) 73 – 80.

[11] BEKBOLET M., SUPHANDAG A. S., UYGUNER C. S., *An investigation of the photocatalytic efficiencies of TiO2 powders on the decolourisation of humic acids*, Journal of Photochemistry and Photobiology A: Chemistry 148 (2002) 121–128.

[12] UYGUNER C. S., BEKBOLET M., *A comparative study on the photocatalytic degradation of humic substances of various origins,* Desalination 176 (2005) 167-176.

[13] WISZNIOWSKI J., ROBERT D., SURMACZ – GÓRSKA J., MIKSCH K., WEBER J. V., *Photocatalytic decomposition of humic acids on TiO2 Part I: Discussion of adsorption and mechanism*, Journal of Photochemistry and Photobiology A: Chemistry 152, (2002) 267–273.

[14] PALMER F.L., EGGINS B.R., COLEMAN H.M., *The effect of operational parameters on the photocatalytic degradation of humic acid,* Journal of Photochemistry and Photobiology A: Chemistry 148 (2002) 137–143.

[15] X.Z. LI, C.M. FAN, Y.P. SUN, *Enhancement of photocatalytic oxidation of humic acid in TiO2 suspensions by increasing cation strength,* Chemosphere 48, (2002) 453–460.

[16] RADWAN AL-RASHEED, DAVID J. CARDIN, *Photocatalytic degradation of humic acid in saline waters. Part 1. Artificial seawater: influence of TiO2, temperature, pH, and airflow*, Chemosphere 51 (2003) 925–933.

[17] RADWAN AL-RASHEED, DAVID J. CARDIN, *Photocatalytic degradation of humic acid in saline waters Part 2. Effects of various photocatalytic materials*, Applied Catalysis A: General 246 (2003) 39–48.

[18] UYGUNER C. S., BEKBOLET M., *Photocatalytic degradation of natural organic matter: Kinetic considerations and light intensity dependence*, Int. Journal of Photoenergy, 06 (2004).

Physicochem. Probl. Miner. Process. 45(2010) 29-38

journal homepage
www.minproc.pwr.wroc.pl/journal/

Physicochemical Problems of Mineral Processing

Index No. 32213X ISSN 1643-1049

Ewelina GRABOWSKA *, Hynd REMITA **, Adriana ZALESKA *,

PHOTOCATALYTIC ACTIVITY OF TiO_2 LOADED WITH METAL CLUSTERS

Received March 22, 2010; reviewed; accepted May 10, 2010

TiO_2 was surface modified with silver, gold and platinum ion clusters to improve its photocatalytic activity. The effect of metal content, the kind of dopant and titanium dioxide source (commercial – P25 and ST-01) used during preparation procedure on photoactivity were investigated. The photocatalytic activity was estimated by measuring the decomposition rate of 0.21 mM phenol aqueous solution under UV-Vis and visible (λ>400 nm). The highest photoactivity was observed for TiO_2 loaded with silver (2%Ag on P25), gold (1%Au on P25) and platinum (0.5% Pt on ST-01) clusters. After 60 min. of irradiation under UV light phenol solution was degraded in 91%, 49% and 91%, respectively

keywords: photocatalysis, metal clusters, modified TiO_2

1. INTRODUCTION

Photodegradation of various pollutants using semiconductors has been intensively studied in recent years for its wide application in environmental protection. TiO_2 is a very promising photocatalyst due to its strong oxidation capacity, high photochemical and biological stability, non-toxicity and low cost [1]. Addition or doping with noble metal, such as platinum [2], palladium [3], silver [4] and gold [5] ions allow to extend

* Department of Chemical Technology, Faculty of Chemistry, Gdansk University of Technology, Gdańsk, Poland, egrab@chem.pg.gda.pl (E. Grabowska)

** Laboratoire de Chimie Physique, Universite Paris-Sud, 91405 Orsay, France

the light absorption of band gap semiconductors to the visible light. Noble metals could be introduced to the surface of TiO_2 by various methods such as: electrolysis, chemical reduction, UV photoreduction, γ-reduction deposition from colloids or adsorption of metal clusters [6-10].

It was proved that doping with $[Pt_3(CO)_6]n^{2-}$ (n=3-10) clusters could enhance the photoconversion yield by inhibition of the electron hole recombination [11-13]. Kowalska et al. [14] modified titania with platinum ions (Pt(II) or Pt(IV)) or clusters ($[Pt_3(CO)_6]_6^2$). TiO_2 was modified with noble metals by direct surface adsorption of Pt(IV) ($PtCl_6^{2-}$) or Pt(II) ($PtCl_4^{2-}$) in aqueous or mixed alcohol-water solutions (metal/TiO_2 = 1-2% w/w). Pt salts or clusters were put into contact with TiO_2 under stirring for several hours. Pt(IV) was introduced from aqueous solution (10^{-3} M) and stirred in the dark for 3 h. Pt(II) surface adsorption was carried out during stirring in the dark. Platinum clusters $[Pt_3(CO)_6]_6^{2-}$ were used as surface adsorbates. These clusters were synthesized by radiolytic reduction (using a ^{60}Co γ-source of 3000 Ci, dose of 800 grays) of Pt(II) in water/2-propanol solutions (10^{-3} M) under 1 atm of CO. The samples obtained by Pt clusters and Pt(II) deposition at the surface of P 25 exhibited a visible light activity for phenol and Rhodamine B degradation [14].

Here, we report the preparation method and characteristics of silver, gold and platinum modified TiO_2 photocatalysts. Metal clusters with controlled nuclearity had been deposited at the TiO_2 surface by radiolytic reduction (using a ^{60}Co γ-source of 3000 Ci, dose of 800 grays) of metal precursors (Au(III), Ag(I) and Pt(IV)) in water/alcohol solutions in the presence of ligands (such as CO), surfactants or polymers.

2. MATERIALS AND METHODS

TiO_2 ST-01 powder having anatase crystal structure was obtained from Ishihara Sangyo, Japan (surface area 300 m^2/g, particle size 7 nm) and P25 (70:30% anatase-to-rutile mixture with a BET surface area of 55 ± 15 m^2g^{-1} and crystallite sizes of 30 nm in 0.1 μm diameter aggregates) from Degussa GmBH, Germany. 98% $KAuCl_4$, 99.5% $AgClO_4$ and 99% H_2PtCl_6 from Aldrich Chem. Co were used as gold, silver and platinum source.

TiO_2-based photocatalysts were obtained according to procedures presented by a simplified block diagram in Figure 1. Silver and gold modified TiO_2 was prepared by one-pot method. Ag-TiO_2 and Au-TiO_2 were prepared by radiolytic reduction (using a ^{60}Co γ-source) of Ag(I) and Au(III), in the presence of suspended TiO_2 in methanol under N_2 atmosphere. Platinum modified titania was synthesized by a two-step method. In the first step, platinum clusters were synthesized by radiolytic reduction (using a ^{60}Co γ-source) of Pt(II) in water/methanol under 1 atm of CO. Obtained platinum

clusters were adsorbed at the TiO_2 surface. The modified TiO_2 photocatalysts were separated by centrifugation and dried at 60ºC.

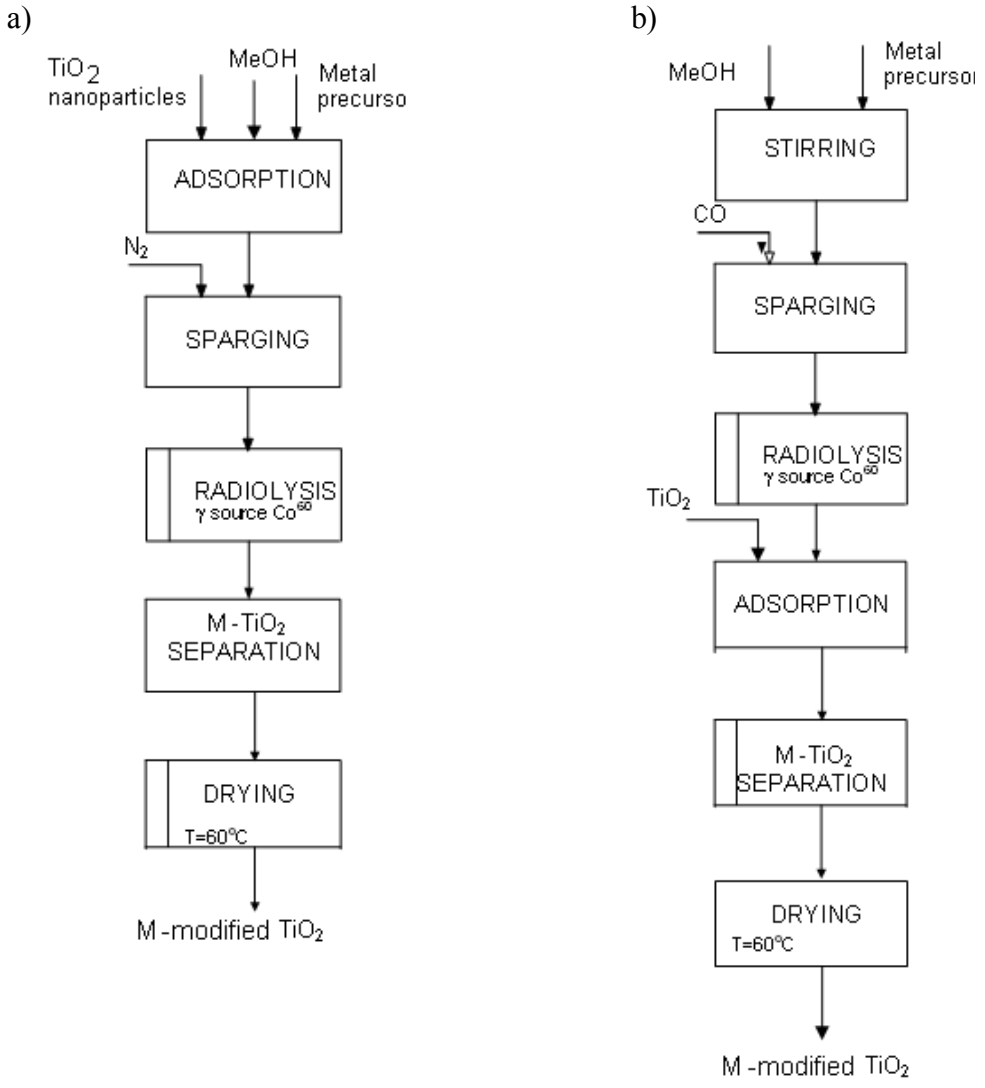

Fig. 1. Block diagram of Me-doped TiO_2 prepared by radiolysis method: (a) one-pot method (metal clusters are reduced directly at the surface of TiO_2 nanoparticles, and (b) two-step method (metal cluster reduction are followed by adsorption at the TiO_2 surface)

The photocatalytic activity of the obtained powders in ultraviolet and visible light was estimated by measuring the decomposition rate of phenol (0.21 mmol/dm^3) in an aqueous solution. Photocatalytic degradation runs were preceded by blind tests in the absence of photocatalyst or illumination. 25 cm^3 of catalyst suspension (125 mg) was stirred using magnetic stirrer and aerated (5 dm^3/h) prior to and during the photocatalytic process. Aliquots of 1.0 cm^3 of the aqueous suspension were collected at regular time periods during irradiation and filtered through syringe filters (Ø=0.2 μm) to remove catalyst particles. The suspension was irradiated using 1000 W Xenon lamp (Oriel), which emits both UV and Vis light. To limit the irradiation wavelength, the light beam was passed through GG400 filter to cut-off wavelengths shorter than 400 nm. Phenol concentration was estimated by colorimetric method using UV-VIS spectrophotometer (DU-7, Beckman).

3. RESULT AND DISCUSSION

All photocatalysts obtained by radiolytic reduction of $AgClO_4$ (0.5; 1; and 2 wt.%) at the surface of ST-01 or P25 were pinky to violet. The samples prepared by modification of ST-01 or P25 with $KAuCl_4$ (0.5; 1; and 2 wt.%) were pinky-violet or light grey, respectively. The samples prepared by γ-radiation of H_2PtCl_6 (0.5; 1; and 2 wt.%) followed by adsorption at the ST-01 and P25 surface were creamy-grey. It was reported that surface modification with Pt clusters caused the grey color of the sample, possibly due to the presence of Pt^0 or PtO_2 [15]. Sample labeling, preparation method and coloration of the samples after metal modification are given in Table 1. For selected samples, the size of metal aggregates was confirmed by microscopy analysis (STEM) and equaled about 2 nm.

The photocatalytic activities of metal loaded TiO_2 samples were quantified in terms of the oxidative degradation of phenol in aqueous solution under UV-Vis irradiation. The observed reaction rate with various metal loaded TiO_2, which were prepared at metal ion concentration from 0.5 to 2 wt.%, are listed in Table 2. Under UV-Vis light irradiation, the rate of phenol degradation in the presence of pure ST01-TiO_2 was estimated to be 0.82 $\mu mol \cdot dm^{-3} \cdot min^{-1}$. The observed rate was increased slightly to 1.02, 1.05 and 1.2 $\mu mol \cdot dm^{-3} \cdot min^{-1}$ in the presence of ST01 loaded with silver and gold clusters prepared by γ-reduction of the solution containing 0.5 wt.% of Ag(I), 2 wt.% of Ag(I) and 0.5 wt.% of Au(III), respectively. However, the increase in Au(III) concentration from 0.5 to 2 wt.% during radiolytic preparation, resulted in the decrease on photoactivity of the obtained photocatalysts, see details in Table 2. Platinum modified ST01 showed significantly enhanced photocatalytic activities under UV-Vis irradiation as compared to pure ST01. Phenol degradation rate was

3.15 $\mu mol \cdot dm^{-3} \cdot min^{-1}$ for the sample Pt-ST01(0.5).

Table 1. Preparation method and coloration of the samples after metal modification

Sample label	Metal precursor	TiO_2 matrix	Content of metal precursor [wt. %]	Preparation method	Sample color
Au-ST01(0.5)	$KAuCl_4$	ST-01	0.5	one-pot	pink/ violet
Au-ST01(1)		ST-01	1	one-pot	pink/ violet
Au-ST01(2)		ST-01	2	one-pot	pink/ violet
Au-P25(0.5)	$KAuCl_4$	P25	0.5	one-pot	light grey
Au-P25(1)		P25	1	one-pot	light grey
Au-P25(2)		P25	2	one-pot	light grey
Ag-ST01(0.5)	$AgClO_4$	ST-01	0.5	one-pot	light pink
Ag-ST01(1)		ST-01	1	one-pot	pink
Ag-ST01(2)		ST-01	2	one-pot	pink
Ag-P25(0.5)	$AgClO_4$	P25	0.5	one-pot	pink
Ag-P25(1)		P25	1	one-pot	pink
Ag-P25(2)		P25	2	one-pot	violet
Pt-ST01(0.5)	H_2PtCl_6	ST-01	0.5	two-step	creamy-grey
Pt-ST01(1)		ST-01	1	two-step	green
Pt-ST01(2)		ST-01	2	two-step	creamy-grey
Pt-P25(0.5)	H_2PtCl_6	P25	0.5	two-step	grey
Pt-P25(1)		P25	1	two-step	grey
Pt-P25(2)		P25	2	two-step	deep grey
Pt-P25(1a)	$(NH_3)_4PtCl_2 \cdot H_2O$	P25	1	one-pot	green-grey
P25	-	P-25	0	-	white
ST-01	-	ST-01	0	-	white

Figure 2 shows the results of phenol degradation under UV-Vis irradiation in the presence of TiO_2 modified with platinum. All powders, prepared by radiolytic reduction of H_2PtCl_6 followed by adsorption of platinum clusters at the ST01 surface, exhibited higher photoactivity than pure ST-01 TiO_2. The highest photoactivity was observed for lower dopant amount (0.5 wt. %). In the presence of the sample Pt-ST01(0.5), phenol

was degraded in 91% after 60 min of irradiation.

Table 2. Photocatalytic activity of pure TiO_2 and samples prepared by metal modification

Sample label	Rate of phenol degradation [μmol dm^{-3} min^{-1}]	
	UV-Vis	Vis
Au-ST01(0.5)	1.2	-
Au-ST01(1)	0.75	0.08
Au-ST01(2)	0.27	-
Au-P25(0.5)	1.25	0.5
Au-P25(1)	1.94	0.54
Au-P25(2)	1.53	0.52
Ag-ST01(0.5)	1.02	-
Ag-ST01(1)	0.58	-
Ag-ST01(2)	1.05	-
Ag-P25(0.5)	2.69	0.33
Ag-P25(1)	2.28	0.78
Ag-P25(2)	3.14	0.27
Pt-ST01(0.5)	3.15	1.07
Pt-ST01(1)	2.15	0.44
Pt-ST01(2)	3.09	0.19
Pt-P25(0.5)	3.45	1.42
Pt-P25(1)	3.71	0.85
Pt-P25(2)	3.64	1.15
Pt-P25(1a)	3.43	-
P25	2.0	0.55
ST-01	0.82	0.25

Degussa P25 is highly photoactive in phenol degradation under UV-Vis light. After 60 min of irradiation, 52% of phenol was degraded. The same time of irradiation resulted in 22% of phenol degradation under visible light. P25 modified with gold clusters revealed lower photoactivity than pure P25 both under UV-Vis and visible light

irradiation. However, deposition of silver or platinum clusters at the surface of P25 nanoparticles resulted in higher photoactivity. Phenol degradation rate was 2.69, 2.28 and 3.14 $\mu mol \cdot dm^{-3} \cdot min^{-1}$ for the samples obtained by radiation of P-25 suspension containing 0.5, 1 and 2 wt.%. of $AgClO_4$, respectively.

All photocatalysts obtained by radiolytic reduction of $AgClO_4$ in the presence of P25 showed higher photoactivity than the samples prepared with ST01. From all the samples prepared by radiolysis reduction of platinum salts in the presence of P25, the highest photoactivity was observed for the samples obtained by γ-irradiation of 1 wt.% H_2PtCl_6 and 1 wt.% $NH_3)_4PtCl_2 \cdot H_2O$ solution followed by adsorption of metal cluster at the P25 surface. Phenol decomposition rate was 3.71 and 3.43 $\mu mol \cdot dm^{-3} \cdot min^{-1}$ for the sample Pt-P25(1) and Pt-P25(1a), respectively. It was observed

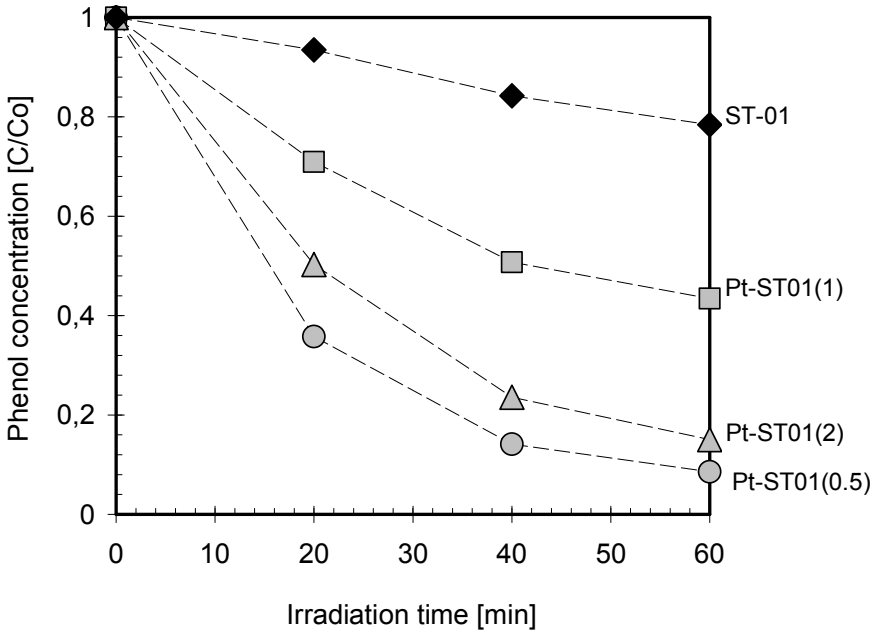

Fig. 2. Photoactivity under UV-Vis light of ST01-TiO_2 modified with platinum clusters deposited by radiolytic reduction of H_2PtCl_6. Experimental conditions: C_o=0.21 mM; m (TiO_2) = 125 mg, T=10°C, Q_{air}=5 l/h

Figure 3 shows the comparison characteristics of the most photoactive metal-modified P25 samples prepared using three types of metal precursors: $KAuCl_4$, $AgClO_4$ and H_2PtCl_6. All photocatalysts revealed the highest photoactivity under UV-Vis light comparable to that of pure TiO_2. Phenol degradation rate was 3.14 $\mu mol \cdot dm^{-3} \cdot min^{-1}$ for

the Ag-P25(2) sample, 3.15 μmol·dm^{-3}·min^{-1} for the Pt-ST01(0.5) sample, and 1.94 μmol·dm^{-3}·min^{-1} for the AuP25(2) sample.

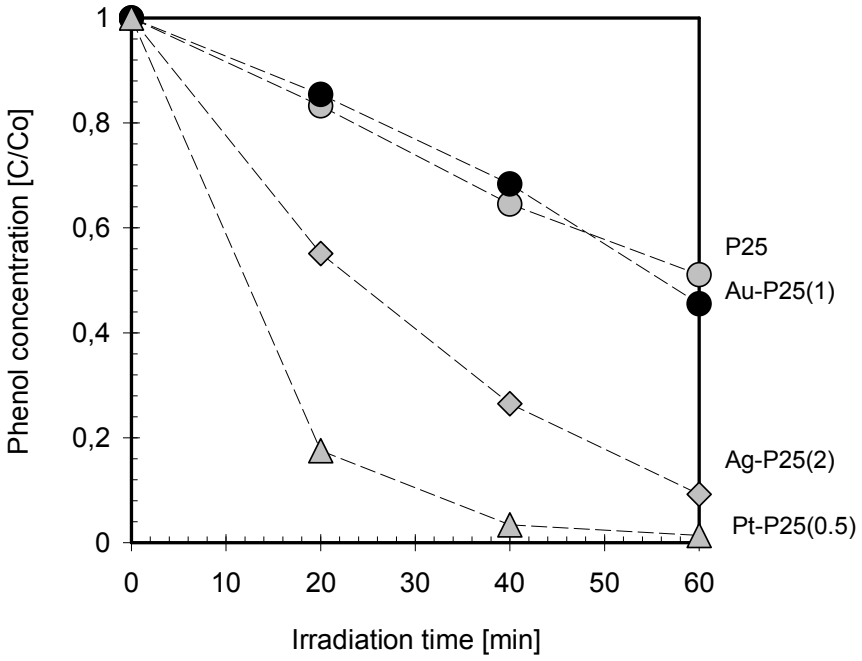

Fig. 3. Photoactivity under UV-Vis light of Au, Ag, Pt-TiO_2 photocatalysts. Experimental conditions: C_o=0.21 mM; m (TiO_2) = 125 mg, T=10°C, Q_{air}=5 l/h

Visible light activity was measured only for the samples revealed high photoactivity under UV-Vis light. The highest photoactivity was observed for the sample prepared by reduction Ag(I) (1 wt.%) on P25 and Pt(IV) (0.5% wt.) on ST-01 nanoparticles. Phenol degradation rate equaled 0.78 and 1.07 μmol·dm^{-3}·min^{-1} for the sample Ag-P25(1) and Pt-ST01(0.5), while it was 0.55 and 0.25 μmol·dm^{-3}·min^{-1} for pure P25 and ST01, respectively. We did not observe any increase in photoactivity under visible light in the case of gold surface modification of P25. All obtained powders prepared by radiolytic reduction of $KAuCl_4$ in the presence of P25 had almost the same photoactivity under visible light (about 0.5 μmol·dm^{-3}·min^{-1}).

Among all tested Pt-TiO_2 samples, Pt-P25(1) showed the best both UV-Vis and visible light photoactivity for phenol degradation. After 60 min irradiation, phenol was degraded in 99 and 38% under UV-Vis and visible light, respectively. According to the literature data under UV irradiation platinum acts as a charge scavenger hindering

charge recombination. Under visible light irradiation a sensitization mechanism should be considered such as absorption of light by platinum clusters.

4. CONCLUSION

The effect of the metal modification on the photocatalytic activity depends on the type of metal, metal precursor concentration used during synthesis and the origin of titania. Generally, Degussa P25 surface modified with silver, gold and platinum clusters exhibits better efficiency in phenol photooxidation than ST01-based photocatalysts. It was found that titania surface modification with silver and platinum enables the increase of the photocatalytic activity both under UV and visible irradiation.

ACKNOWLEDGMENTS

This work was supported by Ministry of Science and Higher Education (contract No.: N N523 420137)

REFERENCES

[1] FUJISHIMA A,.RAO T.N., TRYK D.A., (2000) *Titanium dioxide photocatalysis* J. Photochem. Photobiol. C 1, 1-21

[2] KITANO M., TEKAUCHI M., MATSUOKA M., THOMAS J.M., ANPO M., (2007) *Photocatalytic water splitting using Pt-loaded visible light-responsive TiO_2 thin film photocatalysts* Catal. Today 120, 133-138

[3] KUMAR S., FEDOROV A.G., GOLE J.L. (2005) *Photodegradation of ethylene using visible light responsive surfaces prepared from titania nanoparticle slurries* Appl. Catal. B 57, 93-107

[4] DAMM C., IZRAEL G.,(2007) *Photoelectric properties and photocatalytic activity of silver-coated titanium dioxides* Dyes Pigments 75, 612-618

[5] ORLOV A., JEFFERSON D. A., MACLEOD N., LAMBERT R. M. (2004) *Photocatalytic properties of TiO_2 modified with gold nanoparticles in the degradation of 4-chlorophenol in aqueous solution* Catal. Lett. 92 1, 41-47

[6] HWANG S., LEE M. C., CHOI W., (2003) *Highly enhanced photocatalytic oxidation of CO on titania deposited with Pt nanoparticles: kinetics and mechanism* Appl. Catal., B, 46, 49-63

[7] CHAO H. E., YUN Y. U., XINGFANG H. U., LARBOT A.,., (2003) *Effect of silver doping on the phase transformation and grain growth of sol-gel titania powder* J. Eur. Ceram. Soc 23, 1457-1464

[8] TORIMOTO T., NAKAMURA N., IKEDA S., OHTANI B., (2002) *Discrimination of the active crystalline phases in anatase–rutile mixed titanium(IV) oxide photocatalysts through action spectrum analyses* Phys. Chem. Chem. Phys. 4, 5910-5914

[9] ZHU Y., QIAN Y., HUANG H., ZHANG M., LIU S., (1996) *Sol-gel γ-radiation synthesis of titania-silver nanocomposites* Mater. Lett., 28, 259-261

[10] EL-AZAB A., GAN S, LIANG Y., (2002) *Binding and diffusion of Pt nanoclusters on anatase TiO_2(0 0 1)-(1 x 4) surface* Surf. Sci., 506, 93-104

[11] LONGONI, G.; CHINI, P. (1976) *Synthesis and Chemical Characterization of Platinum Carbonyl Dianions* $[Pt_3(CO)_3(m\text{-}CO)_3]n^{2-}$ *(n=10,6,5,4,3,2,1). A New Series of Inorganic Oligomers* J. Am. Chem. Soc. 98, 7225-7231

[12] TREGUER M., REMITA H., BELLONI J., KEYZER R., (2002) *Carbonyl platinum clusters as silver halide dopant for photographic latent image formation. J. Imaging Sci. Technol.* 46, 193-199

[13] BELLONI J., TREGUER M., REMITA H., DE KEYZER R., (1999) *Enhanced yield of photoinduced electrons in doped silver halide crystals* Nature 402, 865-867

[14] KOWALSKA E., REMITA H, COLBEAU-JUSTIN C., HUPKA J, BELLONI J. (2008) *Modification of Titanium Dioxide with Platinum Ions and Clusters: Application in Photocatalysis* J. Phys. Chem. C 112. 1124-1131

[15] BURGETH G., KISCH H., (2002) *Photocatalytic and photoelectrochemical properties of titania–chloroplatinate(IV)* Coord. Chem. Rev. 230, 41-47

Physicochem. Probl. Miner. Process. 45(2010) 39-47

journal homepage
www.minproc.pwr.wroc.pl/journal/

Physicochemical Problems of Mineral Processing

Index No. 32213X ISSN 1643-1049

Joanna GRZECHULSKA - DAMSZEL *

APPLICATION OF TITANIA COATING AS PHOTOACTIVE REFILL IN THE REACTOR FOR PURIFICATION OF WATER CONTAMINATED WITH ORGANICS

Received March 16, 2010; reviewed; accepted May 10, 2010

The aim of the present work was to remove organic impurities from water using a reactor with photoactive refill. Application of the photoactive refill solves the problem of the replacement of the reactor or its parts when the photocatalyst activity decreases. In case of photocatalytic activity drop, only the photoactive refill can easily be replaced. Titanium dioxide coating was immobilized on the glass fabric as a thin layer from the alcoholic suspension followed by thermal stabilization.

The results of studies revealed that the titania coating shows a high photocatalytic potential for the decomposition of the model organic compounds (azodye Acid Red 18, phenol and methylene blue) in water. The coating exhibits high stability in repeated cycles of water treatment.

keywords: photocatalysis, titania coating, photoactive refill, water purification

1. INTRODUCTION

Methods used for purification of coloured wastewaters can be in general divided in two groups: (i) chemical or physical methods and (ii) biological methods. The physical methods include precipitation methods (coagulation, flocculation, sedimentation),

* Institute of Chemical and Environment Engineering, West Pomeranian University of Technology in Szczecin, Pułaskiego 10, 70-322 Szczecin, Poland, e-mail: joanna.grzechulska@zut.edu.pl

adsorption (activated carbon, silica gels), filtration, reverse osmosis and the like. Reduction, oxidation, ion exchange and neutralization are example chemical methods. Biological treatment can be operated in aerobic or anaerobic conditions.

Advanced oxidation processes, especially photocatalysis, gained much interest last years since they are able to deal with the problem of organic pollutant destruction in aqueous systems [1-10]. Processes of the photocatalytic degradation of organic impurities in majority operate in the systems where the photocatalyst is suspended in the reaction mixture. However, in this case the photocatalyst should be separated from reaction mixture after the process is completed. Removal of the catalyst from the reaction mixture is an additional step in the process that increases its costs. Different researchers have tried to minimize these problems by immobilizing TiO_2 on various solid supports or on the reactor walls, which eliminates arduous step of separation [11-19]. Immobilization of the photocatalyst on the reactor walls or on its other parts shows its disadvantages when the activity of the catalyst decreases and it has to be replaced. Thus, the better solution is to immobilize the photocatalyst on the replaceable elements that can easily be removed and placed again in the reactor. Such supports have the other advantage of providing a good contact of the treated medium with the photocatalyst surface and also of allowing deeper light penetration in the reactor. A flexible textiles seemed to be an adequate support for the photoactive titania coatings. However, textiles are organic materials and can undergo the photocatalytic degradation themselves.

The aim of the present work was to remove organic impurities from water using a reactor with photoactive refill. Titanium dioxide was immobilized on the base material as a thin layer from the alcoholic suspension followed by thermal stabilization. The glass fabric was applied as a support for the titania coating.

2. MATERIALS AND METHODS

The commercial anatase form of titanium dioxide produced by Chemical Factory „Police" (Poland) was used as a photocatalyst. In order to evaluate the photoactivity of the prepared titania coating, decomposition behavior of methylene blue (MB), phenol and azo-dye Acid Red 18 (AR18) was studied. MB and phenol were chose since these compounds are widely used as a model compounds in the photocatalytic studies, whereas AR18 is commonly used azo-dye and was the subject of previous investigations of this paper author [20-24].

The process of photocatalytic oxidation was conducted using a laboratory installation (Figure 1) whose main component was the flow reactor (Trojan Technologies, Canada) with a refill covered with a titania coating. The mercury lamp emitting UV radiation in the range of 250 – 800 nm, with high maximum at 254, 436

and 546 nm, was placed inside the reactor, in its centre. The photoactive refill was also placed inside the reactor in such a way as to stick the inner walls of the reactor. The photocatalyst was fixed to the glass fabric according to the following procedure. The suspension of TiO_2 in ethanol was sonicated for 1 h with a frequency of 40 kHz. The glass fabric was immersed in such prepared suspension and then dried for at 105°C. The procedure was repeated twice. After that the coating was stabilized by thermal treatment at the temperature of 150°C overnight. The excess of the immobilized photocatalyst was rinsed with the water flowing through the reactor before the photocatalytic process. The solution of organics was pumped to the reactor by peristaltic pump from the container and than circulated through the reactor with the flow rate of 36 dm^3/h. The solution circulated in the reactor for 15 minutes without illumination to reach the adsorption equilibrium. The adsorption onto photocatalyst surface was low, only about 5 % (by weight).

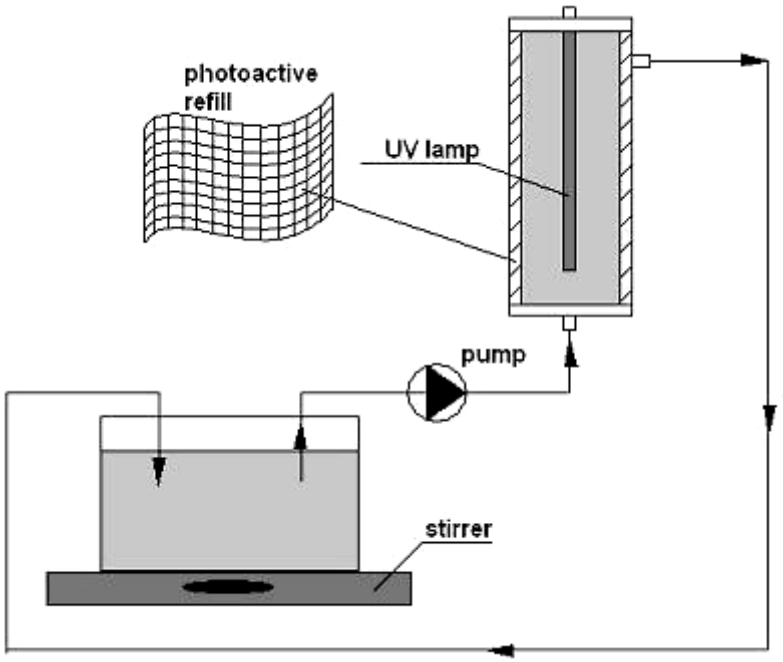

Fig. 1. The scheme of installation for the process of photocatalytic oxidation of MB, phenol and AR18.

The changes of reactants concentration in the solution were determined by absorbance measurement at the maximum absorption wavelength of 664, 270 and 507 nm, respectively for MB, phenol and AR18. (Jasco V-530 spectrometer, Japan). Total organic carbon (TOC) concentration was measured by "multi N/C 2000" analyzer (Analytik Jena, Germany). Total dissolved solids

(TDS) content, conductivity and pH of the solution (Ultrameter 6P, Myron L Company, USA) were also monitored during the process.

3. RESULTS AND DISCUSSION

At the beginning of the studies, blank experiments were performed. No decomposition occurred when an aqueous solution of studied compounds flowed through the reactor in the dark and the direct photolysis was also negligible (0,5 – 1,5%).

Figures 2 – 4 show the changes in concentration, respectively for MB, phenol and AR18, during the photocatalytic process. In case of all studied organic compounds, the concentration decreased the fastest in the first 10 hours of the process performance.

In case of MB, the initial dye concentration in the solution was equal to 5 mg/dm^3 and the total volume of the reaction solution was 2.5 dm^3. Three consecutive tests applying the same photoactive refill were performed (Fig. 2).

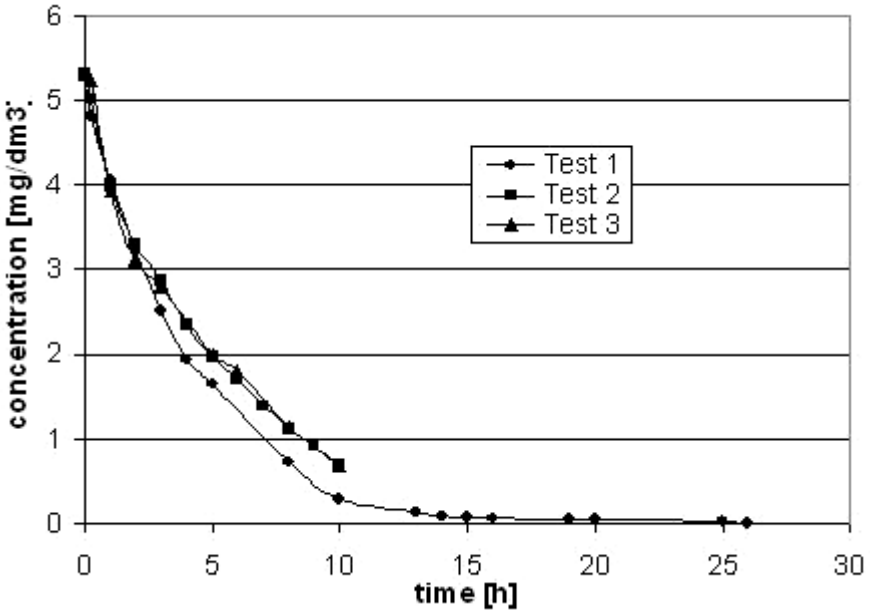

Fig. 2. Changes in concentration of MB during the photocatalytic process (three consecutive tests applying the same photoactive refill).

The dye concentration decreases with the time of the process. As can be seen from Figure 2, the color removal is the highest during the first hours of the process. After

that, the rate of color removal decelerates however a complete discoloration of the solution was achieved. The first test was conducted until the solution was colourless while the time of next tests was set to be 10 hours. The best results were obtained in the first test where after 10 h of the process performance, the decrement of concentration of MB was 94.7%. The complete discolouration of the solution during this test was obtained in 26 hours. The next two tests also gave very good results. During the second test, the concentration of MB decreased from 5.3 mg/dm3 to 0.68 mg/dm3 giving 87% decrement of concentration. The third test showed similar result as the second one. Such a good results obtained in relatively short time indicate that the photoactive refill applied in the studies shows high photocatalytic activity and this activity is stable in the repeated cycles of water treatment.

Figure 3 presents the changes in phenol concentration during the photocatalytic process for three tests performed with the same photoactive refill. The initial phenol concentration applied in the studies was equal to 20 mg/dm^3 and the total volume of the reaction solution was 2.5 dm^3. During the first test, the phenol decomposition degree was equal to 64.4% after the first 5h of the photocatalytic process and complete phenol decomposition was obtained in 23h. In the second tests, the phenol concentration in the solution after 10 h of illumination was a little higher comparing to the first one; however, the third tests showed comparable time of decomposition as the second one.

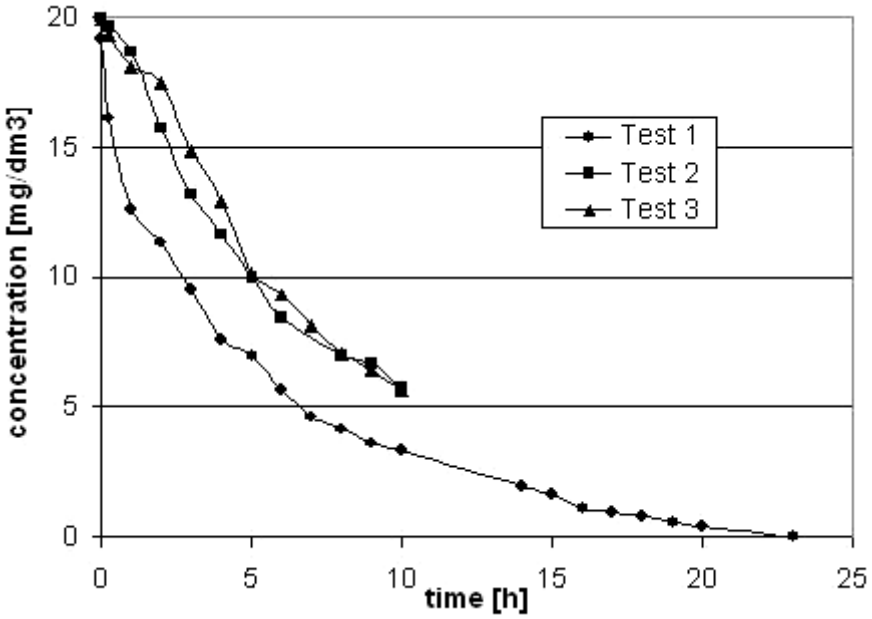

Fig. 3. Changes in concentration of phenol during the photocatalytic process (three consecutive tests applying the same photoactive refill).

For AR18, the results of five separated tests applying the same photoactive refill are presented in Figure 4. The initial AR18 concentration applied in the studies was equal to 10 mg/dm^3 and the total volume of the reaction solution was 2.5 dm^3. Similarly as for MB and phenol, the best results were obtained in the first run. The degree of degradation equal to 72% was achieved already after 5h while the degradation was completed after 15h of the photocatalytic process. The average value of concentration decrement after 5h of the process during the tests from 2 to 5 was about 60%.

Just as it was observed for MB and phenol, the activity of the photoactive refill decreased after the first usage and stabilized at a certain level during the next runs. However, starting from the sixth test, the time required for complete discoloration of AR18 solution elongated and during the eleventh test was doubled comparing to the firs one. Therefore, it can be stated that the lifetime of the photoactive refill amounts to about 200 hours and after that time the refill should be replaced with a new one.

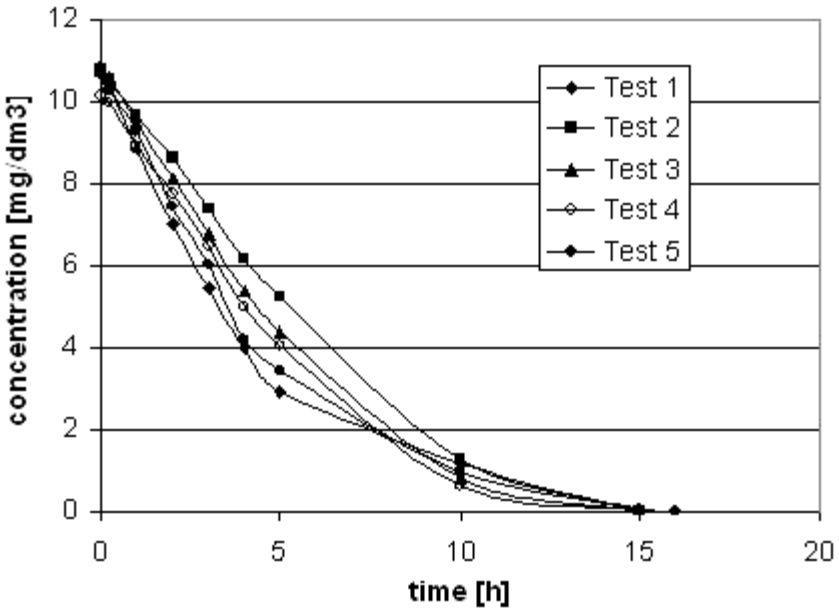

Fig. 4. Changes in concentration of AR18 during the photocatalytic process (five consecutive tests applying the same photoactive refill).

Except for the concentration of the studied compounds, the TOC, TDS, conductivity and pH of the reaction solutions have also been monitored during the photocatalytic process. Changes of these parameters give a wider picture of the organics degradation process since they do not always undergo the complete mineralization. The degradation of the primary structure is analytically observed as decrease in concentration but the degradation products can still remain in the reaction mixture. Figure 5 shows the

changes of TOC, TDS, conductivity and pH during the first test conducted with AR18 solution. The tendency of changes for the other tests conducted with AR18 and also with MB or phenol was similar.

The TOC concentration in the reaction solution for all the studied cases was decreasing during the photocatalytic process however a complete TOC removal was not achieved. This indicates incomplete mineralization of the treated compounds. In order to obtain the complete mineralization of organics leading to inorganic compounds, the time of the photocatalytic reaction should be elongated. It should be yet noticed that the values of TOC concentration in all the studied cases meet the legal regulation concerning the TOC concentration in water. The values of TDS and conductivity gradually increased during the process. This indicates the increase of dissolved compounds and ions in the reaction mixture showing also the progressive degradation of the initial compounds. The progressive degradation of organics was also confirmed by pH decrease (from 6.03 to 5.56) indicating generation of such decomposition products as carboxylic and mineral acids.

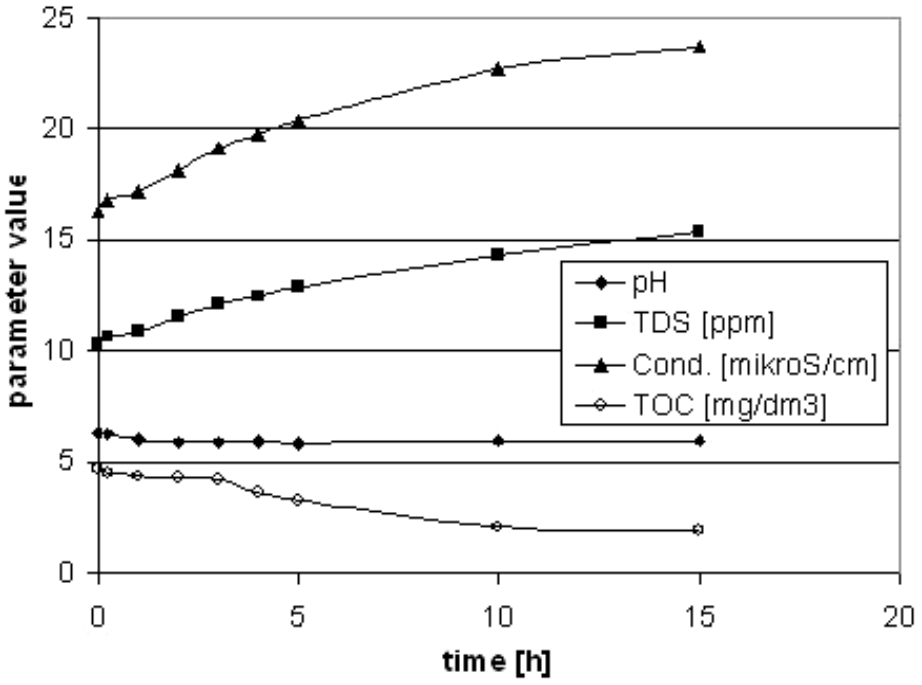

Fig. 5. Changes of TOC, TDS, conductivity and pH during the first test with AR18 solution

4. CONCLUSIONS

The results of the studies revealed that the titania coating shows high photocatalytic potential for the decomposition of the model organic compounds (methylene blue, phenol and Acid Red 18) in water. The coating prepared exhibits high stability in repeated cycles of water treatment. The photoactive refill solves the problem of reactor or its parts replacement necessity. The lifetime of the photoactive refill amounts to about 200 hours and when the photoactivity decreases, only the photoactive refill can easily be replaced. The application of glass fabric is advantageous since it is resistant to UV radiation and on the contrary to the natural fabrics, it does not undergo any photocatalytic decomposition.

REFERENCES

[1] Handbook: *Advanced photochemical oxidation processes*. (1998). United States Environmental Protection Agency, EPAl6251R-981004

[2] FUJISHIMA A., RAO T. N., TRYK D. *Titanium dioxide photocatalysis*. J. Photochem. Photobiol. C: Photochem. Rev. 1(1), 1 – 21.

[3] MUNTER R. (2001). *Advanced oxidation processes – current status and prospects*. Proc. Estonian Acad. Sci. Chem. 50(2), 59 – 80.

[4] ESPLUGAS S., GIMENEZ J., CONTRERAS S., PASCUAL E., RODRIGUEZ M. (2002). *Comparison of different advanced oxidation processes for phenol degradation*. Water Res. 36(4), 1034 – 1042.

[5] GOGATE P. R., PANDIT A. B. (2004). *A review of imperative technologies for wastewater treatment I: oxidation technologies at ambient conditions*. Adv. Environ. Res. 8(3-4), 501 – 551; *A review of imperative technologies for wastewater treatment II: hybrid methods*. Adv. Environ. Res. 8(3-4), 553 – 597.

[6] HASHIMOTO K., IRIE H., FUJISHIMA A. (2005). *TiO_2 photocatalysis: a historical overview and future prospects.* Jap. J. Appl. Phys. 44(12), 8269 – 8285.

[7] HERRMANN J.-M., DUCHAMP C., KARKMAZ M., BUI THU HOAI, LACHHEB H., PUZENAT E., GUILLARD C. (2007). *Environmental green chemistry as defined by photocatalysis*. J. Hazard. Mater. 146(3), 624 – 629.

[8] FUJISHIMA A., ZHANG X., TRYK D. A. (2007). *Heterogeneous photocatalysis: from water photolysis to applications in environmental cleanup*. Int. J. Hydrogen Energ. 32(14), 2664 – 2672.

[9] MALDONADO M. I., PASSARINHO P. C., OLLER I., GERNJAK W., FERNANDEZ P., BLANCO J., MALATO S. (2007). *Photocatalytic degradation of EU priority substances: a comparison between TiO_2 and Fenton plus photo-Fenton in a solar pilot plant*. J. Photoch. Photobio. A 185(2-3), 354 – 363.

[10] GAYA U. I., ABDULLAH A. H. (2008). *Heterogeneous photocatalytic degradation of organic contaminants over titanium dioxide: a review of fundamentals, progress and problems*. J. Photoch. Photobio. C 9(1), 1 – 12.

[11] FERNÁNDEZ, A., LASSALETTA, G., JIMÉNEZ, V.M., JUSTO, A., GONZÁLEZ-ELIPE, A.R., HERRMANN, J.-M., TAHIRI, H., AIT-ICHOU, Y. (1995). *Preparation and characterization of TiO_2 photocatalysts supported on various rigid supports (glass, quartz and stainless steel). Comparative studies of photocatalytic activity in water purification*. Appl. Catal. B: Environ. 7 (1-2), 49 – 63.

[12] GRZECHULSKA, J., MORAWSKI, A.W. (2003). *Photocatalytic labyrinth flow reactor with immobilized P25 TiO_2 bed for removal of phenol from water*. Appl. Catal. B: Environ. 46(2), 415 – 419.

[13] GELOVER S., MONDRAGÓN P., JIMÉNEZ A. (2004). *Titanium dioxide solegel deposited over glass and its application as a photocatalyst for water decontamination*. J. Photoch. Photobio. A 165(1-3), 241 – 246.

[14] PARRA S., STANCA S. E., GUASAQUILLO I., THAMPI K. R. (2004). *Photocatalytic degradation of atrazine using suspended and supported TiO_2*. Appl. Catal. B 51(2), 107 – 116.

[15] MOZIA S., TOMASZEWSKA M., MORAWSKI A. W. (2005). *Decomposition of nonionic surfactant in a labyrinth flow photoreactor with immobilized TiO_2 bed*. Appl. Catal. B 59(3-4), 155 – 160.

[16] GUNLAZUARDIA J., LINDU W. A. (2005). *Photocatalytic degradation of pentachlorophenol in aqueous solution employing immobilized TiO_2 supported on titanium metal*. J. Photoch. Photobio. A 173(1), 51 – 55.

[17] KRYSA J., WALDNER G., MESTANKOVA H., JIRKOVSKY J., GRABNER G. (2006). *Photocatalytic degradation of model organic pollutants on an immobilized particulate TiO_2 layer. Roles of adsorption processes and mechanistic complexity.* Appl. Catal. B 64(3-4), 290 – 301.

[18] TRYBA B. (2008). *Immobilization of TiO_2 and Fe–C–TiO_2 photocatalysts on the cotton material for application in a flow photocatalytic reactor for decomposition of phenol in water*. J. Hazard. Mater. 151(2-3), 623 – 627.

[19] GOETZ V., CAMBON J. P., SACCO D., PLANTARD G. (2009). *Modeling aqueous heterogeneous photocatalytic degradation of organic pollutants with immobilized TiO_2*. Chem. Eng. Process. 48(1), 532 – 537.

[20] GRZECHULSKA-DAMSZEL J., MORAWSKI A. W. (2007). *Removal of organic dye in the hybrid photocatalysis/membrane processes system*. Pol. J. Chem. Tech. 9(2), 104 – 108.

[21] GRZECHULSKA – DAMSZEL J., MORAWSKI A. W. (2009). *Water purification using a novel reactor with photoactive refill*. Catal. Lett. 127, 222-225.

[22] GRZECHULSKA – DAMSZEL J., TOMASZEWSKA M., MORAWSKI A. W. (2009). *Integration of photocatalysis with membrane processes for purification of water contaminated with organic dyes*. Desalination. 241, 118-126

[23] GRZECHULSKA – DAMSZEL J., MORAWSKI A. W. (2009). *Water purification using a novel reactor with the photoactive refill*. Pol. J. Chem. Tech. 11(1), 61-63.

[24] GRZECHULSKA – DAMSZEL J., MORAWSKI A. W. (2009). *Removal of organic dyes in hybrid photocatalysis/nanofiltration system*, Asia-Pac. J. Chem. Eng. Special Issue: Membrane Reactors. 4, 239-245.

Physicochem. Probl. Miner. Process. 45(2010) 49-56

journal homepage
www.minproc.pwr.wroc.pl/journal/

Physicochemical Problems of Mineral Processing

Index No. 32213X ISSN 1643-1049

Andreas HÄNEL *, Piotr MOREŃ *, Adriana ZALESKA *, Jan HUPKA *

PHOTOCATALYTIC ACTIVITY OF TiO_2 IMMOBILIZED ON GLASS BEADS

Received March 29, 2010; reviewed; accepted April 18, 2010

This paper reports the study of the photocatalytic activity of immobilized pure and boron-modified TiO_2 on glass beads. In situ formation and a dip-coating technique fixing catalyst onto the support surface was used. The photoreactor consists of a cylindrical quartz tube (i.d. 40 mm, length 100 mm) and was packed with the immobilized catalyst. The photocatalytic activity was determined by the degradation of phenol in water (0.21 mmol/dm^3). The pure TiO_2 catalyst could be reused for at least 3 cycles.

keywords: Titanium dioxide; photocatalysis, TiO_2, immobilization, photoreactor

1. INTRODUCTION

Heterogeneous photocatalysis in the presence of semiconductors is a promising technology, which decomposes and mineralizes organic contaminants in water by the generation of radicals ($^{\bullet}OH$, $O_2^{\bullet-}$) under irradiation (Fujishima et al., 2000). TiO_2 is the most widely used photocatalyst because of its high photocatalytic activity, non-toxicity and durability (Han et al., 2009). It exhibits a band gap of 3.2 eV and thus radicals are

* Department of Chemical Technology, Gdansk University of Technology ul. G. Narutowicza 11/12, 80-233 Gdańsk, Poland, ahaenel@student.pg.gda.pl (A. Hänel)

formed under UV irradiation. In our previous investigation, we presented a boron-modified photocatalyst (B-TiO_2), which is active in the presence of visible light (Zaleska et al., 2009). The photocatalytic activity was investigated in a slurry type reactor.

Slurry type reactors are commonly used whereupon the photocatalyst particles have to be separated by filtration, coagulation, flocculation or centrifugation achieving a catalyst free solution and recycling the catalyst. These downstream processes are costly, which is a reasonable limitation of using a slurry reactor on an industrial scale. To avoid the separation step the photocatalyst has to be attached onto a support. Immobilization and the support material influence the photocatalyst activity. The surface area of the catalyst is minimized since the coating layer has a lower porosity (Balasubramanian et al., 2004). It was reported that also the type of support material influences the adsorption characteristics and consequently the decomposition rate of pollutants (Sakthivel et al., 2002). Furthermore, immobilized catalyst showed flow rate dependence of the reaction (Bideau et al., 1995; Kobayakawa et al., 1998). Thus, the support should have the following characteristics (Pozzo et al., 1997): (a) transparent to irradiation; (b) strong surface bonding with the TiO_2 catalyst without negatively affecting the reactivity; (c) high specific surface area; (d) good absorption capability for organic compounds; (e) separability; (f) facilitating mass transfer processes and (g) chemical inert.

In view of technical application, the reactor has to be designed in the way so that optimal irradiation of the immobilized catalyst is guaranteed and that it is operated continuously. Several designs were proposed, like fixed bed, fluidized bed, floating bed, coated reactor tube wall, falling film and a kind of membrane "sandwich" reactor (Balasubramanian et al., 2004; Pozzo et al., 1997; O'regan et al., 1990).

In the present paper, both pure and doped TiO_2 deposited at the surface of glass beads were used to study the efficiency of model wastewater treatment. Pure TiO_2 and boron modified TiO_2 were immobilized at the support by in-situ formation and dip-coating technique and the photocatalytic activity was tested in a fixed-bed photoreactor equipped with a parabolic mirror.

2. MATERIALS AND METHODS

The following chemicals were used without further purification: titanium (IV) isopropoxide (97%, Aldrich Chem. Co.), ethanol (POCh, 96%), boric acid triethyl ester (99%), phenol (POCh, pure p.a.), hydrochloric acid (2M) and diluted hydrofluoric acid (5 wt.%). The glass beads used as a support material were obtained from Metal-Chem Sp. Z o.o. (ø 5 mm, $\rho = 2.5$ g/cm^3 for pure TiO_2, ø 4 mm, $\rho = 2.5$ g/cm^3 for B-TiO_2). ST-01 from Ishihara Sangyo, Japan (anatase, surface area 300 m^2/g, particle size 7 nm)

was used as TiO_2 source for boron doped photocatalyst preparation. Before coating, the beads were etched for 24 h in diluted hydrofluoric acid, washed thoroughly with deionized water and dried at 105 °C for 2 h. The immobilization of pure TiO_2 was carried out by in situ formation of TiO_2 procedure similar to the method reported by Kobayakawa et al. (1998). 30 cm^3 titanium (IV) isopropoxide and 200 cm^3 ethanol were mixed with 5.4 cm^3 HCl. A hydroxide sol was obtained by hydrolysis of titanium (IV) isopropoxide. The surface modified glass beads were immersed for 10 min in the hydroxide sol. Subsequently, they were filtrated and dried at 105 °C in an oven and calcinated at 450 °C for 2 h. The procedure was repeated until the beads were coated with 5 layers. Boron modified catalyst was prepared, according to the method reported in our previous investigation (Zaleska et al., 2009). ST-01 powder was grinded with boric acid triethyl ester in an agate mortar achieving boron content of 2 wt.%. The obtained powder was dried at 80 °C and calcinated at 400 °C for 1 h. The resulting powder was dispersed in deionized water achieving coating suspension with 30 g/l catalyst. Glass beads were dipped into suspension for 10 min. After coating, they were dried at 110 °C and calcinated at 400 °C for 1 h.

Fig. 1 shows the experimental setup used for photocatalytic measurements. The photoreactor, made of a cylindrical quartz tube (i.d. 40 mm, length 100 mm), was filled with TiO_2-coated glass beads and positioned over an aluminum parabolic mirror. Two liters of phenol solution (0.21 mmol/dm^3) were pumped in a loop with a flow rate of 1.2 cm^3/s. The TiO_2 immobilized photocatalyst was reused 3 times with a new stock solution. The immobilized B-TiO_2 catalyst was used for a single cycle. The fixed bed was irradiated by UV-Vis light using a 1000 W Xenon lamp (Oriel). Phenol concentration was determined by a colorimetric method measuring the UV-Vis absorbance with spectrophotometer (DU-7, Beckman). UV-flux was measured by UV-power meter (Hamamatsu Photonics, measurements range: 310 nm to 380 nm).

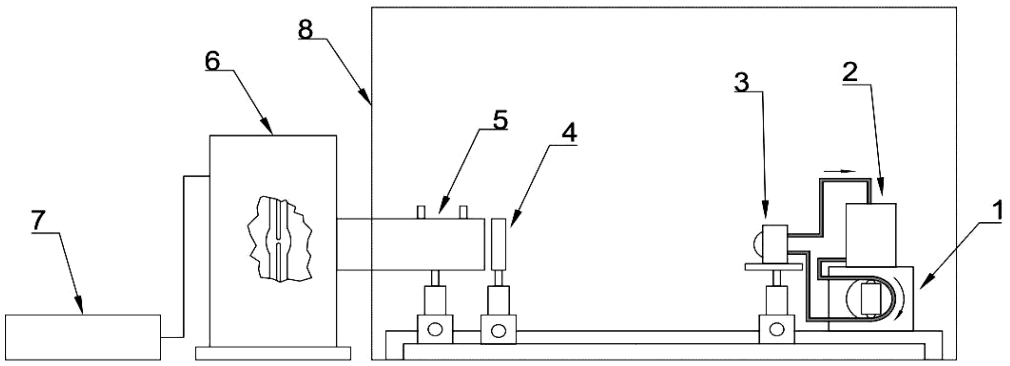

Fig. 1. Experimental setup: 1) peristaltic pump, 2) storage tank, 3) photoreactor with parabolic mirror, 4) filter, 5) IR filter, 6) Xenon lamp, 7) power supply, 8) darkroom

3. RESULT AND DISCUSSION

Table 1 and Fig. 2 show the change in phenol concentration vs. time profile observed during the photocatalytic degradation in the presence of glass beads coated with pure and boron-doped TiO_2. It has been observed that the temperature of phenol solution increased during irradiation and converged against 40 °C. The glass beads coated with pure TiO_2, prepared by sol-gel method, were used for 3 cycles. Considering the phenol solution flow rate (1.2 cm^3/s) it can be estimated that the whole volume of wastewater solution (2 dm^3) was circulated through the photoreactor almost 11 times during one cycle of irradiation (300 min). Under the experimental conditions, the efficiency of phenol removal in the presence of glass beads coated with pure TiO_2 was 30, 28 and 23% for the first, second and third cycle, respectively. Thus, the obtained result suggests that photocatalyst obtained by deposition of TiO_2 at the glass beads surface could be reused at least three times with negligible loss in photoactivity. The mass of the coated beads was measured before the first cycle and after the third one and the mass loss, due to TiO_2 removal, was 0.75 g. Thus, the decrease of phenol degradation rate is contributed to depletion of photocatalyst.

Table 1. Reaction conditions and photocatalytic activity of immobilized pure TiO_2 for three reactor runs with the same catalyst beads and immobilized B-TiO_2 under UV-Vis irradiation

Reaction time (min)	1st cycle			2nd cycle			3rd cycle			B-TiO_2		
	T (°C)	UV flux (mW/cm2)	Efficiency of phenol degradation C/C_0	T (°C)	UV flux (mW/cm2)	Efficiency of phenol degradation C/C_0	T (°C)	UV flux (mW/cm2)	Efficiency of phenol degradation C/C_0	T (°C)	UV flux (mW/cm2)	Efficiency of phenol degradation C/C_0
0	21	14.8	1	26	16.1	1	30	19	1	30	10.8	1
60	31	14.9	0.86	33	17.5	0.97	32	19.5	0.96	32	13.2	0.73
120	35	14.9	0.82	35	18.1	0.94	35	19.8	0.97	34	13	0.7
180	37	16.2	0.73	39	18.2	0.87	38	20.7	0.89	36	13.9	0.69
240	38	16.1	0.71	40	18.3	0.79	38	20.8	0.83	38	14.1	0.68
300	39	16.2	0.7	41	18.3	0.72	39	21.1	0.77	38	13.8	0.67

Slightly higher efficiency of phenol degradation was determined for the photocatalyst in the form of glass beads coated with boron-doped TiO_2. 300 min irradiation resulted in 33% of phenol degradation. After one cycle, the immobilized B-TiO_2 had changed its color from brownish to white and 0.23 g catalyst mass was removed. Thus, the B-TiO_2 catalyst was not reused for an additional cycle. We believe that the high loss of the catalyst is subjected to the high flow rate (72 cm^2/min). In comparison, the maximum flow rate of Kobayakawa et al. (1998) was 15 cm^2/min.

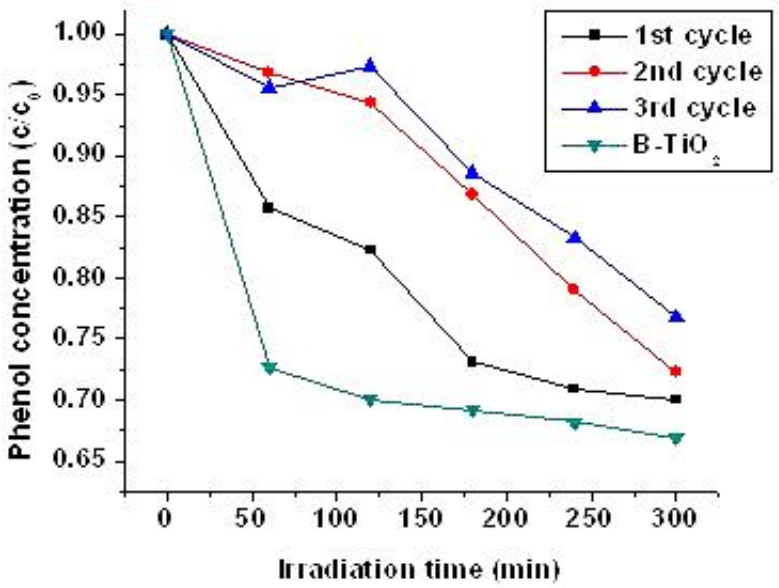

Fig. 2. Efficiency of phenol degradation in the presence of pure and B-TiO_2 under UV-Vis irradiation

Table 2 shows that the phenol degradation efficiency in the fixed-bed photoreactor was much lower than the efficiency, obtained for the system with suspended TiO_2 in the laboratory photoreactor, as reported in our previous investigation. However, it is worth mentioning that these results were achieved for a 10 times greater volume of an irradiated solution. Moreover, the ratio of TiO_2 amount to phenol solution amount was much lower than for the fixed-bed photoreactor system. In this regard, it was confirmed that the fixed-bed photoreactor system with pure or doped TiO_2 immobilized at the glass beads surface proved efficient for a photocatalytic reaction. The observed phenol degradation rate per gram of immobilized B-TiO_2 photocatalyst was higher than for pure TiO_2 supported on glass beads. The degradation rate per gram was 0.42 and 0.15 μmol dm^{-3} h^{-1} g^{-1} for B-TiO_2 and pure TiO_2, respectively.

Table 2. Comparison of fixed-bed photoreactor system and laboratory setup for phenol oxidation (initial phenol concentration: 0.21 mmol/dm^3, UV-Vis irradiation)

Processing Conditions		Fixed-bed photoreactor	Laboratory setup with suspended TiO_2
Volume of oxidized solution [dm^3]		2	0.025
Volume of photoreactor [dm$_3$]		0.125	0.025
Volume of irradiated solution [dm^3]		0.074*	0.025
Irradiation time [min]		300	60
Reaction conditions		polytropic temperature profile	isothermal
Temperature [ºC]		28 – 40	10
Power of radiation source [W]		1000	1000
Mass of the photocatalyst per loading [g]		~1.23 (pure TiO_2) 0.6 (B-TiO_2)	0.125
Irradiation power per reactor volume [W/dm^3]		8000	40000
Introducing gas		-	air
Gas flow rate [dm^3/h]		-	5
Rate of phenol degradation [μmol·dm^{-3}·min^{-1}]	Pure TiO_2	0.18	2.8
	B-TiO_2	0.25	2.9
Rate of phenol degradation per gram of catalyst [μmol·dm^{-3}·min^{-1}·g^{-1}]	Pure TiO_2	0.15	22.4
	B-TiO_2	0.42	23.2

*Calculated according to: $V_{ir} = V_r - V_{gb}$, where V_{ir} – volume of irradiated solution, V_r – volume of photoreactor, V_{gb} – volume of glass beads

The lifetime and regeneration of supported TiO_2 for the degradation of phenol under UV-C light in a batch reactor was investigated by Tasbihi at al. (2007). Three type of TiO_2 material using sol-gel technique were obtained: TiO_2 supported on glass beads, silica gel and quartz sand. The reaction time of 6 h, an initial phenol concentration varied from 25 to 115 mg/dm^3 and 0.25 g of each photocatalyst (supported on 30 g of different support) were chosen for each cycle. After each cycle the photocatalyst was re-calcinated at 600ºC for TiO_2/quartz sand and TiO_2/silica gel, while it was 700ºC for TiO_2/glass beads. TiO_2 supported on quartz sand gave the highest efficiency with 90% degradation of 50 mg/dm^3 phenol solution in 6h, followed by TiO_2 supported on silica gel and glass beads with 86% and 74%, respectively. The supported TiO_2 was found to be stable for repeated use. Their results suggested that TiO_2/quartz sand and TiO_2/glass

beads gave very good performances in the phenol degradation reaction. However, with TiO_2/silica gel, the percentage of degradation decreased to about 11% when used for the second time. Unfortunately, they did not report if depletion of photocatalyst took place, which might be the reason of the degradation decrease after reusing.

4. CONCLUSION

TiO_2 and B-TiO_2 photocatalyst supported on glass beads were synthesized using in-situ formation (sol-gel method) and dip-coating technique for pure and doped-TiO_2, respectively. The boron-doped TiO_2 supported on glass beads was used for the first time in this research. Photocatalytic degradation of phenol was observed for both immobilized catalysts. The adherence of photocatalyst has to be improved for both, TiO_2 and B-TiO_2, since depletion was observed.

ACKNOWLEDGMENTS

This research was supported by Polish Ministry of Science and Higher Education (Contract No.: N N523 483334 and N N 523 420137).

REFERENCES

[1] BALASUBRAMANIAN, G., DIONYSIOU, D.D., SUIDAN, M.T., BAUDIN, I., LAÎNÉ, J.-M., (2004). *Evaluating the activities of immobilized TiO2 powder films for the photocatalytic degradation of organic contaminants in water*. Applied Catalysis B: Environmental, 47, 73-84.

[2] BIDEAU, M., CLAUDEL, B., DUBIEN, C., FAURE, L., KAZOUAN, H., (1995). *On the "immobilization" of titanium dioxide in the photocatalytic oxidation of spent waters*. Journal of Photochemistry & Photobiology, A: Chemistry, 91, 137-144.

[3] FUJISHIMA, A., RAO, T.N., TRYK, D.A., (2000). *Titanium dioxide photocatalysis.* Journal of Photochemistry and Photobiology, C: Photochemistry Reviews, 1, 1-21.

[4] HAN, F., KAMBALA, V.S.R., SRINIVASAN, M., RAJARATHNAM, D., NAIDU, R., (2009). *Tailored titanium dioxide photocatalysts for the degradation of organic dyes in wastewater treatment: A review.* Applied Catalysis A, General, 359, 25-40.

[5] KOBAYAKAWA, K., SATO, C., SATO, Y., FUJISHIMA, A., (1998). *Continuous-flow photoreactor packed with titanium dioxide immobilized on large silica gel beads to decompose oxalic acid in excess water*. Journal of Photochemistry & Photobiology, A: Chemistry, 118, 65-69.

[6] O'REGAN, B., MOSER, J., ANDERSON, M., GRAETZEL, M., (1990). *Vectorial electron injection into transparent semiconductor membranes and electric field effects on the dynamics of light-induced charge separation*. Journal of Physical Chemistry, 94, 8720-8726.

[7] POZZO, R.L., BALTANAS, M.A., CASSANO, A.E., (1997). *Supported titanium oxide as*

photocatalyst in water decontamination: state of the art. Catalysis Today, 39, 219-231.

[8] SAKTHIVEL, S., SHANKAR, M.V., PALANICHAMY, M., ARABINDOO, B., MURUGESAN, V., (2002). *Photocatalytic decomposition of leather dye Comparative study of TiO2 supported on alumina and glass beads*. Journal of Photochemistry & Photobiology, A: Chemistry, 148, 153-159.

[9] TASBIHI, M., NGAH, C.R., AZIZ, N., MANSOR, A., ABDULLAH, A.Z., TEONG, L.K., MOHAMED, A.R., (2007). *Lifetime and regeneration studies of various supported TiO2 photocatalysts for the degradation of phenol under UV-C light in a batch reactor*. Ind. Eng. Chem. Res, 46, 9006-9014.

[10] ZALESKA, A., GRABOWSKA, E., SOBCZAK, J.W., GAZDA, M., HUPKA, J., (2009). *Photocatalytic activity of boron-modified TiO2 under visible light: The effect of boron content, calcination temperature and TiO2 matrix*. Applied Catalysis B, Environmental, 89, 469-475.

Physicochem. Probl. Miner. Process. 45(2010) 57-71

journal homepage
www.minproc.pwr.wroc.pl/journal/

Physicochemical Problems of Mineral Processing

Index No. 32213X ISSN 1643-1049

Toshihiro ISHIKAWA *

STRONG PHOTO-CATALYTIC FIBER AND ITS WIDE APPLICATION

Received March 18, 2010; reviewed; accepted March 20, 2010

In order to avoid large problems regarding peeling of the titania layer coated on the substrate, we developed an epoch-making "strong titania fiber" consisting of photoactive surface layer with a nanometer-scale compositional gradient, which can effectively oxidize any kind of organic materials. An effective water-purification system using this fiber has been also developed. The basis of this technology is to incorporate a selected low-molecular-mass additive ($Ti(OC_4H_9)_4$) into a precursor polymer from which the ceramic forms. After melt-spinning the resulting precursor polymer, thermal treatment of the spun fiber leads to controlled phase separation ("bleed-out") of the additive; subsequent calcination stabilizes the compositionally changed surface region, generating a functional surface layer. This fiber consists of the silica-based core-structure and the gradient-like surface titania layer, which are strongly sintered. We also developed a water-purifier using this fiber (felt material). Any bacteria (common bacterium, legionera pneumophila, colon bacillus, heterotrophic bacteria, and so forth) and organic chemicals (dioxin, PCB, and so forth) were effectively decomposed into CO_2 and H_2O passing through the above purifier.

keywords: strong titania fiber, water purification, photocatalysis

1. INTRODUCTION

Many types of polymer-derived ceramic fibers have been developed using a

* Inorganic Specialty Products Research Laboratory, Ube Industries, Ltd., 1978-5 Kogushi, Ube City, Yamaguchi Prefecture, 755-8633, Japan, E-mail: 24613u@ube-ind.co.jp

polycarbosilane (-SiH(CH_3)-CH_2-)$_n$ as the starting material [1-4]. Through research, many modifications have been made to obtain much higher heat-resistant fibers [2-4]. Of these, we developed in 1998 [3] the highest heat-resistant SiC polycrystalline fiber (Tyranno SA fiber) possessing the excellent heat-resistance up to 2000°C. This fiber was synthesized from polyaluminocarbosilane prepared by addition of very small amount of organic compound of aluminum, which serves as a sintering aid. Using a polyaluminocarbosilane precursor made it easy to control the aluminum concentration less than an upper concentration limit of the solid-soluble aluminum in the SiC crystal. This led Tyranno SA fiber to having excellent mechanical properties (3 GPa) and stability up to very high temperatures (~2000 °C). This fiber has very high thermal conductivity (64 W/mK), and some applications, which require good thermal shock resistance and high thermal conductivity, have been examined. In that time, we also developed unique fiber-bonded ceramic (SA-Tyrannohex), which was composed of highly ordered, close-packed structure of very fine hexagonal columnar fibers with very thin interfacial carbon layer between fibers for creating high fracture toughness.

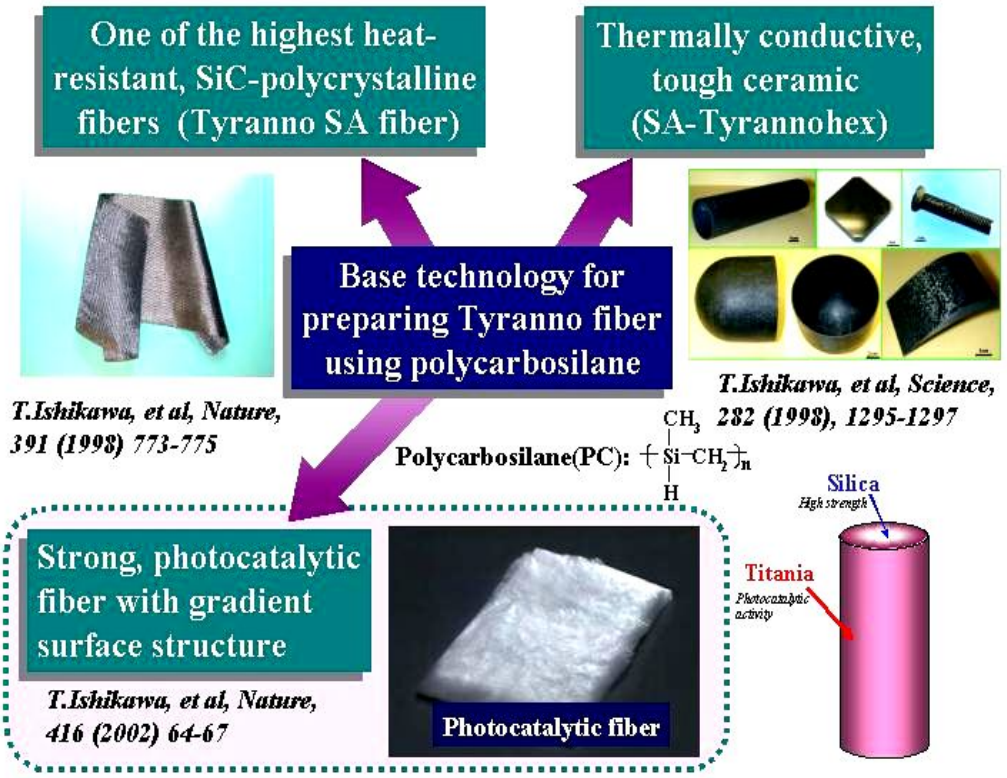

Fig. 1. Background of our technology

This ceramic is one of biomimetic ceramics aiming for natural wood structure or shell structure. Each fiber element consists of the same SiC polycrystalline structure as the above-mentioned Tyranno SA fiber. Accordingly, SA-Tyrannohex shows steady strength and very high fracture energy up to 1700°C in air.

Recently, using this base technology, we developed a new type of functional ceramic fiber with gradient surface structure [6,7]. This fiber was produced from a polycarbosilane containing an excess amount of selected low-molecular-mass additive, which can be converted into a functional ceramic by heat-treatment. Thermal treatment of the precursor fiber leads to controlled phase separation ("bleed out") of the low-molecular-mass additives from inside to outside of the precursor fibers. After that, subsequent calcination generates a functional surface layer during the production of bulk ceramic components. As the embodied functional material of our new process, we developed a strong photocatalytic fiber composed of anatase-TiO_2 surface structure and silica core structure. The above-mentioned technical background is summarized in Fig.1.

Anatase-TiO_2 is well known as a semiconductor catalyst, which exhibits a better photocatalytic activity by irradiation of a light with energy greater than the band gap (3.2eV) [8]. The photocatalytic activity appears by irradiation of an ultraviolet (UV) light with wavelength shorter than 387nm (=3.2eV). The decomposition of harmful substances using the photocatalytic activity of anatase-TiO_2 has attracted a great deal of attention [9-16]. This effect is attributed to the strong oxidant (hydroxyl radical), which generates at the surface of the TiO_2 crystals by the irradiation of UV light. The fundamental mechanism of the photocatalytic activity of titania is shown in Fig. 2.

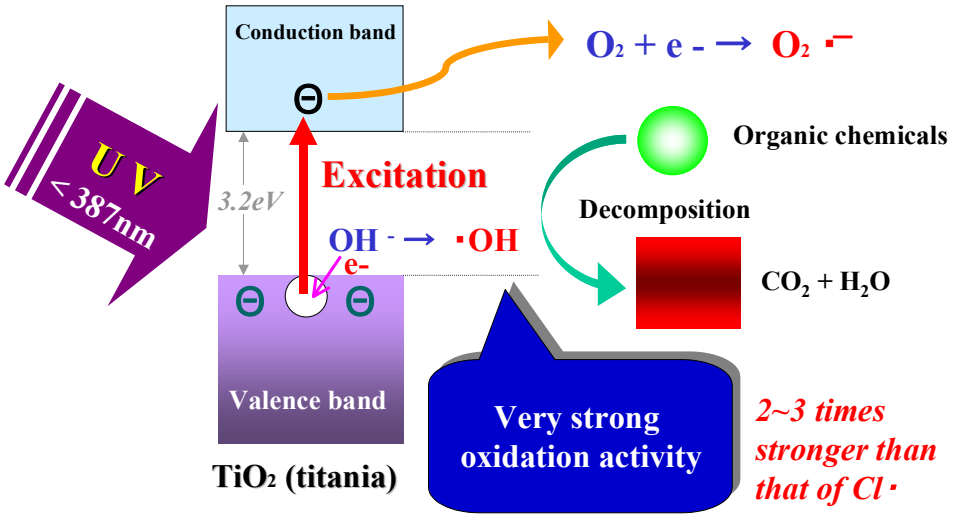

Fig. 2. Fundamental mechanism of the photocatalytic activity of titania

At present, most research have been performed using powder material or coated material on the substrate. Of these, powdery photocatalysts have some difficulties in practical use [9]. For example, they have to be filtrated from treated water. Coated photocatalysts on the substrate cannot provide sufficient contact area with harmful substances [9]. In addition, coated layer is easily peeled off from the substrate during usage. In order to avoid those problems, other types of research concerning fibrous photocatalysts have been conducted [10]. However, up to the present, a combination of excellent photocatalytic activity and high fiber strength has not been achieved using sol-gel method or simple polymer-blend [17,18]. According to the aforementioned new process, we achieved the development of a new photocatalytic, strong (2.5 GPa) and continuous fiber with small diameter (5~7 μ m), namely, a type of titania-dispersed silica-based fiber with a sintered anatase-TiO_2 layer on the surface. The surface gradient layer composed of nanoscale TiO_2 crystals (8 nm) was strongly sintered and exhibited excellent photocatalytic activity, which can lead to the efficient decomposition of harmful substances and any bacterium contained in air and/or water by irradiation of UV light. In this paper, the abovementioned photocatalytic fiber produced by our new *in situ* process and its actual applications are described.

2. SYNTHESIS OF OUR NEW PHOTOCATALYTIC FIBER

Polytitanocarbosilane containing an excess amount of titanium alkoxide was synthesized by the mild reaction of polycarbosilane $(\text{-SiH(CH}_3\text{)-CH}_2\text{-})_n$ (20 kg) with titanium (IV) tetra-n-butoxide (20 kg) at 220 ^{o}C in nitrogen atmosphere. The obtained precursor polymer was melt-spun at 150 ^{o}C continuously using melt-spinning equipment. The spun fiber, which contained excess amount of unreacted titanium alkoxide, was pre-heat-treated at 100 ^{o}C and subsequently fired up to 1200 ^{o}C in air to obtain continuous, transparent fiber (diameter: 5~7 μ m). In the initial stage of the pre-heat-treatment, effective bleeding of the excess amount of unreacted titanium (IV) tetra-n-butoxide from the spun fiber occurred to form the surface gradient layer containing large amount of titanium (IV) tetra-n-butoxide. During the next firing process, the pre-heat-treated precursor fiber was converted into a titania-dispersed, silica-based fiber covered with gradient titania (our photocatalytic fiber). The fundamental concept of the new production process for our photocatalytic fiber is shown in Fig.3.

Figure 4 shows the surface appearance and the cross section of our photocatalytic fiber. As can be seen from this figure, the surface of the fiber is densely covered with nanoscale anatase-TiO_2 particles (8 nm), which are strongly sintered with each other directly or through with amorphous silica phase.

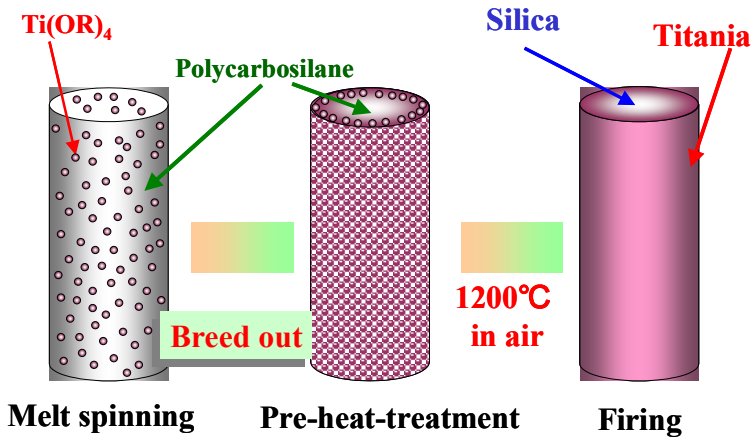

Fig. 3. Fundamental concept of our photocatalytic fiber

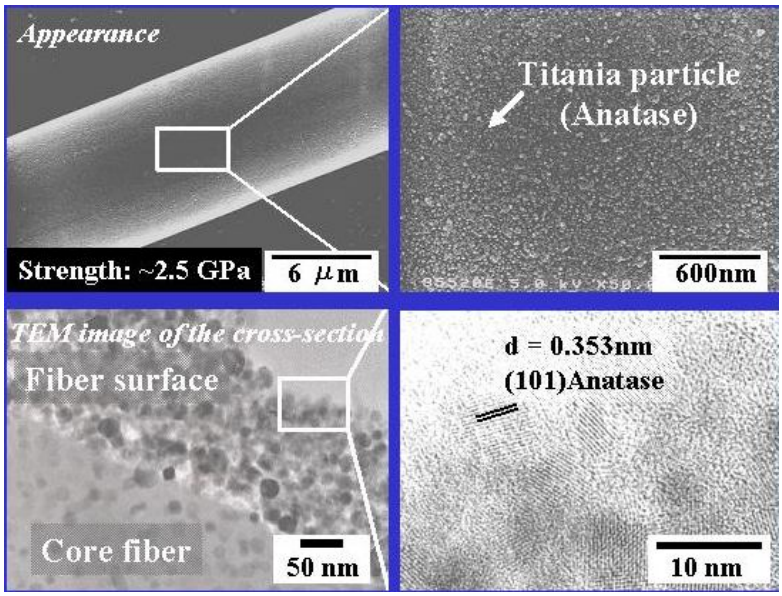

Fig. 4. The surface and cross-section of our photocatalytic fiber

The thickness of the surface TiO_2 layer is approximate 100~200 nm. The tensile strength of this fiber as measured by a single filament method was 2.5GPa on the average using an Orientec UTM-20 with a gauge length of 25 mm and cross-head speed of 2 mm/min. This mechanical strength is markedly superior to that of existing photo-catalytic TiO_2 fibers (<1GPa), which were produced by a sol-gel method [17] or using

polytitanosiloxanes [18]. The high strength of our photocatalytic fiber is closely related to the dense structure without pores, which is caused by its higher firing temperature compared with other TiO_2 fibers.

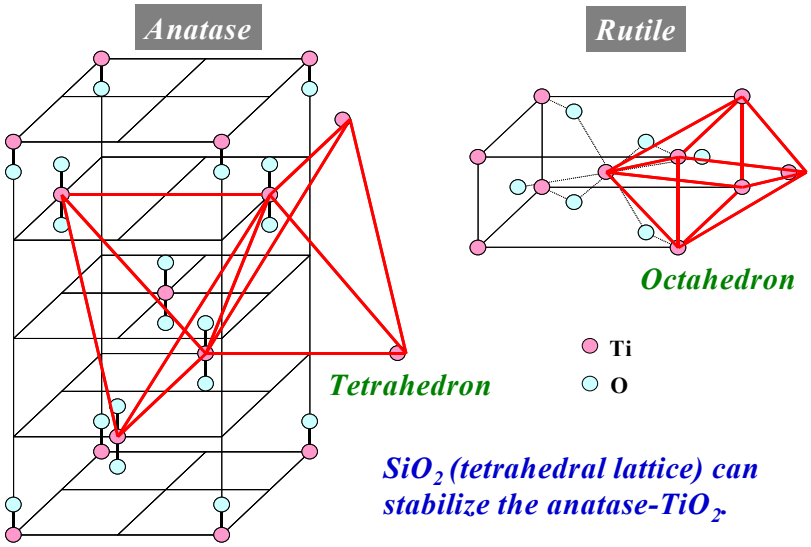

Fig. 5. The crystalline structure of titania along with the relationship between titania and silica

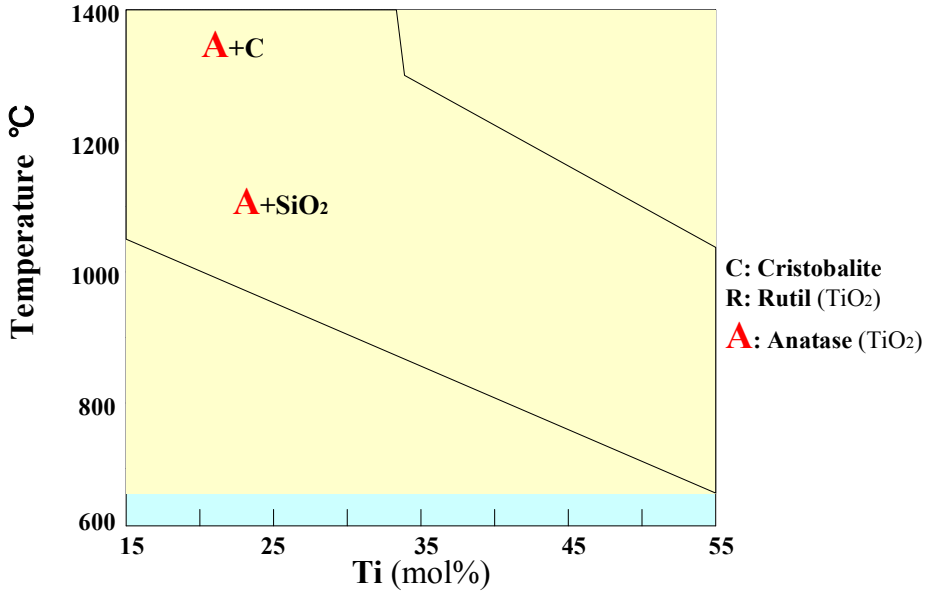

Fig. 6. The phase diagram of titania-silica phases

The photocatalytic activity of our fiber is caused by the anatase-titania on the surface of each fiber. It is well known that anatase-titania converts to rutile at temperatures ranging from 700°C to 1000°C [16]. In particular, pure nanocrystalline anatase easily converts to rutile at lower temperature (~500°C) [20]. In our case (firing temperature: 1200°C), it is thought that the surrounding silica phase caused the stabilization of the anatase phase. At the interface between titania and silica, atoms constituting titania are substituted into the tetrahedral silica lattice forming tetrahedral Ti sites [21]. The interaction between the tetrahedral Si species and the tetrahedral Ti sites in the anatase is thought to prevent the transformation to rutile. Figure 5 and 6 show the crystalline structure of titania along with the relationship between silica and titania, and phase diagram for the titania-silica phases, respectively.

3. APPLICATION OF OUR PHOTOCATALYTIC FIBER

We developed a water-purifier for pollutants using a felt material made of the aforementioned photocatalytic fiber (Fig.7). The average intensity of UV light on the photocatalytic fibers should be 10mW/cm^2 to obtain the good decomposition activity.

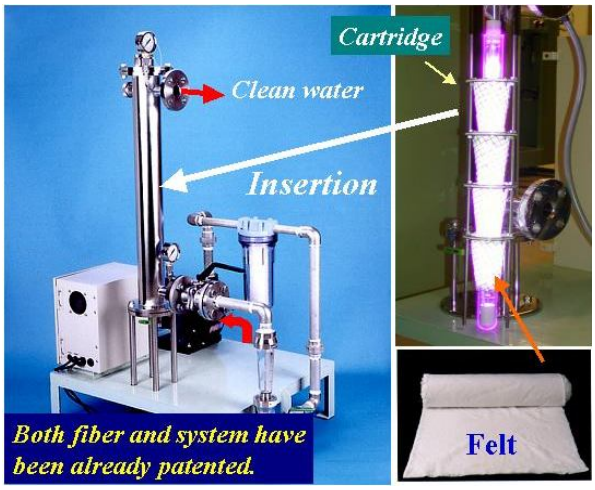

Fig. 7. Water-purifier using our photocatalytic fiber

This is a very simple purifier with a module composed of the cone-shaped felt material (made of our photocatalytic fiber with a very high quantum efficiency (~40%) [19]) and UV lamp. Purification of water of collective bathtubs and swimming pools was performed using this purifier. The muddiness of the pool water was remarkably improved (Fig.8) by the passage through the purifier. Organic filth and chloramines

also decreased after passage through the purifier.

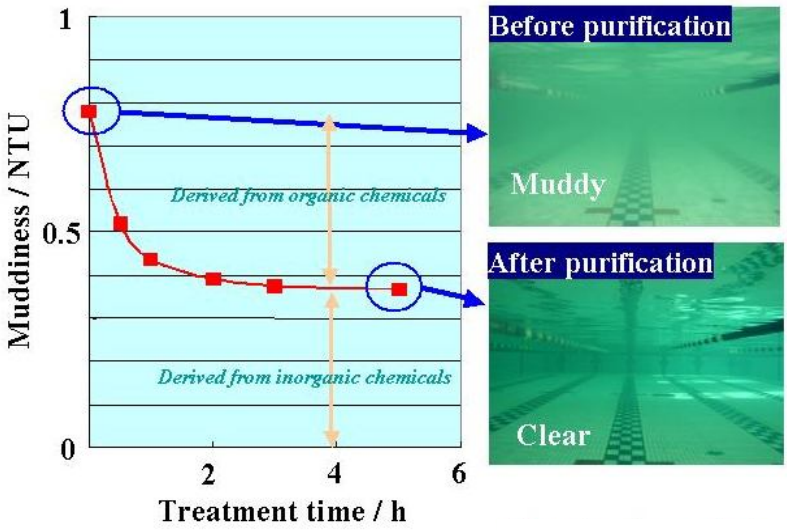

Fig. 8. Purification of the pool-water by the purifier using our photocatalytic fiber

In addition, many bacteria (common bacterium, legionera pneumophila and coliform), which existed in the initial bath water, were effectively decomposed into CO_2 and H_2O. The experimental data on the sterilization of legionera pneumophila is shown in Fig.9.

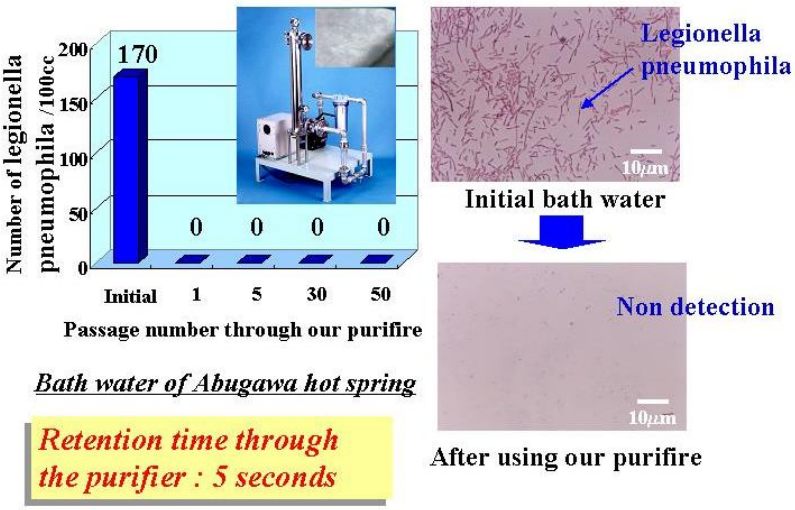

Fig. 9. Sterilization of legionera pneumophila by the purifier using our photocatalytic fiber

As shown in figure 9, the legionera pneumophila were perfectly decomposed by single passage through the water-purifier using our photocatalytic fiber. In this case, the retention time for the single passage through the purifier was only 5 s. Although this time may seem too short, it is sufficiently long compared with the lifetime of hydroxyl radical (10^{-6} s). Each oxidation reaction ought to proceed within the aforementioned lifetime of hydroxyl radical. Accordingly, the decomposition reaction can be accomplished like this, as long as the number of photons is sufficient during the passage.

The result on the decomposition of colon bacillus by our photocatalytic fiber irradiated by UV light is shown in Fig.10 along with the comparison data obtained by only UV irradiation.

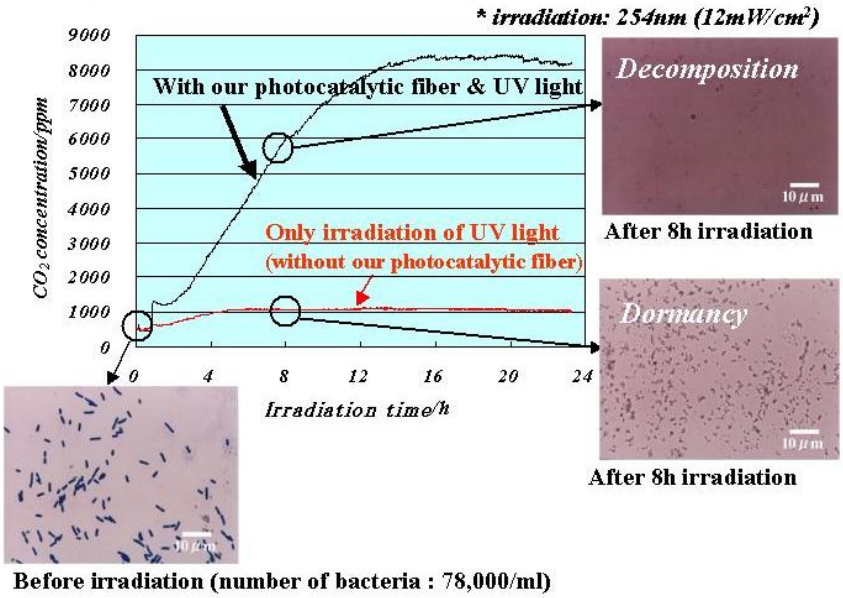

Fig. 10. Decomposition of colon bacillus using our photocatalytic fiber

As can be seen from this figure, use of our photocatalytic fiber led to effective decomposition of colon bacillus accompanied by the generation of carbon dioxide. On the other hand, irradiation of UV light alone resulted in the many dead bodies of colon bacillus with no apparent decomposition. A damaged colon bacillus is shown in Fig.11. Although almost all of colon bacillus was perfectly decomposed into carbon dioxide and water, some residual bacteria were also remarkably damaged. This type of decomposition reaction proceeds on the surface of the photocatalytic fiber when colon bacillus contacts each fiber irradiated by UV light.

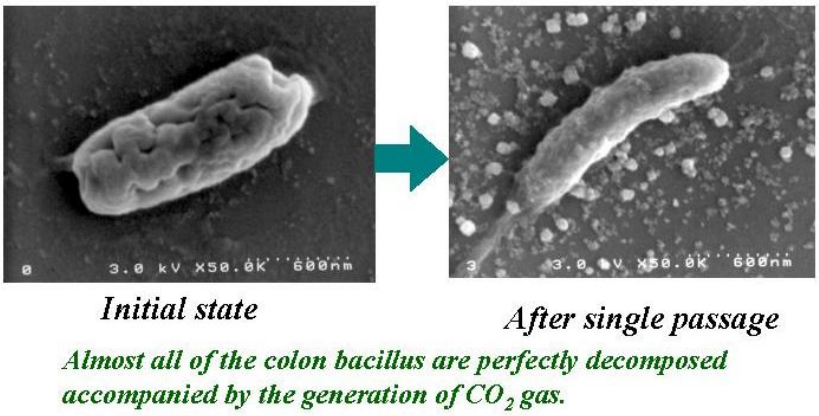

Fig. 11. Damaged colon bacillus after single passage through the purifier using our photocatalytic fiber

Fundamentally, this can be applied to purification system of any kind of organic chemicals. Figure 12 shows the result of the field test on decomposition of dioxin. Dioxin is one of many persistent organic pollutants (POPs). It has been recognized that the perfect decomposition of POPs is very difficult. However, the use of our photocatalytic water-purifier enables the oxidation of dioxin into carbon dioxide and water. This result is caused by the oxidation activity of hydroxyl radical generated on the surface of our photocatalytic fiber irradiated by the UV light.

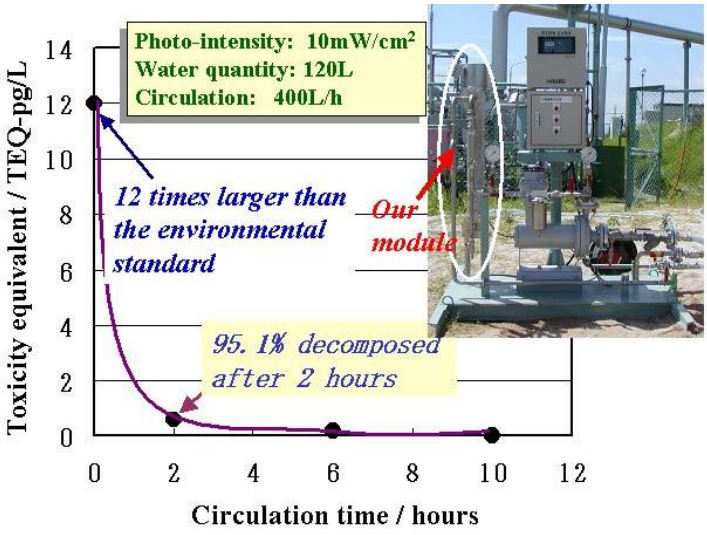

Fig. 12. The result of the field test on decomposition of dioxin

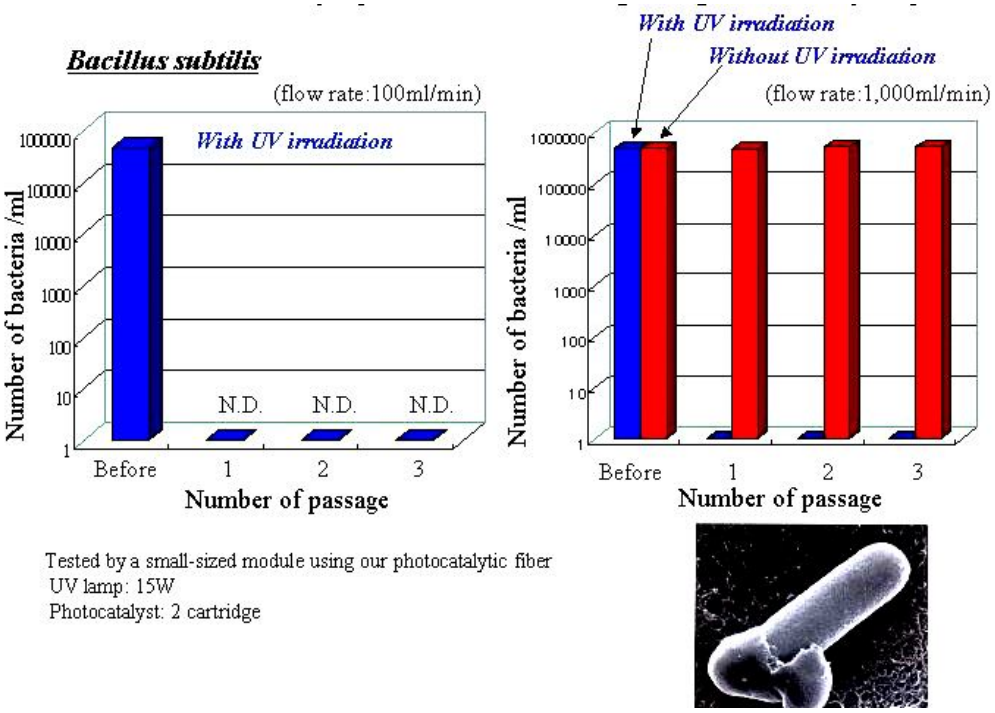

Fig. 13. The result of the purification test on bacillus subtilis

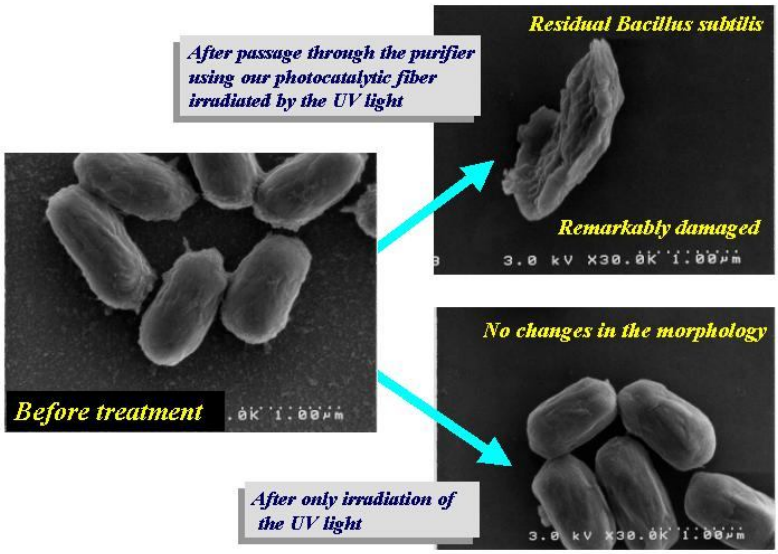

Fig. 14. Damaged hard shell of the bacillus subtilis by contact with our photocatalytic fiber

By the effective formation of the anatase-titania on the surface of each fiber, our photocatalytic fiber can show the excellent decomposition activity of any kind of organic chemicals. Figure 13 shows the result of a purification test of the water containing bacillus subtilis, which is covered with hard shell out of the body. Our purifier enabled to decompose the shell structure by only single passage. From the result obtained without UV irradiation, it is found that the decrease in the number of bacillus subtilis was not caused by filtration.

Figure 14 shows evidence that the hard shell of the bacillus subtilis was actually damaged by contacting our photocatalytic fiber irradiated by UV light.

It is well known that botulinus and anthrax are a variety of the aforementioned bacillus subtilis. And this type of bacteria hardly diminished by boiling water or chlorine. Accordingly, the water-purifier using our photocatalytic fiber is found to be very effective for avoidance of this type of hazard.

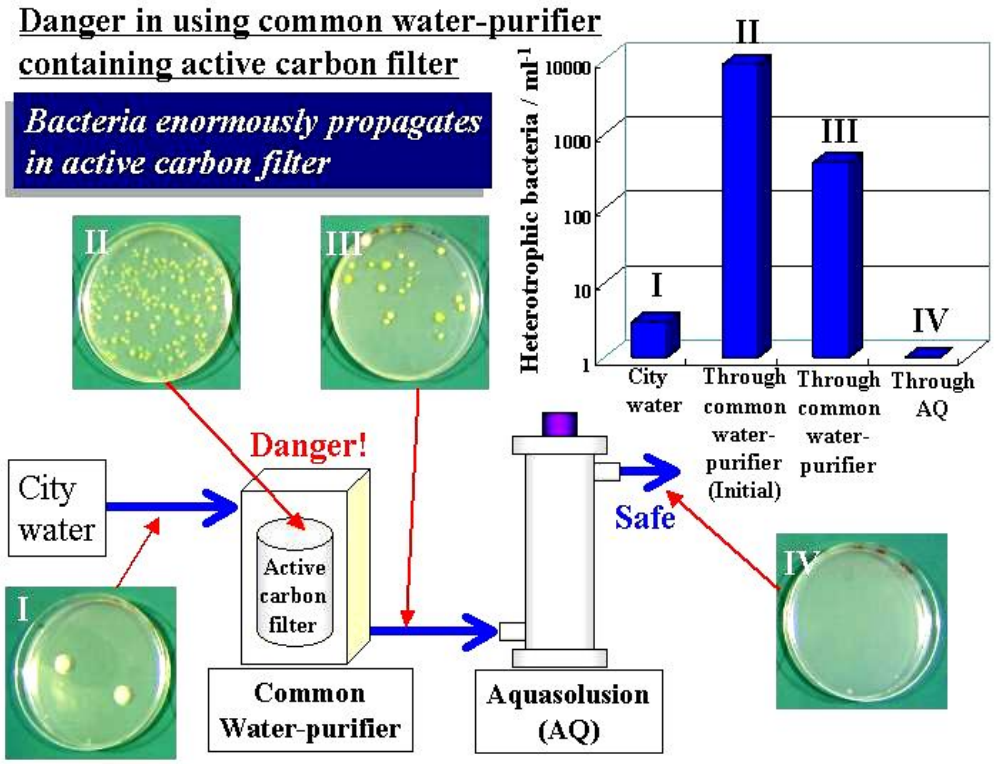

Fig. 15. Danger of the outlet water from the active carbon filter

Regarding drinking water, you are also endangered if you use common water-purifier containing some active carbon filter. In the active carbon filter, lots of bacteria can

propagate. We detected the number of heterotrophic bacteria in the outlet water from the active carbon filter (Fig.15). As can be seen from this result, there are found to be tremendous number of heterotrophic bacteria in the outlet water from the active carbon filter. This is very dangerous for people. Even such water could be perfectly purified by the use of our photocatalytic purifier (Aquasolution: AQ in Fig.15).

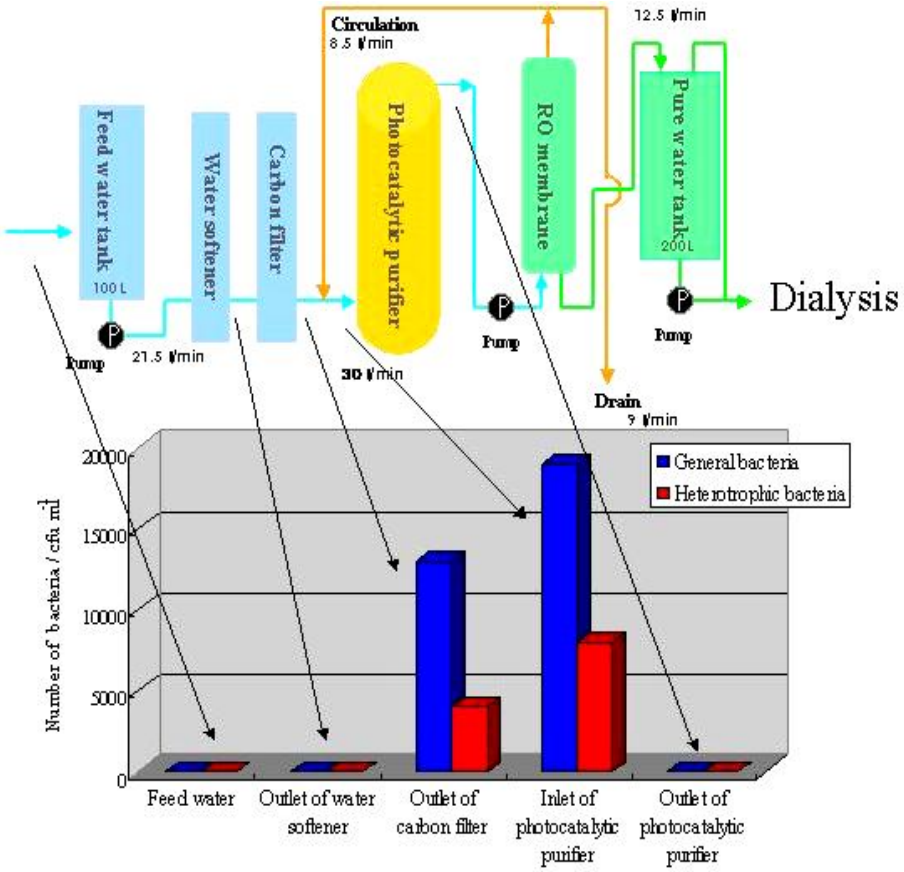

Fig. 16. Purification of the medical water using photocatalytic purifier

This dangerous phenomenon was also confirmed in the field of medical water. Figure 16 shows the changes in the number of bacteria in the purification system for preparing the water for dialysis. Active carbon filter is used in this system. In this case, a tremendous number of bacteria were detected in the outlet water from the active carbon filter. However, after a single passage through our photocatalytic purifier behind the active carbon filter, all of bacteria were decomposed.

As can be seen from the aforementioned information, we need to reconsider the use of active carbon filter, which is often believed to be a safe purification system. In fact,

active carbon filter should be recognized as a kind of breeding zone of bacteria. In order to avoid such dangerous situation, the photocatalytic purification system must be very effective.

Furthermore, we have also confirmed the effective purification of the water for rinsing mouth or tooth-grinder in the dental systems.

4. SUMMARY AND CONCLUSION

On the basis of a precursor method using a polycarbosilane, we developed a new *in situ* process for preparing functional ceramic fibers with a gradient surface layer. This process treated a polycarbosilane containing an excess amount of selected low-molecular-mass additives, which can be converted into functional ceramics by heat-treatment. Thermal treatment of the precursor fiber leads to controlled phase separation ("bleed out") of the low-molecular-mass additives from inside to outside of the fiber. After that, subsequent calcination generates a functional ceramic fiber with a gradient surface structure during the production of bulk ceramic components. As the embodied functional ceramic fiber, we developed a strong photocatalytic fiber composed of a surface gradient titania-crystalline layer and a silica-based core structure. This fiber showed an excellent photocatalytic activity, that is to say, the very high quantum efficiency (~40%) and a decomposition ability of organic chemicals and any kind of bacteria, and so forth, by irradiation of UV light. Very tough bacteria such as bacillus subtillis and anthrax, which are covered with hard shell and hardly decomposed by chlorine or boiled water, can be also effectively decomposed by our photocatalytic purifier. Our system has been successfully applied to purification of many types of water in wide fields.

REFERENCES

[1] S. YAJIMA, Y. HASEGAWA, K. OKAMURA, T. MATSUZAWA, *"Development of High Tensile Strength Silicon Carbide Fiber Using an Organosilicon Polymer Precursor",* Nature, 273, 525-527 (1978).

[2] M. TAKEDA, J. SAKAMOTO, A. SAEKI, Y. IMAI, and H. ICHIKAWA, *"High Performance Silicon Carbide Fiber Hi-Nicalon for Ceramic Matrix Composites"*, Ceram.Eng.Sci.Proc., 16[4], 37-44 (1995).

[3] T. ISHIKAWA, Y. KOHTOKU, K. KUMAGAWA, T. YAMAMURA & T. NAGASAWA, *"High-Strength Alkali-Resistant Sintered SiC Fibre Stable to 2200 ^{o}C",* Nature, 391, 773-775 (1998).

[4] J. LIPOWITZ, J. A. RABE, G. A. ZANK, A. ZANGVIL, Y. XU, *"Structure and Prooperties of Sylramic ^{TM} Silicon Carbide Fiber – A Polycrystalline, Stoichiometric SiC Composition"*, Ceram.Eng.Sci.Proc., 18[3], 147-157 (1997).

[5] T. ISHIKAWA, S. KAJII, K. MATSUNAGA, T. HOGAMI, Y. KOHTOKU & T. NAGASAWA, "*A Tough, Thermally Conductive Silicon Carbide Composite with High Strength up to 1600 ^{0}C in Air"*, Science, 282, 1295-1297 (1998).

[6] T. ISHIKAWA, H. YAMAOKA, Y. HARADA, T. FUJII, T. NAGASAWA, *"A general process for in situ formation of functional surface layers on ceramics"*, Nature, 416, 64-67 (2002).

[7] T. ISHIKAWA, Y. HARADA, H. HAYASHI, S. KAJII, *"Silica-Group Composite Oxide Fiber and Process for the Production"*, US Patent 6,541,416 B2 (Foreign Application Priority Date: June 13, 2000).

[8] I. SOPYAN, S. MURASAWA, K. HASHIMOTO, and A. FUJISHIMA, *"Highly Efficient TiO2 Film Photocatalyst, Degradation of Acetaldehyde",* Chemistry Letters (The Chemical Society of Japan), pp.723-726 (1994).

[9] T. ISHIKAWA, *"Ceramic Fiber with Decomposition Ability of Dioxine",* Miraizairyo, *3(2), 26-33 (2003).*

[10] H. KOIKE, Y. OKI, and Y. TAKEUCHI, Mater.Res.Soc.Sym.Proc., *549, 141 (1999).*

[11] A. MATSUDA, Y. KOTANI, T. KOGURE, M. TATSUMISAGO, T. MINAMI, *"Transparent Anatase Nanocomposite Films by the Sol-Gel Process at Low Temperatures"*, J.Am.Ceram.Soc., 83[1], 229-231 (2000).

[12] D. R. PARK, J. ZHANG, K. IKEUE, H. YAMASHITA, M. ANPO, *"Photocatalytic Oxidation of Ethylene to CO_2 and H_2O on Ultrafine TiO_2 Photocatalysts in the Presence of O_2 and H_2O",* J.Catal., 185, 114-119 (1999).

[13] T. ISHIKAWA, *"Photocatalytic Fiber with Gradient Surface Produced from a Polycarbosilane and its Applications"*, International Journal of Applied Ceramic Technology, 1[1], 49-55 (2004).

[14] T. ISHIKAWA, *"Advances in Inorganic Fibers",* Adv. Polym. Sci., 178, 109-144 (2005).

[15] N. TAKEDA, M. OHTANI, T. TORIMOTO, S. KUWABATA, H. YONEYAMA, *"Evaluation of Diffusibility of Adsorbed Propionaldehyde on Titanium Dioxide-Loaded Adsorbent Photocatalyst Films from Its Photocomposition Rate"*, J.Phys.Chem.B, 101, 2644-2649 (1997).

[16] C. K. CHAN, J. F. PORTER, Y. G. LI, W. GUO, C. M. CHAN, *"Effects of Calcination on the Microstructures and Photocatalytic Properties of Nanosized Titanium Dioxide Powders Prepared by Vapor Hydrolysis"*, J.Am.Ceram.Soc., 82[3], 566-572 (1999).

[17] H. KOIKE, Y. OKI, Y. TAKEUCHI, *"Preparing Titania fibers and their Photo-catalytic Activity"*, Mater.Res.soc.Sym.Proc., 549, 141-146 (1999).

[18] T. GUNJI, I. SOPYAN, Y. ABE, *"Synthesis of Polytitanosiloxanes and their Transformation to SiO_2-TiO_2 Ceramic Fibers"*, J.Polym.Sci., Part A Polym.Chem., 32, 3133-3139 (1991).

[19] T. ISHIKAWA, *"Photocatalytic Fiber with Gradient Surface Structure Produced from a Polycarbosilane and Its Application"*, Int.J.Appl.Chem.Technol., 1[1], 49-55 (2004).

[20] P. I. GOUMA, P. K. DUTTA, M. J. MILLS, *"Structural Stability of Titania Thin Films"*, Nano Structured Materials, 11(8), 1231-1237 (1999).

[21] C. ANDERSON, A. J. BARD, *"Improved Photocatalytic Activity and Characterization of Mixed TiO_2/SiO_2 and TiO_2/Al_2O_3"*, J.Phys.Chem.B, 101, 2611-2616 (1997).

Physicochem. Probl. Miner. Process. 45(2010) 73-84

journal homepage
www.minproc.pwr.wroc.pl/journal/

Physicochemical Problems of Mineral Processing

Index No. 32213X ISSN 1643-1049

Izumi KUMAKIRI *, Christian SIMON *, Krzysztof SZCZEPANOWICZ **, Dawid WODKA **, Paweł NOWAK **, Lilianna SZYK-WARSZYŃSKA **, Piotr WARSZYŃSKI **

REMOVAL OF NATURAL ORGANIC MATTER FROM POTABLE WATER USING PHOTO-CATALYTIC MEMBRANE REACTOR

Received April 29, 2010; reviewed; accepted May 31, 2010

The application of photo-catalysis combined with membrane filtration for the oxidation of humic acid substances (HA) which is one of the major natural organic matters (NOMs) is discussed in this paper. Theoretical model shows a potential advantage of photo-catalytic filtration under low flux conditions. Cross-flow filtration is applied for HA removal using a TiO_2 membrane under UV conditions. An increase of the flux through the membrane was observed by applying UV light.

keywords: Natural organic matter (NOM), humic acid, membrane filtration, photocatalyst, potable water

1. INTRODUCTION

Natural organic matter (NOM) is a major cause of colour and odour in potable water. Moreover, the combination of NOM and chlorine, a common additive in potable water, has been pointed out to be a source of possible formation of carcinogens [1,2].

* SINTEF, P.O. Box 124 Blindern, N-0314 Oslo, Norway
** Polish Academy of Sciences, Institute of Catalysis and Surface Chemistry, Krakow, Poland
Corresponding author: Izumi.kumakiri@sintef.no

While more than 90% of NOM can be removed by membrane filtration or by coagulation, removing small concentrations of NOM, especially small to medium size, with reasonable cost and efficiency is a challenging task.

Photo-catalytic oxidation has a potential as a process to remove small to medium sized NOM. Table 1 shows examples of photo-catalytic oxidation of humic acid (HA), which is one of the major components of surface water and often represented as NOM.

Table 1. HA decomposition by photo-catalysis

Feed	HA conc. (mg/L)	TiO_2 conc. (g/L)	pH	Degradation rate constant (10^{-2} min^{-1})	$t_{1/2}$ (min)	ref.
HA from river	50	0.25	6.5 ± 0.5	0.83	84	[3]
HA salt from Aldrich	50	0.25	6.5 ± 0.5	1.60	43	[3]
HA (Aldrich) in sea water with air flow	40	1	4.5	2.6		[4]
HA (Aldrich) in sea water with oxygen flow	40	1	4.5	4.1		[4]

Photo-catalysts are often applied in powder form dispersed in water [5,6]. In such a case an extra task to separate the photo-catalyst from the treated water is required. Powdered catalyst may not be preferred in the application of potable water treatment, as remaining photo-catalysts can be a health concern.

Photo-catalysts immobilized on/in substrates offer an alternative to powders. Various materials, such as polymers, inorganic materials, are used as supports [7,8]. The configuration of immobilized photo-catalytic system can be classified into either flow-over reactors [9–11] or flow-through (filtration) reactors [12] as show in Figure 1. A higher photo-catalytic surface area per volume of the reactor combined with sufficient light supply to the catalysts will reduce the module size in both cases.

Flow-through reactor is a configuration where NOM removal can be achieved not only by the photo-oxidation properties but also by the sieving properties of the photo-catalytic substrates. Fouling is reported as one of the major difficulties in membrane filtration with NOM containing solutions [13]. The application of photo-catalytic oxidation may clean the membrane surface and avoid fouling during the filtration. Photo-catalytic oxidation may be enhanced by additional chemicals in some cases [14]. Membrane contactor has been an alternative configuration that opens for an efficient addition of helping agents to the reaction field [15].

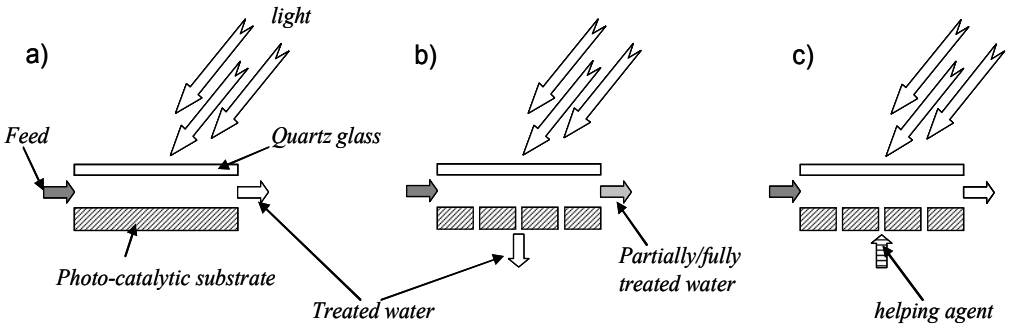

Fig. 1. Various photo-catalytic reactor configurations:

a) Flow-over reactor: water flows over a photo-catalytic substrate and organics in the water are oxidized during the contact with the substrate
b) Membrane filtration combined with photo-catalysis: The photo-catalytic substrate is porous and water permeates through it due to overpressure on the feed side. Organics in water are oxidized not only by flowing over the photo-catalytic substrate but also by permeating through it. Organics are also removed by the sieving property of the substrate. The concentration of organics in the retentate may decrease depending on the operating conditions.
c) Membrane contactor combined with photo-catalysis: Water flows over the photo-catalytic substrate. Helping agents, such as oxidants, can be supplied from the other side of the membrane.

In this study, application of a photo-catalytic membrane filtration to HA removal is studied. The operating conditions for a possible removal of HA are estimated based on theoretical models. Cross flow filtration with TiO_2 membrane is performed under UV to remove HA.

1.1..Models

1.1.1 Membrane filtration

Kedem-Katchalsky described the membrane transport as follows [16]:

$$J_v = L_P(\Delta P - o \cdot \Delta\pi)$$

$$J_S = P(C_2 - C_3) + (1-\sigma)C_a J_V$$

In the case of pure water permeation, the equation above is simplified to:

$$J_v = L_P \Delta P$$

In this model, the membrane performance is represented by three parameters: L_p, o

and P. These parameters are independent on the operating conditions, while flux through the membrane and the ability to remove the solute from the solution changes with e.g. an increasing pressure at the feed side.

The pore model relates the membrane morphology to the permeation and the separation properties of the membrane [17]. Cylindrical pores and spherical molecules are assumed in this model:

$$L_P = (r_P^2 / 8\mu)(\mathrm{A}_k / \Delta x)$$

$$o = 1 - S_F \left\{1 + (16 + 9)q^2\right\}$$

$$P = D \cdot S_D (\mathrm{A}_k / \Delta x)$$

where,

$$q = \frac{r_s}{r_p}$$

$$S_F = (1-q)^2 \left\{2 - (1-q)^2\right\}$$

$$S_D = (1-q)^2$$

If solute is either partially or fully rejected during membrane filtration, the concentration of the solute at the membrane surface becomes higher than its concentration in the bulk at the feed side. This phenomenon is called concentration polarization.

Concentration polarization can be estimated by taking the material balance in the boundary layer [18]:

$$J_v C - D \frac{dC}{dx} = J_v C_3$$

Under the boundary conditions (x =0: C =C_b, x =δ; C =C_m), the equation above becomes:

$$\frac{C_2 - C_3}{C_1 - C_3} = \exp \frac{J_v}{k}$$

The mass transfer coefficient, k, in the boundary layer can be estimated from the flow conditions:

$$S_h \equiv \frac{dk}{D}$$

Sherwood number (Sh) is described as follows in case of a turbulent flow [19]:

$$S_h = 0.023 R_e^{0.875} S_c^{0.25}$$

where;

$$R_e \equiv \frac{\rho d u}{\mu} \text{ and } S_c \equiv \frac{\mu}{\rho D}$$

For typical operating conditions such as 4000<Re<10000, the mass transfer coefficient will vary in the range of 2 to 5 (10^{-6} m s^{-1}). In this study, k value is estimated to be 3.5 (10^{-6} m s^{-1}).

The size of HA (r_s) is assumed to be 5.4 nm by using the diffusivity value reported [20] and by applying the Stokes equation: $r_s = \frac{\kappa T}{6\pi\mu D}$. Note that the size distribution of HA is not taken into account in this study.

Target application is potable water treatment, which solution contains very low HA concentration, such as <1 mg/l. The Van't Hoff equation is applied to estimate the osmotic pressure in the estimation.

1.1.2. Photo-catalytic oxidation combined with membrane filtration

The following assumptions are made to examine the possible operating conditions for photo-catalytic membrane filtration:

- The membrane has sieving abilities at the surface
- Oxidation of non-sieved organics occurs during the permeation through the photo-catalytic layer
- The photo-catalytic layer has cylindrical pores with thickness of 10μm where light source can penetrate through and photo-catalysis does not affect the water permeation through the membrane

Photo-catalysis is often described by the first order equation: $\ln \frac{C_t}{C_0} = -Kt$. Contact time, t, is estimated as a function of the inverse of flux through the membrane: $t = \frac{A_k \cdot \Delta x}{J_V}$.

2. EXPERIMENTAL

Photo-catalytic membranes were prepared by depositing commercial photo-catalysts

(ST-01, Ishihara Sangyo LTD) on porous α-alumina disks (Keranor Ø 38 mm). 25 µg/l of sodium HA salt (Sigma Aldrich) was used as feed solution. Three black light lamps (8W, main wave length: 350nm) were combined and used as light source. All the experiments were performed at room temperature. Concentration change of HA solutions during the treatment was measured by UV-vis analysis (Shimadzu, UV-1800).

Membrane filtration tests were performed under cross-flow filtration conditions with a flow rate of 1 l/min. Both pure water flux and HA solution flux through the membrane were measured. The measurements were performed at increasing pressure. After reaching the maximum pressure, the pressure was reduced to the minimum value. The flux was measured several times to confirm the steady state.

3. RESULTS AND DISCUSSION

3.1. Membrane filtration combined with photo-catalysis

Figure 2 shows the maximum possible removal of HA with a variety of ratios between the membrane pore size and HA size. The estimated pore size based on the average HA size is also included in the figure. When the membrane pore size is smaller than the size of HA, HA will not permeate through the membrane and a 100% removal

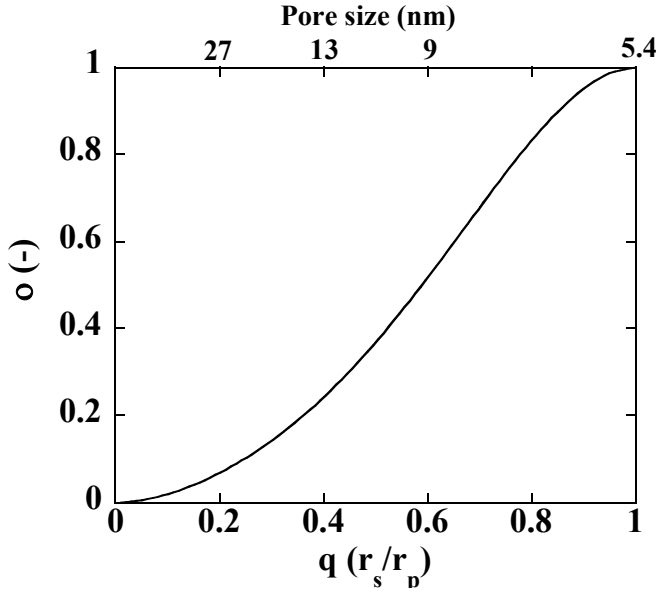

Fig. 2. Potential of HA removal as a function of the membrane pore size

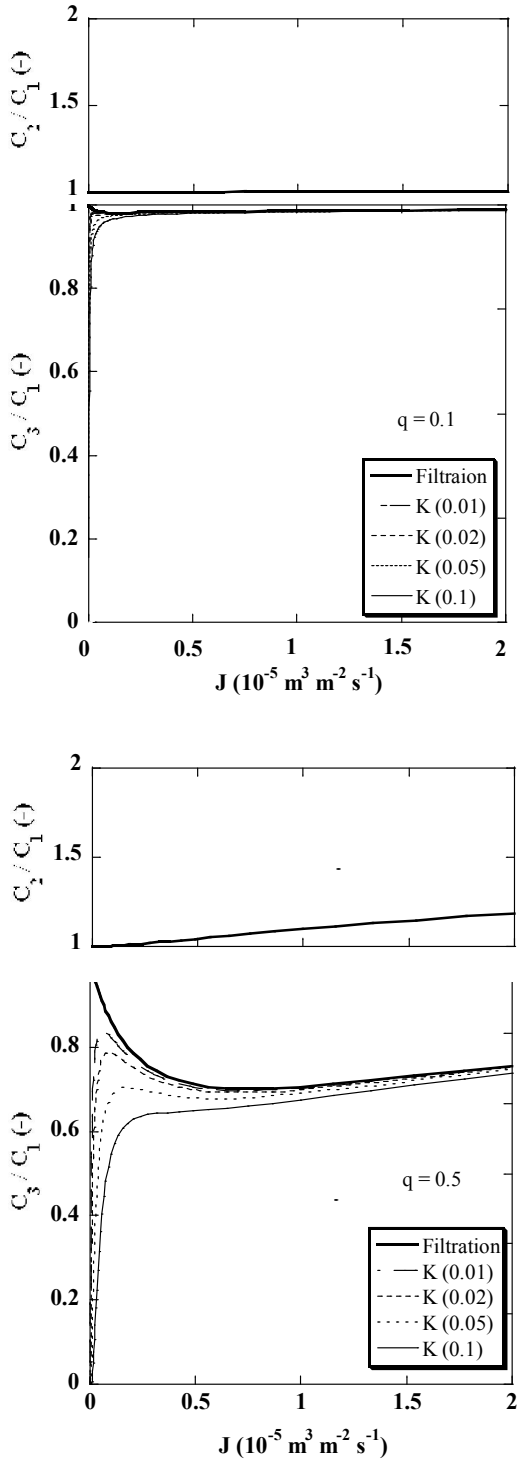

(o = 1 in the figure) will be achieved. On the contrary, the degree of removal will depend on the pore size of the membrane with pore size larger than the size of HA. For example, 50% of HA can potentially be removed with a membrane having pores 170% larger than the size of HA.

Oxidation of HA during the permeation through membrane is one potential application of photo-catalysis combined filtration. Figure 3 illustrates the HA concentration decrease after passing through the membrane. The change is shown as the ratio of concentration in the permeate solution (C_3) and in the feed solution (C_1). Both conventional membrane filtration and photo-catalysis combined filtration with various kinetic constants are illustrated in Figure 3. Kinetic constants are varied from k= 0.01 to 0.1, are of similar order as the value for HA oxidation reported in Table 1. Figure shows membranes with three different pore sizes.

HA concentration in the permeated solution is high under low flux through membrane and becomes lower when increasing the flux that will be achieved by applying higher pressure. This tendency is observed as the contribution of permeation by diffusion becomes smaller with increasing volume fluxes, as

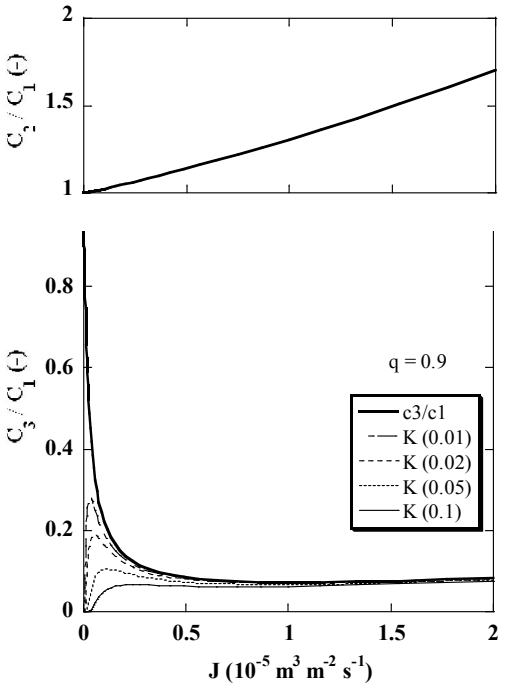

Fig. 3. HA concentration as a function of flux through membrane

results from the Kedem-Katchalsky equation. The concentration polarization (C_2/C_1) becomes higher with increasing flux and with increasing sieving property. When about 90% of the HA is removed by filtration (C_3/C_1<0.1), the concentration of HA at the membrane surface can be more than 1.5 times higher than the concentration in the bulk feed. An increase of the HA concentration may enhance the adsorption of HA onto the membrane and might cause a permeation resistance layer. The combination of photo-catalysis with membrane filtration can reduce the HA concentration in the permeated solution.The contribution of photo-catalytic oxidation varies with the operating conditions and the membrane pore size. This contribution becomes significant at low membrane fluxes, hence when the contact time between HA and photo-catalyst is long at low flux conditions. With kinetic constant K>0.05, the photo-catalytic filtration can prevent the increase of HA concentration in the feed due to the contribution of the diffusion. Low flux condition requires low pressure at the feed side that can reduce housing and operation costs. Photo-catalytic membrane filtration may be an alternative for small scale treatment.

On the contrary, the influence of photo-oxidation is almost negligible at high fluxes, e.g.> $1x10^{-5}$ $m^3/m^2/s$ (>0.9 $m^3/m^2/day$). Under such conditions, the HA removal is mainly determined by the membrane pore size.

Even though the kinetic constant is 5 to 10 times faster than assumed, it is not enough to treat large volume flux solution.

Another potential advantage of combining photo-catalysis and membrane filtration is the self-cleaning ability of the membrane surface during filtration [21]. Figure 4 shows HA removal property and flux as a function of the overpressure between the feed side and the permeate side. The flux in HA filtration at 0.2 bar overpressure was almost the

same as pure water flux, suggesting that fouling is negligible under these conditions. Flux in HA filtration becomes smaller than in the case of pure water flux at overpressures higher than 0.4 bar. The decrease suggests a formation of a permeation resistance layer. After reaching the maximum pressure, the differential pressure was reduced back to 0.2 bar. The flux was smaller compared to the starting value as shown with closed keys in the figure. The flux measured by reducing the pressure shows a linear change with the pressure difference, suggesting a stable permeation resistance. Fouling caused by HA seems irreversible. The membrane surface after filtration was red due to the adsorbed HA, which was difficult to remove by standard washing with water. Although, the feed contains very dilute HA and operation conditions were in low flux conditions, HA fouling is much stronger than the ability to oxidise HA by photo-catalysis under black lamps. Stronger light sources may improve the self-cleaning and reduce the fouling effect but it may increase the operation cost.

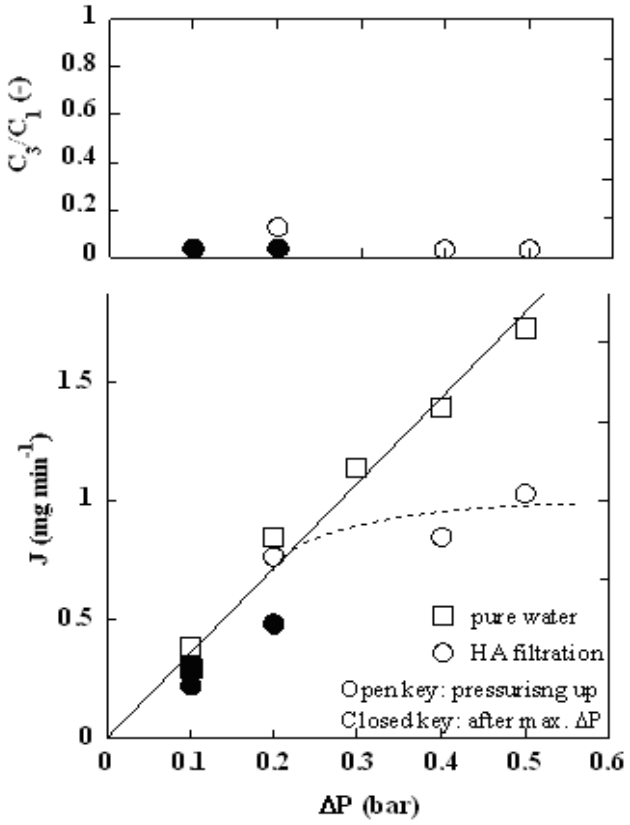

Fig. 4. HA cross-flow filtration under UV light

The photo-catalyst had some influence on the flux. Figure 5 shows the change of flux through the membrane under a stable operating pressure. The flux increased to about 120% almost instantly after applying UV light on the membrane surface. The increase in flux may be due to a change of the surface properties, such as becoming more hydrophilic. The flux did not change in dark after UV radiation for about 30 min.

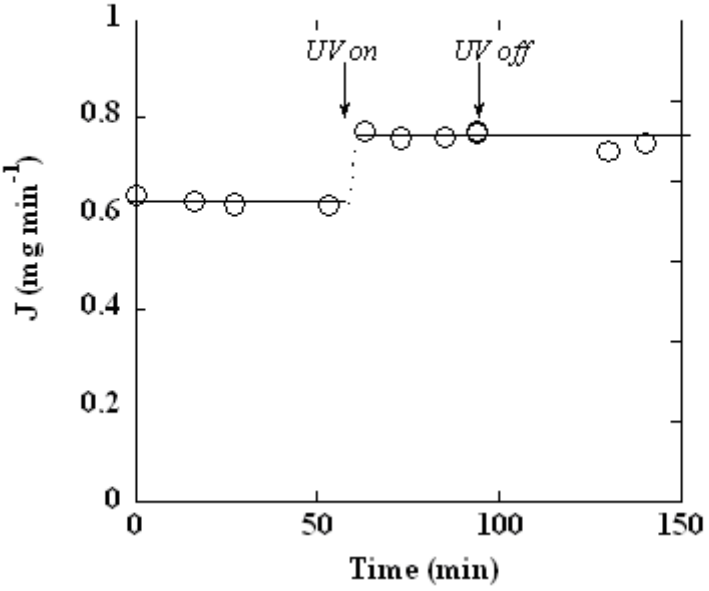

Fig. 5. Flux through the membrane in dark conditions and under UV light exposure (the pressure difference across the membrane (ΔP) was maintained at 0.2 bar)

4. CONCLUSION

Combining photo-catalysis with membrane filtration has a potential to improve the HA removal rate under low flux (low pressure) conditions such as $< 0.2 \times 10^{-5}$ m^3 m^{-2} s^{-1}. Photo-catalysis has not significant influence on the HA removal with membranes having a flux larger than 1×10^{-5} m^3 m^{-2} s^{-1}. Photo-catalytic oxidation needs to be improved to eliminate fouling caused by HA during filtration. Photo-catalytic surface increases the flux through the membrane by applying UV light.

ACKNOWLEDGEMENT

The authors acknowledge the EEA grant (PL0084) for the financial support through NOMRemove project.

REFERENCES

[1] GERECKE AC, S. D. Environmental Science & Technology **2003**, *37*, 1331.
[2] LEIKNES T, O. H., Myklebust H. Journal of Membrane Science **2004**, *242*, 47.
[3] UYGUNER CS, B. M. Desalination **2005**, *176*.
[4] AL-RASHEED R, C. D. Chemosphere **2003**, *51*, 925.
[5] CHEN DW, R. A. Water Research **1998**, *32*, 3223.
[6] ABELLAN MN, D. R., GIMENEZ J, et al. Journal of Photochemistry and Photobiology A-Chemistry **2009**, *202*, 164.
[7] BIDEAU M, C. B., DUBIEN C, et al. Journal of Photochemistry and Photobiology A-Chemistry **1995**, *91*, 137.
[8] ZHANG YL, W. S., ZHANG HY, et al. Journal of Colloid and Interface Science **2009**, *339*, 434.
[9] REN M, V. K. Separation and Purification Technology **2008**, *62*, 523.
[10] LIN HF, V. K. Journal of Applied Electrochemistry **2005**, *35*, 699.
[11] MATSUNAGA T, Y. H., Ohtani S, et al. Applied Catalysis A-General *351*, 231.
[12] TSURU T, K.-N. T., YOSHIOKA T, et al. Catalysis Today **2003**, *82*, 41.
[13] LEE NH, A. G., CROUE JP, et al. Water Research **2004**, *38*, 4511.
[14] JUNG JT, K. J., CHOI JY. Research on Chemical Intermediates **2009**, *35*, 243.
[15] BREDESEN R., et atl. WO02074701 **2001**
[16] NAKAO S.-I-, KIMURA S., J.Chem.Eng.Japan, **1982**, 15, 200
[17] TANIMURA S, N. S., KIMURA S Journal of Chemical Engineering of Japan **1991**, *24*, 364.
[18] KIMURA, S. S. SOURIRAJAN AIChEJ **1967**, *13*, 497.
[19] KIMURA S., NAKAO S.-I., 37, kitami, Japan, **1985**
[20] WANG YG, C. C., CLARK MM. Journal of Membrane Science **2001**, *183*, 49.
[21] TURU M, et al., JP 2006-326530 **2006**

NOMENCLATURE

J_v [$m^3\ m^{-2}\cdot s^{-1}$]: Volume flux through the membrane
J_s [$mol\ m^{-2}\cdot s^{-1}$]: solute flux through membrane
ΔP [Pa]: Pressure difference across the membrane
$\Delta\pi$ [Pa]: Osmotic pressure difference across the membrane
C_a [$mol\ m^{-3}$]: Average solution concentration

C_1 [mol m^{-3}]: Solution concentration in the feed
C_2 [mol m^{-3}]: Solution concentration over the membrane at feed side
C_3 [mol m^{-3}]: Solution concentration in the permeate
L_p [$m \cdot s^{-1} \cdot Pa^{-1}$]: Pure water permeability
o [-]: Reflection coefficient
P [$m \cdot s^{-1}$]: Solute permeability
r_p [m]: Pore size of the membrane
r_s [m]: Solute size
A_k [-]: Pore opening ratio
Δx [m]: Thickness of the membrane
μ [Ps s]: Viscosity of water
ρ [kg m^{-3}]: Density of water
k [m s^{-1}]: Mass transfer coefficient
Re [-]: Reynolds number
Sc [-]: Schmidt number
Sh [-]: Sherwood Number
D [$m^2 \cdot s^{-1}$]: Diffusion coefficient
K [s^{-1}]: Rate constant
t [s]: Contact time

Physicochem. Probl. Miner. Process. 45(2010) 85-98

journal homepage
www.minproc.pwr.wroc.pl/journal/

Physicochemical Problems of Mineral Processing

Index No. 32213X ISSN 1643-1049

Krzysztof SZCZEPANOWICZ *, Joanna STEFAŃSKA **, Robert P. SOCHA *, Piotr WARSZYŃSKI *

PREPARATION OF SILVER NANOPARTICLES VIA CHEMICAL REDUCTION AND THEIR ANTIMICROBIAL ACTIVITY

Received April 23, 2010; reviewed; accepted May 18, 2010

A simple and economic method of synthesis of silver colloid nanoparticles with controlled size is presented. By reduction of $[Ag(NH_3)_2]^+$ complex in sodium dodecylsulfate (SDS) micellar solution with three various reducing agents (hydrazine, formalin and ascorbic acid) the nanoparticles were produced with size below 20 nm. The average size, size distribution, morphology, and structure of particles were determined by dynamic light scattering (DLS), scanning electron microscopy (SEM), and UV/Visible absorption spectrophotometry. The influence of the reducing agent on the size of silver particles, fraction of metallic silver and their antimicrobial properties is discussed. In particular, the reduction of silver complex by hydrazine resulted in silver nanoparticles with size below 20nm. They showed high activity against Gram-positive and Gram-negative bacteria (lab isolated strains), and clinical isolated strains including highly multiresistant strains such as Staphylococcus epidermidis, Staphylococcus aureus and Pseudomonas aeruginosa.

keywords: silver, nanoparticles, antimicrobial properties, MIC.

1. INTRODUCTION

Development of new, effective and low cost antimicrobial agents has been an object

* Institute of Catalysis and Surface Chemistry PAS, st. Niezapomianjek 8, 30-239 Kraków, Poland, ncszczep@cyf-kr.edu.pl (K. Sczepanowicz)

** Medical University of Warsaw, Department of Pharmaceutical Microbiology, st. Oczki 3, 02-007 Warsaw, Poland

of research activity of many groups due to build-up of resistance of microbial organisms to traditional antibiotics. It is well known that silver-based compounds are highly toxic to microorganisms. Silver (Ag) has been known for its antibacterial activity since the times of ancient Greece (Silver et al., 1996). It is currently used to control bacterial growth in a variety of applications, including dental work, catheters, and burn wounds (Crabtree, et al., 2003, Catauro, et al., 2004). Recently, silver nanoparticles (Sondi, et al., 2004, Morones, et al., 2005, Baker, et al., 2005). as well as various silver-based compounds containing ionic silver (Butkus, et al. 2003, Chen, et al., 2005) exhibiting antimicrobial activity, have been synthesized. Silver-containing materials and coatings with antimicrobial activity can be used: in medicine to reduce infections in hospitals, in burn treatment, as well as to prevent bacteria colonization on prostheses, catheters, vascular grafts, dental materials, stainless steel materials (Bosetti, et al., 2002, Gauger, et al., 2003, Gosheger, et al., 2004, Rupp, et all., 2004, Strathmann, et al., 2004, Ohashi, et al., 2004, Ulkur, et al., 2005, Parikh, et al., 2005,). Fibers containing silver nanoparticles can be used to eliminate microorganisms on textile fabrics (Yuranova, et al., 2003, Jeong, et al., 2005) . Silver nanoparticles also exhibit a potent cytoprotective activity toward HIV infected cells (Sun, et al., 2005). Reducing the particle size of materials is an efficient tool for improving their bioactivity. Therefore, it is a role of nanotechnology to help overcoming the limitations in the size of efficient particles, which can contribute to the positive change in the public awareness regarding that science in general (Mirkin, et al., 2000). Numerous methods of preparation silver nanoparticles have been developed (Matijevic, 1993, Gutierrez , et al., 1993, Nickel, et al., 2000, Leopold, et al., 2003, Khanna, et al., 2003, Sondi, et al., 2003). The most widespread method of synthesis of silver nanoparticles is based on the chemical reduction of a silver salt solution by a reducing agent. In polysaccharide method, Ag nanoparticles are prepared using water as an environmentally benign solvent and polysaccharides as a capping agent, or in some cases, as both a reducing and a capping agent (Raveendran, et al., 2003). In Tollens method, a synthesis using a Tollens process was used to form silver particles with controlled size in a one-step process. The basic reaction in this process involves the reduction of a silver ammoniacal solution using saccharides (Yin, et al., 2002, Saito, et al., 2003). In that way films with colloidal silver particles ranging from 50 to 200 nm, or silver hydrosols with particles in the order of 20-50 nm, were obtained. Ag nanoparticles can be successfully synthesized by irradiation. For example, laser irradiation (Nd3+-YAG 500nm) of an aqueous solution of Ag salt and surfactant can fabricate Ag NPs with a well-defined shape and size distribution (Abid, et al., 2002). No chemical reducing agent is required in this method. Silver nanoparticles can be also formed by biological method, i.e., extracts from bio-organisms may act both as reducing and capping agents. Reduction of Ag^+ ions was done by combinations of biomolecules found in these extracts such as enzymes/proteins, amino acids,

polysaccharides, and vitamins (Shankar, et al., 2002, Gardea-Torresdey , et al., 2003, Jagadeesh, et al., 2004, Collera-Zuniga, et al. 2005, Shankar , et al., 2005, Richardson , et al., 2006, Li, et al., 2007, Vigneshwaran, et al., 2007, Xie, et al., 2007, Wu, et al., 2008, Sharma, et al., 2009).

The aim of our work was to develop simple and effective method of synthesis of silver nanoparticles with well-defined size and to verify their antimicrobial activity on the series of Gram-positive and Gram-negative bacteria (standard strains and clinical isolated strains including highly multiresistant strains such as *Staphylococcus epidermidis*, *Staphylococcus aureus* and *Pseudomonas aeruginosa*). Our work was concentrated on the chemical reduction method and the effect of reducing agents, hydrazine monohydrate, formalin and ascorbic acid, on the size and antimicrobial activity.

2. MATERIALS AND METHODS

2.1. Materials

Silver nitrate (pure p.a.), ammonia (25% w/w aqueous solution pure p.a.), ascorbic acid -AAC (pure p.a.) and formalin -F (36-38% pure p.a.) were purchased from POCH Gliwice Poland. Sodium dodecyl sulfate –SDS (>90%) and hydrazine monohydrate –H (purum, ≥98.0%) were purchased from Sigma-Aldrich. All materials were used without further purification. Distilled water used in all experiments was obtained with the three-stage Millipore Direct-Q 3UV purification system.

Table 1. The components of Ag $3d_{5/2}$ core excitation for the studied systems.

System	Component A		Component B	
	BE (eV)	Ratio (%)	BE (eV)	Ratio (%)
Ag/formalin	368.2	81.1	369.3	18.9
Ag/hydrazine monohydrate	368.2	90.2	369.8	9.8
Ag/ascorbic acid	368.0	78.0	369.3	22.0

Microorganisms used in this study were as follows: Gram-positive bacteria: *Staphylococcus aureus* ATCC 4163, *Staphylococcus aureus* ATCC 25923, *Staphylococcus aureus* ATCC 29213, *Staphylococcus aureus* ATCC 6538, *Staphylococcus epidermidis* ATCC 12228, *Bacillus subtilis* ATCC 6633, *Bacillus cereus* ATCC 11778, *Enterococcus hirae* ATCC 10541, *Micrococcus luteus* ATCC 9341, *Micrococcus luteus* ATCC 10240 and clinical isolates of *Staphylococcus epidermidis* and *Staphylococcus aureus* (MSSA and MRSA strains), Gram-negative rods: *Escherichia coli* ATCC 10538, *Escherichia coli* ATCC 25922, *Escherichia coli*

NCTC 8196, *Proteus vulgaris* NCTC 4635, *Pseudomonas aeruginosa* ATCC 15442, *Pseudomonas aeruginosa* NCTC 6749, *Pseudomonas aeruginosa* ATCC 27853, *Bordetella bronchiseptica* ATCC 4617 and hospital isolates of *Staphylococcus epidermidis*, *Staphylococcus aureus*, *Pseudomonas aeruginosa* and *Escherichia coli*. Bacterial strains were obtained from the collection of the Department of Pharmaceutical Microbiology, Medical University of Warsaw, Poland.

Table 2. Antimicrobial activity of Ag nanoparticles suspensions and antibacterial drug - ciprofloxacin against standard bacterial strains: Minimal Inhibitory Concenteration (MIC). μg/ml)

Compound / Strain	H	F	Ciprofloxacin
***Staphylococcus aureus* ATCC 4163**	**20**	**80**	**0,5**
***Staphylococcus aureus* ATCC 25923**	**20**	**80**	**0,5**
***Staphylococcus aureus* ATCC 6538**	**20**	**80**	**0,5**
***Staphylococcus aureus* ATCC 29213**	**20**	**80**	**0,5**
***Staphylococcus epidermidis* ATCC 12228**	**10**	**40**	**0,5**
***Bacillus subtilis* ATCC 6633**	**20**	**80**	**<0,125**
***Bacillus cereus* ATCC 11778**	**20**	**80**	**1**
***Enterococcus hirae* ATCC 10541**	**80**	**80**	**4**
***Micrococcus luteus* ATCC 9341**	**5**	**40**	**2**
***Micrococcus luteus* ATCC 10240**	**5**	**40**	**1**
***Escherichia coli* ATCC 10538**	**10**	**40**	**<0125**
***Escherichia coli* ATCC 25922**	**10**	**40**	**<0,125**
***Escherichia coli* NCTC 8196**	**10**	**40**	**<0,125**
***Proteus vulgaris* NCTC 4635**	**10**	**40**	**<0,125**
***Pseudomonas aeruginosa* ATCC 15442**	**10**	**40**	**0,5**
***Pseudomonas aeruginosa* NCTC 6749**	**10**	**40**	**0,5**
***Pseudomonas aeruginosa* ATCC 27853**	**10**	**40**	**1**
***Bordetella bronchiseptica* ATCC 4617**	**10**	**40**	**1**

2.2. Synthesis of silver nanoparticles.

Colloidal silver particles were synthesized by the reduction of $[Ag(NH_3)_2]^+$ complex with hydrazine monohydrate, formalin and ascorbic acid in micellar solution of sodium dodecyl sulfate - SDS. The initial concentrations of the reaction components were 10^{-2} mol/L for $AgNO_3$ and 0.1 mol/L for SDS. SDS used in our experiments was of technical grade (90%), so the ammonia was added to obtain clear and transparent solution of $[Ag(NH_3)_2]^+$, to prevent AgCl precipitation. Reducing agent (hydrazine monohydrate, formaline, ascorbic acid) was added to the reaction system in one step during stirring at 200 rpm, in ratio 1:1 (without excess of reducer). Reduction was

initiated in several minutes after addition of the reducing agent. Reactions were performed at room temperature (20-25 °C).

2.3. Characterization of silver nanoparticles

Size (hydrodynamic diameter) of silver nanoparticles was determined by DLS (Dynamic Light Scattering) using Zetasizer Nano Series from Malvern Instruments with the detection angle of 173^{o} in optically homogeneous square polystyrene cells. All measurements were performed at 25^{o}C. Each value was obtained as average from three runs with at least 10 measurements. The zeta potential of silver nanoparticles was measured by the microelectrophoretic method using Malvern Zetasizer Nano ZS apparatus. Each value was obtained as an average from three subsequent runs of the instrument with at least 20 measurements. Microscopic SEM (scanning electron microscope) observations of silver nanoparticles were performed with a JEOL JSM-7500F, Field Emission Scanning Electron Microscope. UV/VIS absorption spectra of the silver colloids were acquired by using Analytik Jena AG - SPECORD® 40 spectrophotometer. The chemical composition of the particles was determined by X-ray Photoelectron Spectroscopy (XPS). Prior to analysis, the drop of suspension containing particle was deposited on the pure Au foil surface, dried at room temperature in low vacuum then transferred to the analysis chamber. The measurements were performed in the ultrahigh vacuum ($3 \cdot 10^{-10}$ mbar) system equipped with hemispherical analyzer (SES R 4000, Gammadata Scienta).

Table 3. Antimicrobial activity of Ag nanoparticles suspension H against clinical strains of *taphylococcus epidermidis* and *Staphylococcus aureus* (MRSA – methicillin-resistant, MSSA – methicillin-susceptible): Minimal Inhibitory Concentration (MIC, μg/ml)

S.epidrmidis	**MIC**	***S. aureus* (MRSA)**	**MIC**	***S.aureus* (MSSA)**	**MIC**
311/08	**2,5**	**275/08**	**10**	**256/08**	**10**
315/08	**2,5**	**277/08**	**10**	**261/08**	**10**
316/08	**2,5**	**306/08**	**10**	**267/08**	**10**
317/08	**2,5**	**307/08**	**10**	**268/09**	**10**
318/08	**2,5**	**309/08**	**10**	**269/08**	**5**
340/09	**2,5**	**329/08**	**10**	**338/08**	**10**
341/09	**5**	**355/09**	**5**	**339/08**	**10**
342/09	**5**	**356/09**	**10**	**367/09**	**10**
343/09	**5**	**357/09**	**10**	**369/09**	**10**
377/09	**5**	**376/09**	**10**	**372/09**	**10**

The unmonochromatized Mg Kα X-ray source of incident energy of 1253.6 eV was applied to generate core excitation. The spectrometer was calibrated according to ISO 15472:2001. The energy resolution of the system, measured as a full width at half maximum (FWHM) for Ag $3d_{5/2}$ excitation line, was 0.95 eV. The spectra were processed by CasaXPS 2.3.12 program. The calibration was performed for carbon C 1s core excitation at electron binding energy (BE) of 285 eV taken as an internal standard. In the spectra, the background was approximated by a Shirley profile. The spectra deconvolution into a minimum number of the components was done by application of the Voigt-type line shapes (70:30 Gaussian/Lorentzian product). The analysis depth of 9 nm allowed sampling of the particle volume.

2.4. Antimicrobial properties

To eliminate influence of SDS and some by-products of reduction reaction on antimicrobial properties, silver colloid nanoparticles were dialyzed 4 times using distilled water. Reference solution (water taken after last dialysis) didn't show antimicrobial activities. During dialysis of silver nanoparticles reduced by ascorbic acid aggregation process was observed. Suspension of silver nanoparticles were tested in vitro for their antibacterial activity using standard and clinical strains of Gram-positive and Gram-negative bacteria.

Table 4. Antimicrobial activity of Ag nanoparticles suspension H against clinical strains o *Pseudomonas aeruginosa and Escherichia coli*: Minimal Inhibitory Concenteration (MsIC, μg/ml)

P. aeruginosa	MIC	E. Coli	MIC
6m	5	ML1	2.5
7m	5	ML3	2.5
10m	5	ML5	2.5
11m	5	ML6	2.5
12m	5	ML8	2.5
16m	5	ML9	2.5
18m	10	ML12	2.5
22m	10	ML15	2.5
23m	5	ML16	2.5
31m	5	ML17	5

Clinical strains were isolated from different biological materials of patients hospitalized in one of the Warsaw Medical University Hospitals. Minimal Inhibitory Concentrations (MIC) were established by the twofold serial agar dilution technique using Mueller–Hinton II agar medium (Becton Dickinson), according to CLSI guidelines (Clinical and Laboratory Standards Institute, 2006). Concentrations of silver

nanoparticles suspensions reduced by hydrazine monohydrate (H) and by formalin (F) in solid medium ranged from 80 to 1,25µg/ml, concentrations of silver suspension reduced by ascorbic acid (AAC) ranged from 8 to 1,25µg/ml. The final inoculum of bacterial strain was 10^4 CFU/mL (colony forming units per mL), except the final inoculum for *E. hirae* ATCC 10541, which was 10^5 CFU/mL. Minimal inhibitory concentrations were read after 18 h of incubation at 35 °C.

3. RESULTS AND DISCUSSION

Figure 1 demonstrates examples of size distributions of silver suspensions obtained using different reducing agents.

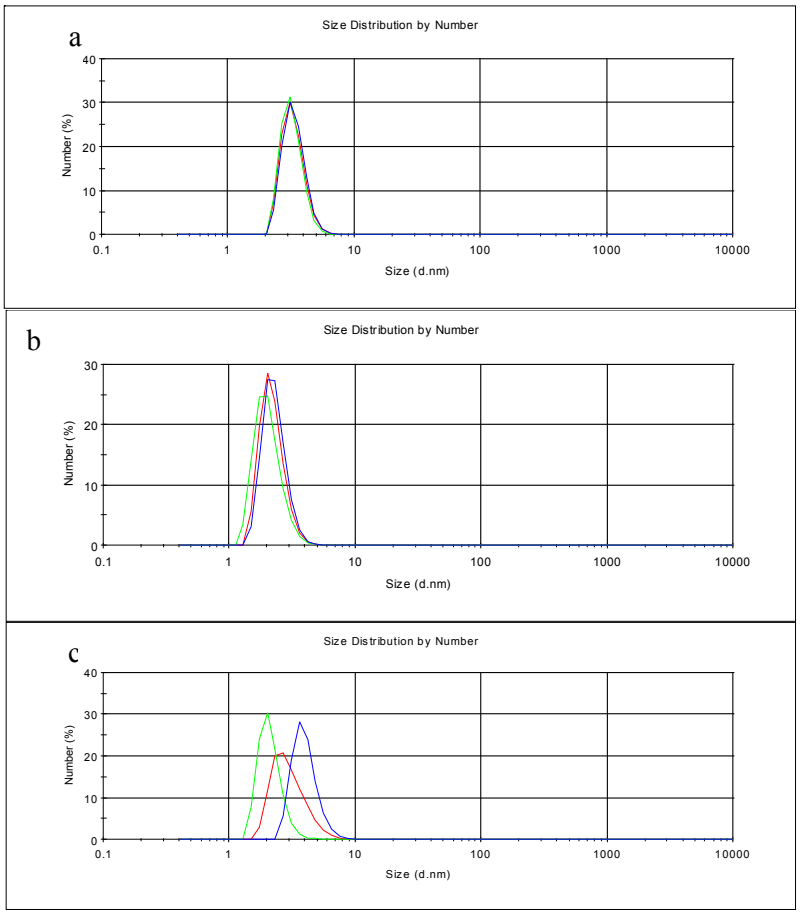

Fig. 1. Size distribution of silver nanoparticles measured by DLS reduced with a) formalin b) hydrazine monohydrate c) ascorbic acid.

One can see that the average size of nanoparticles, 4 nm, was practically not influenced by the type of the reducing agent, hydrazine monohydrate, formaline and ascorbic acid. Therefore, size and stability of the particles was controlled by addition of surfactant - sodium dodecylsulfate (SDS). We found that optimal concentration of SDS in reaction system was ~0.1 mol/L and the average size of nanoparticles, as measured by DLS, was in the range of a few nanometers. SEM micrograph (Fig.2) illustrates silver nanoparticles reduced with hydrazine monohydrate, which were deposited on opposite charged latex particles. The size of the observed particles, below 20nm, is in agreement with the values obtained by DLS. Zeta potential of Ag nanoparticles was negative (c.a. -60mV) due to SDS presence at their surface and slightly increases by c.a. 10mV after dialysis due to removal of excess of SDS.

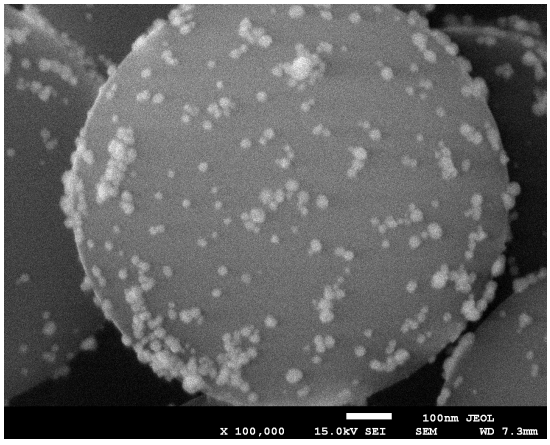

Fig. 2. SEM micrograph of silver nanoparticles reduced with hydrazine monohydrate deposited on oppositely charged Latex particles.

The suspension of 1600 ppm of silver was stable for a year. In the case when ascorbic acid was used as reducer stability of nanoparticles at that concentration was much lower and we observed aggregation in a few minutes after preparation of the Ag suspension. To obtain stable suspension with ascorbic acid we used 10 times lower concentration of $[Ag(NH_3)_2]^+$. In this concentration (160ppm) suspension of silver nanoparticles was stable for a year.

In the UV/VIS absorption spectra (Fig. 3) of silver particles, synthesized using various reducing agents, narrow surface plasmon absorption peaks at the wavelengths 390-420 nm were observed. That confirms the nanocrystalline character of the particles (Schneider, et al., 1994) and the low degree of their polydispersity.

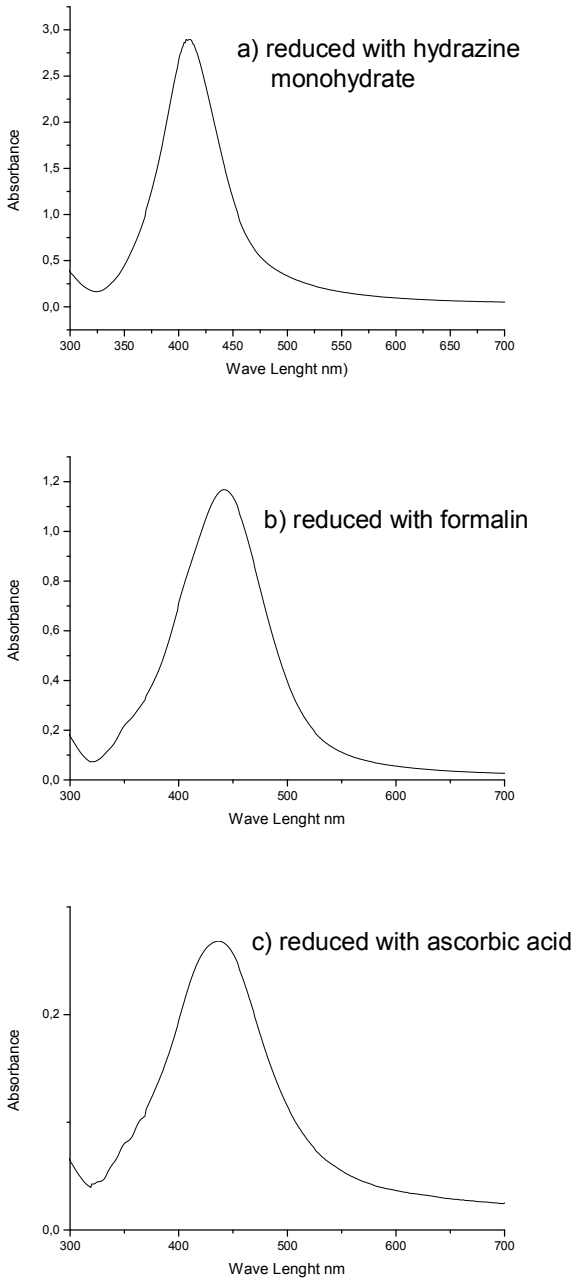

Fig. 3. Absorption spectra of Ag nanoparticle suspension reduced with a) hydrazine monohydrate b) formalin c) ascorbic acid.

Colloids containing particles larger than 100 nm, possess a uniform light absorption at longer wavelengths, a characteristic feature of metal particles of such size. The XPS measurements of the dried Ag suspensions allowed determining of the electronic states of silver in the obtained suspensions. The sample XPS spectrum of Ag 3d core excitation for Ag particles synthesized with the use of hydrazine is shown in Figure 4. This spectrum was deconvoluted into 2 components, where the component A at BE of 368.2 eV was assigned to metallic silver (Moulder, et al., 1992). The other fitting component (B) showed unexpectedly high BE of 369.8 eV that can be related either to the presence of Ag nanoparticles (Shin, et al., 2004) or to silver bonded to organic species [46]. However, the most probable state can be assigned to the peak B is silver immersed in or covered by an organic matrix (Majid, et al., 2003, Shin, et al., 2004, Lim, et al., 2006). The XPS spectra obtained for other systems (Table 1) showed also

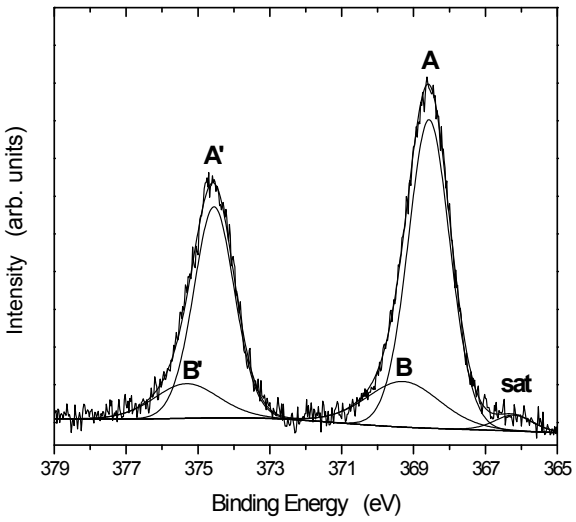

Fig. 4. The Ag 3d core excitation spectrum for Ag Hydrazine monohydrate sample.

two components of the Ag 3d core excitation. The XPS analysis suggests that hydrazine monohydrate used in the particle synthesis results in the lowest amount of the organic-bonded silver fraction. The reduction by ascorbic acid and formaline produces twice as organic-bonded silver as in the case of hydrazine monohydrate. The results of antibacterial tests (MIC) are summarized in tables 2-4. These results demonstrate that silver nanoparticles reduced with hydrazine monohydrate and formalin (suspension H and F) were active against Gram-positive and Gram-negative bacteria. Very good activity was observed for suspension H, MICs values of standard bacterial strains were

between 5 and 20 μg/ml. Suspension F showed good activity (MICs 40-80 μg/ml). On the other hand silver suspension reduced with ascorbic acid (concentration of silver 10 times lower) was inactive against tested strains due to aggregation process during dialysis. The next step of antimicrobial test was the evaluation of activity of silver nanoparticles H against clinical isolates of Gram-positive and Gram-negative bacteria: *Staphylococcus epidermidis*, methicillin-resistant and methicillin-susceptible *Staphylococcus aureus*, *Pseudomonas aeruginosa* and *Eschericha coli.* Species of these bacteria are a biofilm-forming important human pathogens, responsible for a many nosocomial infections. Silver suspension H exhibit very high activity against hospital strains of *Staphylococcus epidermidis* and *Escherichia coli* (MICs values between 2,5 and 5 μg/ml), and good activity against *Staphylococcus aureus,* both methicillin-susceptible and methicillin-resistant strains, and *Pseudomonas aeruginosa* (MICs 5-10 μg/ml).

4. CONCLUSION

Simple and effective method of synthesis of silver nanoparticles with well-defined size and antimicrobial activity was demonstrated. The method was based on the chemical reduction of silver nitrate by reducing agents, hydrazine monohydrate (H), formalin (F) and ascorbic acid (AAC). Size and stability of obtained silver nanoparticles was controlled by presence of surfactant - sodium dodecylsulfate (SDS). The average size of nanoparticles as measured by DLS and SEM micrograph was below 20nm. The UV/VIS absorption spectras of silver particles confirmed the nanocrystalline character of the particles synthesized using various reducing agents. The XPS analysis showed that hydrazine monohydrate used in the particle synthesis results in the lowest amount of the organic-bonded silver fraction. Antimicrobial tests demonstrated that silver nanoparticles reduced with hydrazine monohydrate and formalin were active against Gram-positive and Gram-negative bacteria. The best activity was observed for suspension reduced with hydrazine monohydrate; MICs values of standard bacterial strains were between 5 and 20 μg/ml. On the other hand silver suspension reduced with ascorbic acid (AAC) was inactive against tested strains probably due to aggregation process during dialysis. Nanoparticles reduced with hydrazine monohydrate also showed high activity against clinical isolated strains, included highly multiresistant strains such as *Staphylococcus epidermidis*, *Staphylococcus aureus* and *Pseudomonas aeruginosa*. The received silver antimicrobial agents can be proposed as an alternative strategy for reducing bacterial adhesion and to prevent bacterial bio-film formation.

ACKNOWLEDGMENT

The work was partially financed by MNiSW grant and MATERA ERA-NET project « NANOMEDPART ».

REFERENCES

ABID J.P., WARK A.W., et al. (2002). *Preparation of Silver Nanoparticles in Solution From a Silver Salt By Laser Irradiation*. Chem Commun 792-793.

BAKER C. PRADHAN A., et al. (2005). *Synthesis and Antibacterial Properties of Silver Nanoparticles* J. Nanosci. Nanotechnol. 5: 244-249

BOSETTI M., MASSE A., et al. (2002). *Silver coated materials for external fixation devices; in vitro biocompatibility and genotoxicity*. Biomaterials 23: 887–892

BUTKUS M.A., EDLING L., et al. (2003). *The efficacy of silver as a bactericidal agent: advantages, limitations and considerations for future use*. J. Water Supply Res. Technol-Aqua 52: 407-416

CATAURO M., RAUCCI M.G., et al. (2004). *Antibacterial and bioactive silver-containing Na_2O _ CaO _ $2SiO_2$ glass prepared by sol-gel method*. J Mater Sci Mater Med. 15(7): 831 - 837.

CHEN S.P., WU G.Z., et al. (2005). *Preparation of high antimicrobial activity thiourea chitosan-Ag+ complex*. Carbohydr. Polym. 60: 33-38.

Clinical and Laboratory Standards Institute, (2006). Methods for Dilution Antimicrobial Susceptibility Tests for Bacteria That Grow Aerobically; Wayne, PA, USA, Approved Standard M7-A7.

COLLERA-ZUNIGA O., JIMENEZ F.G., et al. (2005). *Comparative study of carotenoid composition in three mexican varieties of Capsicum annuum* L. Food Chem. 90: 109–114

CRABTREE J.H., BURCHETTE R.J., et al. (2003). *The efficacy of silver-ion implanted catheters in reducing peritoneal dialysis-related infections*. Perit Dial Int. 23(4): 368-374.

GARDEA-TORRESDEY J.L., GOMEZ E., et al. (2003). *Alfalfa Sprouts: A Natural Source for the Synthesis of Silver Nanoparticles*. Langmuir 19: 1357-1361.

GAUGER A., MEMPEL M., et al. (2003). *Silver-Coated Textiles Reduce Staphylococcus aureus Colonization in Patients with Atopic Eczema*. Dermatology 207: 15-21.

GOSHEGER G., HARDES J., et al. (2004). *Silver-coated megaendoprostheses in a rabbit model--an analysis of the infection rate and toxicological side effects*. Biomaterials 25: 5547-5556.

GUTIERREZ M., HENGLEIN A. (1993). *Formation of colloidal silver by push-pull reduction of Ag^+*. J. Phys. Chem. 97: 11368-11370.

JAGADEESH B.H., PRABHA T.N., et al. (2004). *Activities of β-hexosaminidase and α-mannosidase during development and ripening of bell capsicum (Capsicum annuum var. variata)*. Plant Sci. 167: 1263–1271

JEONG S.H., YEO S.Y., et al. (2005). *The effect of filler particle size on the antibacterial properties of compounded polymer/silver fibers*. J Mater Sci. 40: 5407–5411.

KHANNA P .K., SUBBARAO V.V.V.S. (2003). *Nanosized silver powder via reduction of silver*

nitrate by sodium formaldehydesulfoxylate in acidic pH medium. Mater. Lett. 57: 2242-2245

LEOPOLD N., LENDL B. (2003). *A New Method for Fast Preparation of Highly Surface-Enhanced Raman Scattering (SERS) Active Silver Colloids at Room Temperature by Reduction of Silver Nitrate with Hydroxylamine Hydrochloride*. J. Phys. Chem. B 107: 5723-5727.

LI S., SHEN Y., et al. (2007*). Green synthesis of silver nanoparticles using Capsicum annuum* L. extract. Green Chem 9: 852-858.

LIM D.C., LOPEZ-SALIDO I., et al. (2006). *Characterization of Ag nanoparticles on Si wafer prepared using Tollen's reagent and acid-etching*. Apel. Surf. Sci. 253: 959–965

MAJID A., BENSEBAA F., et al. (2003). *Modification of the metallic surface of silver by the formation of alkanethiol self-assembled monolayers with subsequent reaction with chlorosilanes*. Rev. Adv. Mater. Sci. 4: 25-31.

MATIJEVIC, (1993). *Preparation and properties of uniform size colloids*. E. Chem. Mater. 5: 412-426.

MIRKIN CA, TATON TA. (2000). *Semiconductors meet biology*. Nature 405: 626-627.

MORONES J.R., ELECHIGUERRA J.L., et al. (2005). *The bactericidal effect of silver anoparticles*. J. Nanotechnology 16: 2346-2353

MOULDER J.F., STICKLE W.F., et al. (1992). in Handbook of X-ray Photoelectron Spectroscopy (ed. J. Chastain, 2nd edition) Perkin-Elmer Corporation (Physical Electronics),

NICKEL U., CASTELL A.Z., et al. (2000). *A silver colloid produced by reduction with hydrazine as support for highly sensitive surface-enhanced raman spectroscopy*. Langmuir, 16: 9087-9091.

OHASHI S., SAKU S., et al. (2004). *Antibacterial activity of silver inorganic agent YDA filler*. J. Oral Rehabil. 31: 364-367.

PARIKH D.V., FINK T., et al. (2005). *Antimicrobial Silver/sodium Carboxymethyl Cotton Dressings for Burn Wounds* Text. Res. J. 75: 134-138.

RAVEENDRAN P, FU JET, et al. (2003). *Totally green nanoparticle synthesis*. J Am Chem Soc 125: 13940-13941.

RICHARDSON A., JANIEC A., et al. (2006). *Synthesis of silver nanoparticles: An undergraduate laboratory using a green approach*. Chem Ed 11: 331-333.

RUPP M.E., FITZGERALD T., et al. (2004). *Effect of silver-coated urinary catheters: efficacy, cost-effectiveness, and antimicrobial resistance*. Am. J. Infect. Control 32: 445-450.

SAITO Y., WANG J., et al. (2003). *Simple Chemical Method for Forming Silver Surfaces with Controlled Grain Sizes for Surface Plasmon Experiments*. Langmuir 19: 6857-6861.

SCHNEIDER S., HALBIG P., et al. (1994). *Reproducible preparation of silver sols with uniform particle size for application in sur-face-enhanced Raman spectroscopy* Photochem. Photobiol. 60: 605-610.

SHANKAR S.S., AHMAD A., et al. (2002). *Geranium leaf assisted biosynthesis of silver nanoparticles*. Biotechnol Prog 19: 1627-1631.

SHANKAR S.S., AHMAD A., et al. (2005). *Controlling the Optical Properties of Lemongrass Extract Synthesized Gold Nanotriangles and Potential Application in Infrared-Absorbing Optical Coatings*. Chem Mater 17: 566-572.

SHARMA V.K., YNGARD R.A., et al. (2009). *Silver nanoparticles: Green synthesis and their antimicrobial activities*. Advances in Colloid and Interface Science 145: 83–96

SHIN H.S., CHOI H.C., et al. (2004). *Chemical and size effects of nanocomposites of silver and polyvinyl pyrrolidone determined by X-ray photoemission spectroscopy*. Chem. Phys. Lett. 383: 418–422

SILVER S, PHUNG LT., (1996). *Bacterial heavy metal resistance: new surprises*. Annu Rev Microbiol. 50: 753-789.

SONDI I., GOIA D.V., et al. (2003). *Preparation of highly concentrated stable dispersions of uniform silver nanoparticles*. J. Colloid Interface Sci. 260: 75-81.

SONDI I., SALOPEK-SONDI B. (2004). *Silver nanoparticles as antimicrobial agent: a case study on E. coli as a model for Gram-negative.* J. Colloid Interface Sci. 275: 177-182.

STRATHMANN M., WINGENDER J. (2004). *Use of an oxonol dye in combination with confocal laser scanning microscopy to monitor damage of Staphylococcus aureus cells during colonization of silver-coated vascular grafts*. International Journal of Antimicrobial Agents 24: 36-42

SUN R.W.Y., CHEN R., et al. (2005). *Silver nanoparticles fabricated in Hepes buffer exhibit cytoprotective activities toward HTV-1 infected cells*. Chem. Commun. 40: 5059-5061.

ULKUR E., ONCUL O., et al., (2005). *Comparison of silver-coated dressing (Acticoat), chlorhexidine acetate 0.5% (Bactigras), and fusidic acid 2% (Fucidin) for topical antibacterial effect in methicillin-resistant Staphylococci-contaminated, full-skin thickness rat burn wounds*. Burns 31: 874-877

VIGNESHWARAN N., KATHE A.A., et al. (2007). *Silver-protein (core-shell) nanoparticle production using spent mushroom substrate.* Langmuir 23: 7113-7117.

WU Q., CAO H., et al. (2008). *Biomolecule-Assisted Synthesis of Water-Soluble Silver Nanoparticles and Their Biomedical Applications*. Inorg Chem 47: 5882-5888.

XIE J., LEE J.Y., et al. (2007). *Silver Nanoplates*: From Biological to Biomimetic Synthesis. ACSNano 1: 429-439.

YIN Y.D., LI Z., et al. (2002). *Synthesis and characterization of stable aqueous dispersions of silver nanoparticles through the Tollens process.s* J. Mater. Chem. 12: 522-527.

YURANOVA T., RINCON A., et al. (2003). *Antibacterial textiles prepared by RF-plasma and vacuum-UV mediated deposition of silver.* J Photochem. Photobiol. A. Chem., 161: 27-34.

Physicochem. Probl. Miner. Process. 45(2010) 99-112

journal homepage
www.minproc.pwr.wroc.pl/journal/

Physicochemical Problems of Mineral Processing

Index No. 32213X ISSN 1643-1049

Dawid WODKA *, Elżbieta BIELAŃSKA *, Robert P. SOCHA *,
Paweł NOWAK *, Piotr WARSZYŃSKI *

INFLUENCE OF THE DECOMPOSED SUBSTRATES ON THE PHOTOCATALYTIC ACTIVITY OF THE TITANIUM DIOXIDE MODIFIED BY SILVER NANOPARTICLES

Received April 25, 2010; reviewed; accepted April 30, 2010

Photocatalytic activity of Ag/TiO_2 composites obtained by photoreduction treatment (PRT) was investigated. The composite materials, containing 1.0 and 2.1 wt% of silver nanoparticles were obtained by depositing silver on the Evonic–Degussa P25 titania surface. Ag/TiO_2 samples were examined by SEM, XPS and BET techniques. The XPS measurements revealed that silver particles were obtained mainly in metallic form. The photocatalytic activity of pure P25 and Ag/TiO_2 composites was compared in photooxidation reaction of some model compound like: formic acid (FA), rhodamine B (RhB) and methylene blue (MB). Photodecomposition reaction was investigated in a batch reactor containing aqueous suspension of a photocatalyst illuminated by either UV or artificial sunlight (halogen lamp). The tests proved that small amount of silver nanoparticles deposited on titania surface triggers the increase in photocatalytic activity, this increase depends however on the type of substrate. The relation between the type of substrate and the activity of the composite was discussed.

keywords: Titanium dioxide; Photocatalysis; Silver nanoparticles; Organic dyes

---

* Institute of Catalysis and Surface Chemistry, PAS, 30 – 239 Kraków, Poland, ncwodka@cyf-kr.edu.pl (D. Wodka)

1. INTRODUCTION

Heterogeneous photocatalysis is an economically alternative and environmentally safe technology of advanced oxidation processes (AOP) for removal of organic impurities from water. During that process, the semiconductor illuminated by light of the proper wavelength absorbs light and generates active species, which oxidize the organic compounds dissolved in water. The most popular and promising material for this application is TiO_2 because of its high physical and chemical stability, non-toxicity and low price [1]. However its main drawbacks of low quantum yield and limited photoresponse range (< 380 nm) hinder its application and commercialization [2]. To handle those problems researchers have adopted numerous strategies, including phase and morphological control, doping, sensitizations and semiconductor coupling [3-15]. Recently there has been a great interest in the photoelectrochemical properties of nanostructured TiO_2 films such as photovoltaic [16-17], photocatalytic [18], optical [19] and water splitting ability [2]. Further, several researchers reported that modification of the TiO_2 surface with metals, like Pt, Fe, Ag, Au and Pd is promising as a tool to enhance the photocatalytic activity of TiO_2 and to increase the quantum yield [20-23]. In particular, silver nanoparticles deposited on TiO_2 substrate (Ag/TiO_2) have attracted significant attention because of non-toxicity of the metal with remarkable catalytic and antibacterial activity [24-30]. Moreover silver is particularly suitable for industrial applications due to its relatively low price and the ease of preparation when compared to other metals. Activity of those materials has been tested with many organic compounds like organic dyes [31,32], phenols, ketones [25], carboxylic acids [33] in solid - liquid as well as in solid - gas systems. In that kind of reactions the Ag/TiO_2 composite showed usually higher activity than bare titania. The most common and promising methods of Ag/TiO_2 preparation, which make possible approaching the system of high efficiency and low cost are sol-gel [34, 35], PRT [36,37] and CVD [38] ones.

The aim of this work was the determination of the influence of decomposed substrates on the photocatalytic activity of titanium dioxide modified by silver nanoparticles. The composites were synthesized from organic silver salt (silver acetate). The application of acetate in the PRT reaction allowed synthesizing metallic nanoparticles without any additional reducers (sacrificial reagents). In such photoreaction process the organic anion causes reduction of silver cations to the metallic state. It makes that kind of synthesis simple, fast, relatively cheap and makes possible obtaining pure composites without any impurities what is a big advantage when compared to reduction of $AgNO_3$ [39-41]. The Ag/TiO_2 photocatalysts containing silver particles in two silver concentration (1.0 and 2.1 wt%) were tested in decomposition of selected organic compounds: formic acid (FA), rhodamine B (RhB) and methylene blue (MB) [42]. Results recorded for silver modified titania were

compared with pure P25.

In this paper we would like to take a special note on the photosensitization effect occurring for organic dyes on pure titania and antagonistic effect, the decrease of the Ag/TiO_2 composite activity due to the specific interaction of the dye with silver.

2. EXPERIMENTAL

2.1. Materials and reagents

TiO_2 (P25, 25% rutile and 75% anatase) was kindly supplied by Evonic-Degussa. Silver acetate, 99.99% metals basis was purchased form Sigma-Aldrich. Formic acid (FA, 98.0% p.a.) and methylene blue (MB) were obtained from Fluka. Potassium thiocyanate (99.0%, p.a.), nitric acid (65.0%, p.a), rhodamine B and silver nitrate (p.a) were purchased from POCh Gliwice.

All reagents were used as received without further purification. Deionized water of Millipore Direct Q UV quality was used in all experiments.

2.2. Preparation of Ag/TiO_2

The Ag/TiO_2 nanocomposites were prepared by a photoreduction treatment (PRT). The suspensions (40 ml) were prepared by mixing P25 powder (1 g) with different volumes of CH_3COOAg aqueous solution (0.05 M) and deionized water. Then suspension was sonificated for 10 minutes, agitated (300 rpm) and finally irradiated with a high pressure xenon arc lamp (250 W) for 1 hour in quartz flat bottomed cell. The resulting Ag/TiO_2 nanocomposites were recovered by filtration, rinsed with deionized water several times and finally dried at 40 °C in the dark. The composites were prepared for following Ag/TiO_2 ratios (%) in the synthesis mixture: 2 and 20. The analysis of real silver concentration in composite was performed using Volhard titration method, after digesting composite in nitric acid. In the further text the real concentration of silver, expressed in wt% is given.

2.3. Material Characterizations

The scanning electron microscopy (SEM) images and EDXS analysis were performed with a JEOL JSM-7500F Field Emission apparatus operated at 15 kV. The samples were analyzed without any surface treatment.

The X-ray Photoelectron Spectroscopy (XPS) and X-ray excited Auger Electron Spectroscopy (XAES) measurements were performed using an XPS spectrometer equipped with a hemispherical analyzer (R4000, Gammadata Scienta) using MgKα

(1253.6 eV) radiation. The power of the X-ray source was 240 W and the analyzer pass energy was 100 eV, corresponding to a full width at half maximum (FWHM) of 0.9 eV for the Ag $3d_{5/2}$ peak. The area of the sample analyzed was approximately 3 mm^2. The powder samples were pressed onto indium foil and mounted on a dedicated holder. In a case of Ag/TiO_2 suspensions, the drop of liquid sample was dried on the gold sheet surface and then analyzed. The binding energy (BE) was calibrated using Cu, Au and Ag foils as reference materials, according to ISO 15472:2001 procedure.

The Brunauer–Emmett–Teller (BET) surface area of the powder samples was determined with a QuantaChrome Autosorb-1 instrument. The surface area of the samples was obtained from nitrogen adsorption isotherms after outgassing for 18 hours at the temperature of 20°C.

2.4. Photodegradation experiments

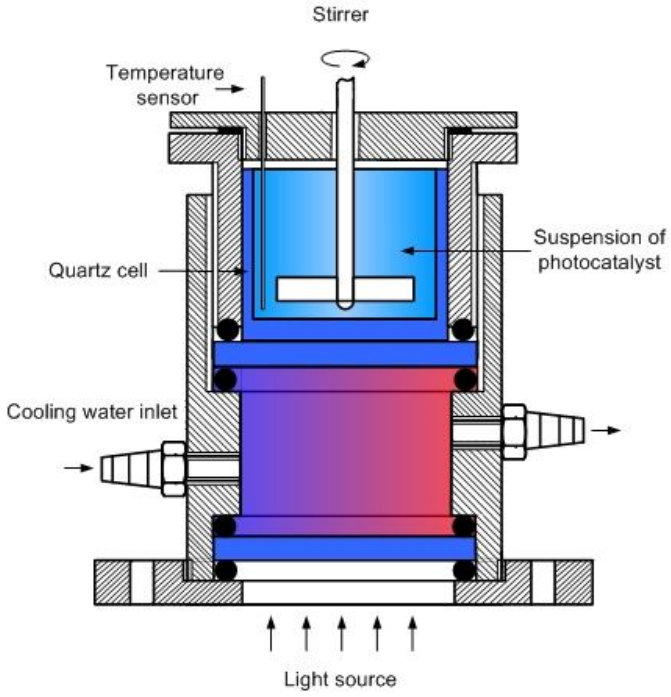

Fig. 1. The scheme of the quartz flat bottomed photoreactor.

The photooxidation experiments were performed in two quartz flat bottomed reactors of the same volume as for the preparation of the composite (40 ml). In the first reactor the halogen lamp (150 W, Philips) was used as an artificial sunlight (ASL) source, in the other one, dedicated for ultraviolet, the high pressure xenon arc lamp (250 W, Optel) was applied. Both lamps were used without any cut-off filters, except

the layer of cooling water flowing below the bottom of the cell. The cell illumination was monitored by the radiometer Radiometer RD 0.2/2/100 (Optel). The distance between the source and the sensor was about 25 cm for ASL and 15 cm for UV light and the illumination area was 16.3 cm^2. The irradiation intensity at the bottom of an empty reactor was 68.8 mW/cm^2 for ALS and 48.8 mW/cm^2 for UV source. The photocatalyst suspensions were stirred during the experiments in both reactors with a mechanical stirrer at a constant rate of 300 rpm. During all experiments the temperature in the reactor was stabilized at 25±0.5°C (Fig. 1).

After the photocatalytic experiment three samples of suspension were taken from the reactor, subjected to 25 min of centrifugation at 15000 rpm to separate TiO_2 and analyzed for the contaminant concentration. The concentration changes of different contaminants were determined by UV-VIS spectrophotometery (Analytik Jena – Specord 40). The most characteristic wavelength of maximum light absorption was chosen for all contaminants. After preliminary experiments the following photocatalyst and contaminant concentrations as well as irradiation times were chosen for testing the activity of the Ag/TiO_2 composites, as shown in Table 1.

Table 1. The experimental parameters of the photodegradation experiments.

Contaminant	**RhB**	**MB**	**FA**
$\mathbf{C_{contaminant}}$	$3x10^{-5}$ M	$3x10^{-5}$ M	$2x10^{-2}$ M
$\mathbf{C_{photocatalyst}}$	500 mg/l	100 mg/l	500 mg/l
Irradiation time	20 min	20 min	60 min
Analytical wavelength	555 nm	665 nm	208 nm

The contaminant concentrations were selected to fit the spectrophotometer absorbance range up to A = 3. The percentage of the decomposed contamination was calculated using following equation (1):

$$\%_{decomp} = \frac{(A_0 - A)}{A_0} \cdot 100 \text{ , (\%)} \tag{1}$$

where A_0 – is the initial absorbance of the suspension (before irradiation) and A is the suspension absorbance after irradiation.

Obtained results showed photocatalytic activity, when the effect of adsorption was eliminated by differential measurement between the reference kept in the dark and the sample illuminated during the same time. Figure 2 shows the process of sample preparation to the spectrophotometric measurement. Stability of decomposed contaminant was checked in a blank experiment without the photocatalyst. After 1h illumination under ASL and UV light the photodecomposition effect was negligible for all used substrates.

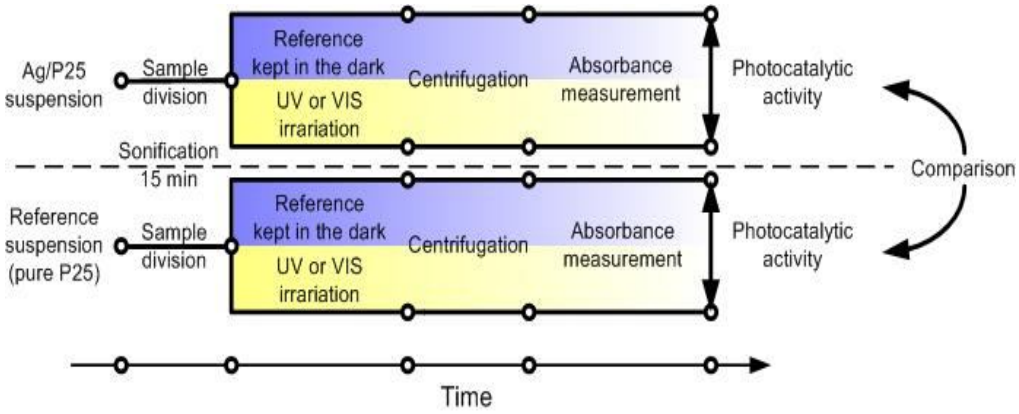

Fig. 2. The process of sample preparation to the spectrophotometric measurement.

3. RESULTS AND DISCUSSION

3.1. Adsorption effect and photocatalytic activity

Table 2. Adsorption effect registered for different substrates.

Substrate	Time [h]	Adsorption on pure P25, %	Adsorption on Ag/TiO_2, %
MB	1.5	3.1	40.4
	3	1.6	40.3
	6	1.7	41.4
	12	1.5	40.2
RhB	1.5	1.7	6.9
	3	1.0	8.9
	6	1.2	9.0
	12	0.9	9.5
FA	1.5	3.3	1.9
	3	1.7	1.0

In the first stage of the experiments the adsorption of investigated substances on TiO_2 and Ag/TiO_2 composites was determined (Table 2). The adsorption was expressed as the % decrease in the concentration of the contaminant in relation to the initial concentration after various times of contact.

Significant adsorption of both RhB and MB on Ag/TiO_2 composite was observed, but the decrease of concentration of FA was very low and similar for TiO_2 and composite. Note that none of the investigated compound adsorbed in a significant degree on pure TiO_2.

As the first model contaminant rhodamine B (RhB) was used. In the case of 2.1 wt% Ag/TiO_2, after UV illumination (Figure 3) RhB got degraded by only 12 % more than in the case of pure P25. ASL light illumination of the silver enriched titania showed no effect on RhB oxidation (1.0 wt% sample) or even some decrease of the reactivity (2.1 wt% sample).

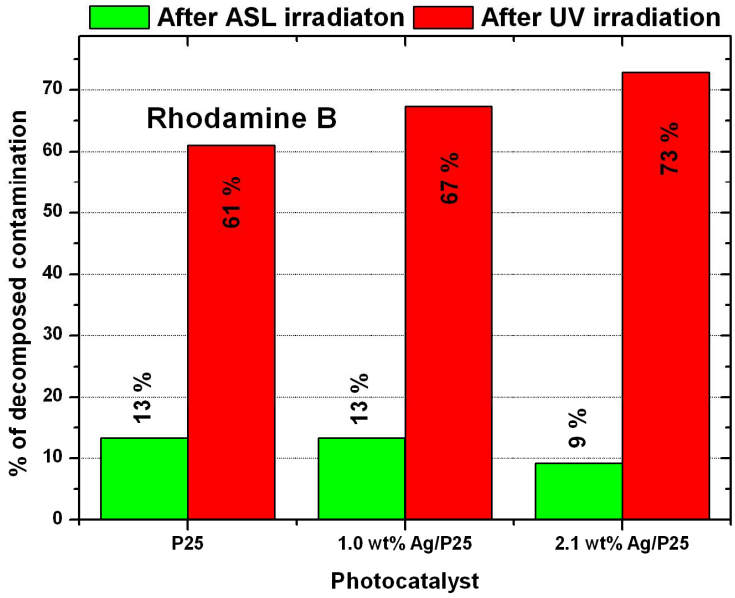

Fig. 3. Photocatalytic degradation of RhB on the pure P25 and silver modified photocatalyst

Methylene blue was also tested. For that compound a decrease of the photoactivity of Ag/TiO_2 as compared to pure TiO_2 was observed under ASL and UV irradiation. Note that decrease of the photoactivity is roughly proportional to the silver concentration on the P25 surface (Figure 4).

The same photocatalytic tests as for RhB and MB were performed for formic acid. Significant increase of activity for Ag modified sample, as compared to pure TiO_2 was observed in the case of UV irradiation (Figure 5). In the case of ASL irradiation of the composites containing 1.0 and 2.1 wt% of Ag the decomposition of FA was practically negligible. The increase of silver concentration to 2.1 wt% resulted in significant increase of the FA degradation under UV irradiation when compared to 1 wt% of Ag.

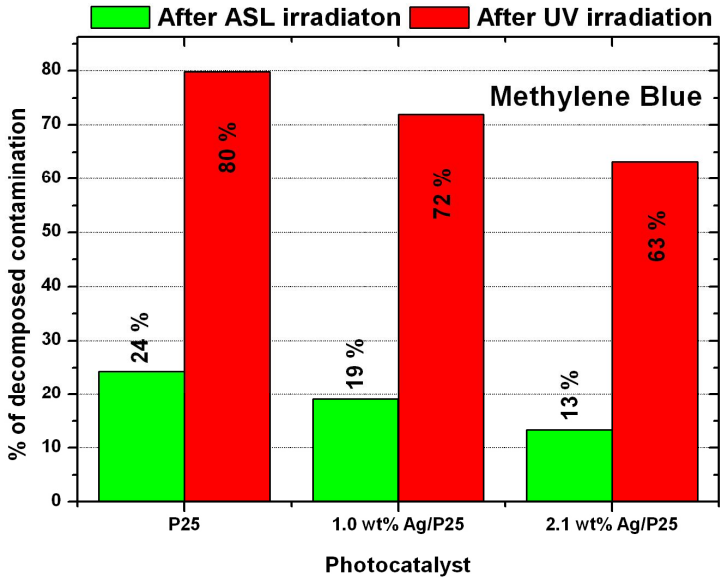

Fig. 4. Photocatalytic degradation of MB on the pure P25 and silver modified photocatalyst.

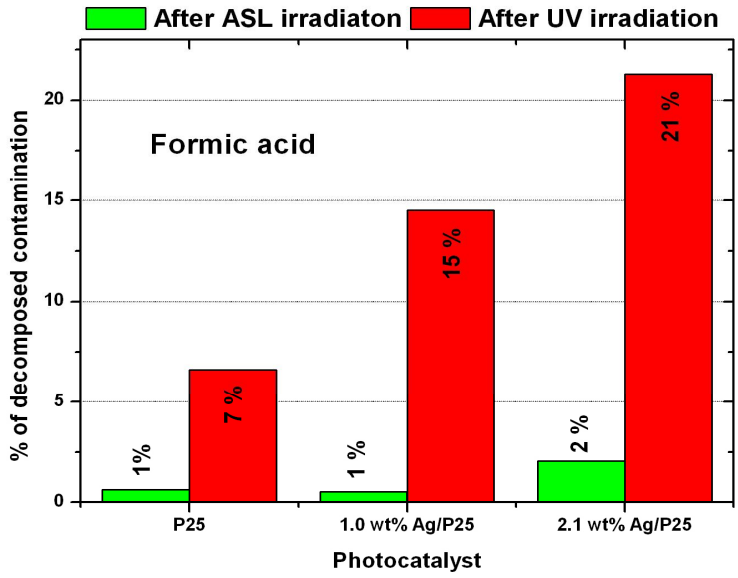

Fig. 5. Photocatalytic degradation of FA on the pure P25 and silver modified photocatalyst

3.2. XPS analysis

The chemical composition of Ag/TiO_2 composite before the photocatalytic tests was analyzed by the XPS method (Table 3, 4). The chemical state of silver in the composite was obtained by analysis of Ag 3d core excitation and Auger spectrum (XAES). The Ag 3d peaks of all composite samples were slightly asymmetric. Good fit was obtained when two doublets were applied in the spectrum fitting procedure. The exemplary spectrum of the just prepared composite is shown in Figure 6.

Table 3. XPS, and EDXS analysis of Ag/TiO_2 – 2.1 wt% composite freshly synthesized, A – ratio of the intensity of the Ag 3d emission line that may be ascribed to metallic silver, B – ratio of the higher BE component .

Ag $3d_{5/2}$ (A)		**Ag $3d_{5/2}$ (B)**		**Ag $L_4N_{45}N_{45}$ (eV)**	**α' (eV)**	**XPS Ag/Ti**
BE (eV)	**%**	**BE (eV)**	**%**			
367.7	78.2	368.6	21.8	358.4	726.1	0.081

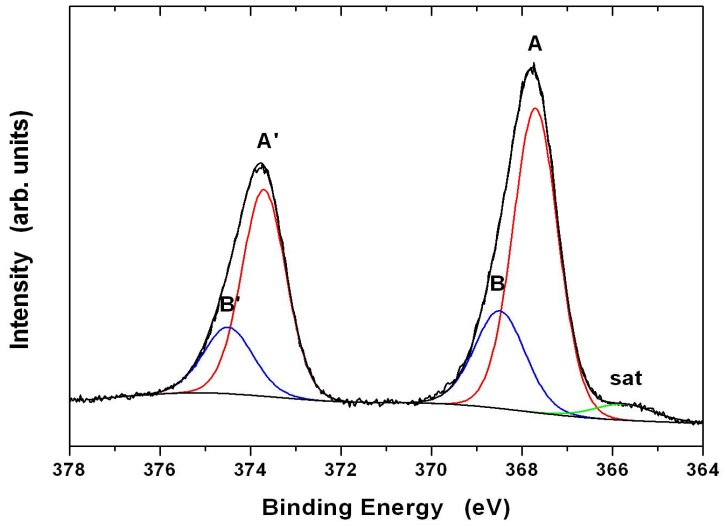

Fig. 6. The deconvoluted spectrum of Ag 3d core excitation obtained for Ag/TiO_2 composite (2.1 wt%).

The electron binding energy (BE) of the most intense peak (A) was found in the range of 367.5-368.0 eV for all studied samples. The Auger parameter (α'= Ag $3d_{5/2}$

(BE) + Ag $L_4N_{45}N_{45}$ (KE)) showed values above 725 eV. Analysis of Ag $3d_{5/2}$ BE and α' parameters showed that metallic silver is main silver species present in the composite [43]. Additionally, because the BE of the Ag 3d core excitation depends on the particle size [44, 45], the presence of the second peak (B) at BE of 368.5-369.2 eV in the XP spectra suggests that part of silver at the TiO_2 surface forms nanoparticles.

Table 4. Silver concentration in 1.0 and 2.1 wt% Ag/TiO_2 composites obtained by XPS and EDXS analysis.

Sample	**XPS measurements**		**EDXS measurements**	
	Ti at% XPS	**Ag at% XPS**	**Ti at% EDXS**	**Ag at% EDXS**
Ag/TiO_2 1.0 wt%	96.0	4.0	98.2	1.8
Ag/TiO_2 2.1 wt%	92.5	7.5	96.1	3.9

XPS analysis allowed calculation of the Ag to Ti atomic ratio (Table 4). The XPS analysis depth for Ag and TiO_2 was estimated to 5.2 and 7.4 nm, respectively [46]. The results showed that surface occupied by silver nanoparticles proportionally increase with the concentration of silver in composite. It means that applying higher concentration of silver salt during synthesis do not trigger the agglomeration or nanoparticles growth. This result was confirmed by EDXS analysis (Table 4) although lower values of the Ag/Ti were found. The EDXS analysis depth is much larger comparing to the XPS, it can approach 1 μm. Taking above into account it may be stated that Ag clusters/nanoparticles decorate the TiO_2 surface.

3.3. SEM and EDXS analysis

Figure 7 presents the SEM images obtained for the Ag/TiO_2 composite containing 1.2 wt% of the silver nanoparticles. The image 7a shows morphology of the composite. In Figure 7b, the back-scattered electrons (BSE) were used to obtain the SEM image sensitive to the larger atomic number (Z). In this picture, the bright spots were identified as the silver nanoparticles. Most of the Ag particles show rather low diameter (up to 20 nm) although there is a small number of relatively large particles (more then 50 nm). The titanium and silver concentrations in the EDXS analyzed points (Fig. 7b) are collected in Table 5. The Ag concentration shows nonuniform distribution over the sample that varies from 1.67 to 5.24 wt%.

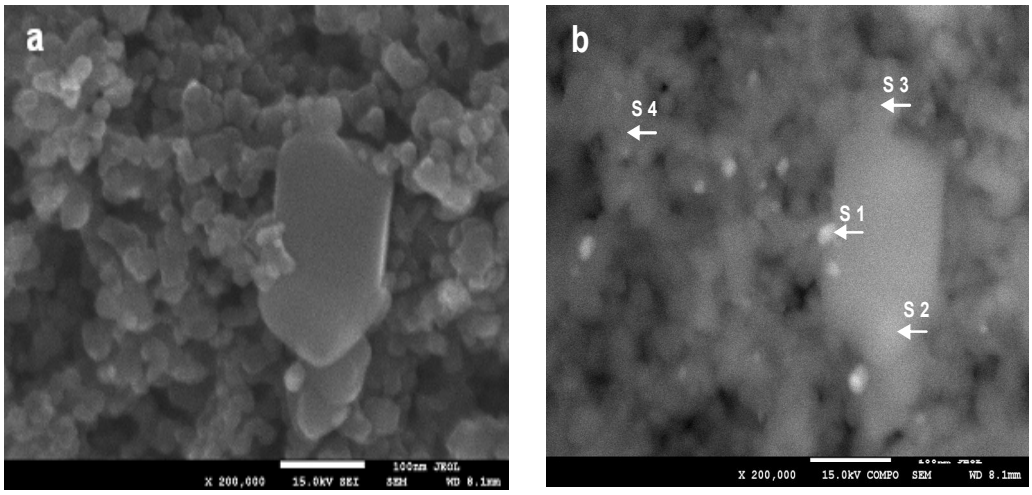

Fig. 7. SEM (a) and BSE (b) images of Ag/TiO_2 composite (1.2 wt%)

Table 5. Distribution of Ag nanoparticles

Spectrum	Spectr. 1	Spectr. 2	Spectr. 3	Spectr. 4	Mean	Std. dev.	Max.	Min.
	Weight%							
Ti	94.8	98.2	98.3	97.7	97.2	1.7	98.3	94.8
Ag	5.2	1.8	1.7	2.3	2.8	1.7	5.2	1.7

3.4. Analysis BET

The surface area obtained for 2.1% Ag/TiO_2 (49.4 m^2/g) was smaller then for pure P25 (56.6 m^2/g). Probably silver nanoparticles are deposited in the cracks and holes of agglomerates of TiO_2.

4. DISCUSSION

Interpretation of the organic dyes behavior in the photodecomposition reactions requires the consideration of the photosensitization effect. In the case of RhB degradation photoactivity increased with the increases in silver concentration slightly and only under UV irradiation (see Figure 3). On the other hand silver composites under ASL light illumination showed no effect on RhB oxidation (1.0 wt% of Ag) or even

some decrease of the reactivity (for 2.1 wt% sample). That behavior can be, at least partially, explained by the occurrence of photoinduced activation (photosensitization mechanism) [17]. Organic dye adsorption modified photocatalyst surface and shifted TiO_2 light absorption to the visible region what increased activity due to wider light spectrum available. The photosensitization is correlated with the effective surface area of TiO_2. Thus the composites with larger amount of silver have smaller active area due to the surface blocking what results in the decrease of activity. In the case of UV light photosensitization mechanism is not so important because the excitation energy is high enough to initiate the photocatalytic process. So, the synergic influence of the silver nanoparticles and titania substrate is stronger than photosensitization effect caused by organic dye which resulted in the increase of photocatalytic activity under UV irradiation. Note, that because photosensitization occurs on bare TiO_2 surface both effects (photosensitization and activation by Ag) interfere with each other. So, in the case when sensitization plays an important role in the photocatalytic process the influence of activation by depositing metal particles on the surface would be masked in the systems where photosensitization occurs.

In the case of MB the decrease of photoactivity were observed under both ASL and UV irradiation when silver was deposited at the surface. Besides the influence of photosensitization this behavior can be explained by blocking of the silver surface by MB due to the creation of Ag-S bond between sulfur atom contained in MB molecule and the surface of silver, which results in poisoning of silver containing composites. So, that part of the surface of TiO_2 which is occupied by silver becomes inactive. Therefore, the more silver at the TiO_2 surface the stronger surface poisoning and the stronger decrease of the photocatalytic process efficiency. Strong adsorption of MB at the surface of silver was confirmed by adsorption measurements. The rate of MB decomposition on TiO_2 was generally very high, much higher then in the case of RhB which is evidently due to the photosensitization effect.

Elimination of the photosensitization mechanism was done by applying colorless substrate, FA. Photodecomposition of that compound in the presence of Ag/TiO_2 composited showed significant increase of activity under UV irradiation (see Figure 5). It means that decomposition of FA could be possible only under UV light irradiation, so the pure photodegradation mechanism was observed only for FA.

4. CONCLUSIONS

The Ag/TiO_2 composites containing various concentrations (1.0 and 2.1 wt%) of the silver nanoparticles on the titania surface were tested as a potential photocatalyst for the removal of organic contaminations from water. It was proved that small amount of silver nanoparticles (2.1 wt%) greatly increase photocatalytic activity, this effect

depends however on the substrate studied. The Ag/TiO_2 composite showed oxidation activity significantly higher than pure P25 in the case of FA. However for RhB the activity of the composite was only slightly higher than the activity of pure TiO_2 and in the case of MB bare P25 was slightly better than the obtained composite. According to our opinion the difference between dyes and other substrates is caused by the interference of the photosensitization effect which neutralizes the influence of silver. So, it may be concluded that organic dyes, commonly applied as testing substances in photocatalytic experiments may not be recommended as testing species in the case of surface-modified titania. What is more, substrate containing sulfur in the molecule could deactivate Ag/TiO_2 composite.

ACKNOWLEDGEMENT

This research was supported by European Economic Area Financial Mechanism. PL0084 (2007-2010) NOMRemove: Effective photocatalytic-membrane methods of removal of organic contaminants for water treatment.

REFERENCES

[1] CARP O., HUISMAN C.L., RELLER A. Prog. Solid State Chem. **2004**, 32, 33–177.
[2] HOFFMANN M.R., MARTIN S.T., CHOI W., BAHNEMANN D.W. Chem.Rev. **1995**, 95, 69–96.
[3] SIVALINGAM G., NAGAVENI K., HEGDE M.S., MADRAS G. Appl. Catal. B **2003**, 45, 23–38.
[4] HU C., TANG Y., JIANG Z., HAO Z., TANG H., WONG P.K. Appl. Catal. A **2003**, 253 389–396.
[5] CHIANG K., LIM T.M, TSEN L., LEE C.C. Appl. Catal. A **2004**, 261, 225–237.
[6] COLEMAN H.M., CHIANG K., AMAL R. Chem. Eng. J. **2005**, 113, 65–72.
[7] ZHANG Z., WANG C., ZAKARIA R., YING J.Y. J. Phys. Chem. B **1998**, 102, 10871–10878.
[8] ARANA J., DONA-RODRIGUEZ J.M., GONZALEZ-DIAZ O., TELLO RENDON E., HERRERA MELIAN J.A., COLON G., NAVIO J.A., PEREZ PENA J. J. Mol. Catal. A **2004**, 215, 153–160.
[9] OHTANI B., IWAI K., NISHIMOTO S., SATO S. J. Phys. Chem. B **1997**, 101, 3349–3359.
[10] HAIBIN L., XUECHEN D., GUOCONG L., XIAOQI L. J. Mater. Sci. **2008**, 43,1669–1676.
[11] EGERTON T.A., MATTINSON J.A. J. Photochem. Photobiol. A **2008**, 194, 283–289.
[12] GAO Y.M., LEE W., TREHAN R., KERSHAV R., DWIGHT K. A. World Mater. Res. Bull. **1991**, 26, 1247–1254.
[13] HERRMANN J.M., DISDIER J., PICHAT P., FERNANDEZ A., GONZALEZ-ELIPE A., MUNUERA G., LECLERCQ C. J. Catal. **1991**, 132, 490–497.
[14] YOUNG C., LIM T.M., CHIANG K., SCOTT J., AMAL R. Appl. Catal. B **2008**, 78, 1–10.
[15] NAZEERUDDIN M.K, KAY A., RODICIO I., HUMPHRY BAKER R., MULLER E., LISKA P., VLACHOPOULOS N., GRÄTZEL M. J. Am. Chem. Soc. **1993**, 115, 6382–6390.
[16] CHEREPY N.J., SMESTAD G.P., GRÄTZEL M., ZHANG J.Z. J. Phys. Chem. B. **1997**, 101, 9342-9351.
[17] O'REGAN B., GRÄTZEL M. Nature **1991**, 353, 737–739.
[18] LANATA M., CHERCHI M., ZAPPETTINI A., PIETRALUNGA S.M., MARTINELLI M. Opt.

Mater. **2001**, 17, 11-14.
[19] FUJISHIMA A., HONDA K. Nature **1972**, 238, 37–38.
[20] LI F.B., LI X.Z. Chemosphere **2002**, 48, 1103–1111.
[21] ZHANG F., JIN R., CHEN J., SHAO C., GAO W., LI L. J. Cat. **2005**, 232, 424–431.
[22] QI X.H., WANG Z.H., ZHUANG Y.Y., YU Y., LI J.L. J. Haz. Mat. **2005**, 118, 219–225.
[23] SAKTHIVEL S., SHANKAR M.V., PALANICHAMY M., ARABINDOO B., BAHNEMANN D.W., MURUGESAN V. Water Research **2004**, 38, 3001– 3008.
[24] VAMATHEVAN V., AMAL R., BEYDOUN D., LOW G., MCEVOY S. J. Photochem. Photobiol. A **2002**, 148, 233–245.
[25] ROBERTSON P.K.J., BAHNEMANN D.W., ROBERTSON J.M.C., WOOD F., Hdb. Env. Chem. **2005**, Vol. 2. Part M, 367–423.
[26] LI. Q., MAHENDRA S., LYON D.Y., BRUNET L., LIGA M.V., LI D., ALVAREZ P.JJ. Water Res. **2008**, 42, 4591–4602.
[27] LINSEBIGLER A.L., LU G., YATES J.T. Chem. Rev. **1995**, 95, 735-758.
[28] HOFMANN M.R., MARTIN S.T., CHOI W., BAHNEMANN D.W. Chem. Rev. **1995**, 95, 69-96.
[29] MILLS A., LE HUNTE S. J. Photochem. Photobiol. A **1997**, 108, 1-35.
[30] KIRIAKIDOU F., KONDARIDES D.I., VERYKIOS X.E. Catal. Today **1999**, 54, 119-130.
[31] SOBANA N., SELVAM K., SWAMINATHAN M. Sep. Pur. Tech. **2008**, 62, 648–653.
[32] LI H., DUAN X., LIU G., LIU X. J. Mater Sci. **2008**, 43, 1669–1676.
[33] LI CH., HSIEH Y., CHIU W., LIU CH., KAO CH. Sep. Pur. Tech. **2007**, 58, 148–151.
[34] HOU X., HUANG M., WU X., LIU A. Chem. Eng. J. **2009**, 146, 42–48.
[35] NAKATA K., UDAGAWA K., TRYK D.A., OCHIAI Y., NISHIMOTO S., SAKAI H., MURAKAMI T., ABE M., FUJISHIMA A. Mat. Lett. **2009**, 63, 1628–1630.
[36] PARAMASIVAM I.; MACAK J.M; GHICOV A.; SCHMUKI P. Chem. Phys.Lett. **2007**, 445, 233-237.
[37] LI H.; DUAN X.; LIU G.; LIU X. J. Mater. Sci. **2008**, 43, 1669–1676.
[38] WANG K.H.; HSIEH Y.H.; CHAO P.W.; CHANG C.T. J. Hazard. Mater. **2002** 95, (1–2) 161-174.
[39] KUBACKA A.; FERRER M.; MARTINEZ-ARIAS A.; FERNANDEZ-GARCIA M. App. Cat. B **2008**, 84, 87–93.
[40] LAI Y.; CHEN Y.; ZHUANG H.; LIN CH. Mat. Let. **2008**, 62, 3688–3690.
[41] MALAGUTTI A.R.; MOURAO H.A.J.L; GARBIN J.R.; RIBEIRO C. App. Cat. B **2009**, l90, 205–212.
[42] WODKA D.; NOWAK P.; WARSZYŃSKI P.; KUMAKIRI I.; SIMON C., Polish Annual Conference on Catalysis, Krakow, **2009**, Book of Abstracts (ISBN 978-83-60514-09-2), p22, p39.
[43] NIST X-ray Photoelectron Spectroscopy Database; http://srdata.nist.gov/xps/.
[44] SHIN H.S.; CHOI H.CH.; JUNG Y.; KIM S.B.; SONG, H.J.; SHIN H.J. Chem. Phys. Lett. **2004**, 4383, 18–422.
[45] LIM D.CH.; LOPEZ-SALIDO I.; KIM; Y.D. Surf. Sci. **2005**, 598, 96–103.
[46] TANUMA S.; POWELL C.J.; PENN D.R. Surf. Interf. Anal. **1993**, 21 165

Physicochem. Probl. Miner. Process. 45(2010) 113-126

journal homepage
www.minproc.pwr.wroc.pl/journal/

Physicochemical Problems of Mineral Processing

Index No. 32213X ISSN 1643-1049

Anna ZIELIŃSKA-JUREK *, Małgorzata WALICKA *, Anna TADAJEWSKA *, Izabela ŁĄCKA **, Maria GAZDA ***, Adriana ZALESKA *

PREPARATION OF Ag/Cu-DOPED TITANIUM (IV) OXIDE NANOPARTICLES IN W/O MICROEMULSION

Received March 23, 2010; reviewed; accepted May 22, 2010

The Cu-TiO_2 and Ag/Cu-TiO_2 nanoparticles have been prepared using a water-in-oil microemulsion system of water/AOT/cyclohexane. The photocatalytic activity of the catalysts was estimated by measuring the decomposition rate of phenol in 0.21 mM aqueous solution under visible light irradiation. The bioactivity of Ag/Cu-doped titanium (IV) oxide nanocomposites was estimated using bacteria *Escherichia coli* and *Staphylococcus aureus*, yeast *Saccharomyces cerevisiae* and pathogenic fungi belonging to *Candida* family. The photocatalysts' characteristics by X-ray diffraction, BET surface area measurements, Scanning Electron Microscopy (SEM) energy dispersive spectroscopy (EDS) analysis showed that a sample with the highest photo- and bioactivity had anatase structure, about 190 m^2/g specific surface area, absorbed light for λ>400 nm and contained 1.45 mass % of silver, 1.40 mass % of copper and 59.4 mass % of Ti.

keywords: Ag/Cu-doped TiO_2, microemulsion, heterogeneous photocatalysis, bioactivity

1. INTRODUCTION

Titanium (IV) oxide nanoparticles is one of the most studied semiconductors for

* Department of Chemical Technology, Chemical Faculty, anna_z@chem.pg.gda.pl (A. Zielińska-Jurek)
** Department of Pharmaceutical Technology and Biochemistry, Chemical Faculty
***Department of Solid State Physics, Faculty of Applied Physics and Mathematics, Gdansk University of Technology, 80-233 Gdańsk, Poland

photocatalytic degradation of hazardous and toxic organic pollutants, solar energy conversion, disinfection and self-cleaning coatings. However, the pure TiO_2 has wide band gap and can only be excited by a small UV fraction of solar light and thus this practically limits the use of sunlight or visible light as an irradiation source in photocatalytic reactions on TiO_2.

For the purpose of overcoming these limitations of TiO_2 and to enhance the photocatalytic activity response into the visible part of the spectrum, the surface modification of TiO_2 with various noble metals [1,2,3], transition metals [4,5,6] or non-metallic elements [7,8] have been widely investigated.

The role of loaded metal is trapping and subsequent transfer of photoexcited electrons on TiO_2 surface. The metals deposited or doped on TiO_2 have the high Schottky barriers and thus act as electron traps, facilitating electron–hole separation and promotes the interfacial electron transfer process. Bamwenda et al. compared the photocatalytic activity of Au-TiO_2 and Pt-TiO_2 nanoparticles in process of hydrogen generation. The maximum hydrogen production yield was observed for platinum- and gold-modified titanium (IV) oxide nanoparticles containing 0.3-1 wt% and 1-2 wt % of noble metal respectively [9]. For the preparation of self-cleaning coatings and water/air filters for reduction the spread of infections and improve the hygienic conditions the silver-doped TiO_2 nanoparticles have been widely investigated.

Hamal et al. reported the preparation and characterization of highly active in visible light new nanoparticle photocatalysts based on silver, carbon and sulfur-doped TiO_2. They found that Ag/(C, S)–TiO_2 nanoparticle photocatalysts degrade the gaseous acetaldehyde 10 and 3 times faster than commercial TiO_2 (P25, Degussa) under visible and UV light, respectively [10]. In recent years, Degussa P25 TiO_2 has set the standard for photoreactivity in environmental applications. Degussa P25 is a nonporous 70:30% anatase-to-rutile mixture with a BET surface area of 55± 15 m^2/g and crystallite sizes of 30 nm in 0.1 μm diameter aggregates.

Keleher et al. obtained Ag-TiO_2 nanoparticles, which exhibited antimicrobial activity against gram-positive and gram-negative bacterial strains. The zone of inhibition diameters for the Ag-TiO_2 particles was found to be comparable with those of the other antimicrobial agents (tetracycline, chloramphenicol, erythromycin, and neomycin) [11].

Our previous study confirmed that Ag-TiO_2 nanoparticles obtained in w/o microemulsion system exhibited visible light activity and antimicrobial activity against *E. coli, St. aureus, S. cerevisiae* and pathogenic fungi belonging to *Candida* family [12].

This paper described the Vis-light photocatalytic activity of the Cu-doped TiO_2 and Ag/Cu-doped TiO_2 nanoparticles prepared in w/o microemulsion system. W/O microemulsion contain inverted micellar aggregates consisting of water droplets surrounded by amphiphiles in a continuous nonpolar system. The particle sizes

generated can be controlled by the nanodroplet size of the inner phase of the microemulsion. The effect of metals amount on photocatalytic activity and antimicrobial properties have been widely investigated.

2. EXPERIMENTAL

2.2. Materials and instruments

Titanium isopropoxide (pure p.a.) was purchased from Aldrich and used as titanium source for the preparation of TiO_2 nanoparticles. Silver nitrate (pure p.a.) was provided by POCh and used as the starting material for the silver nanoparticles. Hydrazine anhydrous (50-60%) was purchased from Aldrich and used as reducing agent. Cyclohexane was used as the continuous oil phase, and sodium bis- (2-ethylhexyl) sulfosuccinate (AOT) purchased from Aldrich as the surfactant, 1-hexanol as the cosurfactant and aqueous solution as the dispersed phase. The crystal structures of the Ag/Cu-TiO_2 nanoparticles were determined from XRD pattern measured in the range of $2\theta = 20–60^o$ using X-ray diffractometer (Xpert PRO-MPD, Philips) with Cu target ($\lambda = 1.542$ Å). The XRD analysis of the crystallite size was based on the Scherrer formula: $d = 0.89\lambda/(Be - Bt)\cos\theta$, where λ is the X-ray wavelength, Be indicates the measured breadth of a peak profile, while Bt is the ideal, non-broadened breadth of a peak and θ is the diffraction angle. The value of Bt was estimated on the basis of the measurements performed for a standard sample of polycrystalline Si with large crystalline grains. The accuracy of the grain size analysis has been estimated to be about 20%. The surface morphology was determined using scanning electron microscope (SEM, LEO 1430 VP) equipped with energy dispersive X-ray spectrometer – EDS, Quantax 200. Nitrogen adsorption–desorption isotherms were recorded at liquid nitrogen temperature (77K) on a Micromeritics Gemini V (model 2365) and the specific surface areas were determined by the Brunauer–Emmett–Teller (BET) method.

2.3. Preparation of Cu-doped TiO_2 and Ag/Cu-doped TiO_2 photocatalysts

The microemulsions were prepared by mixing the aqueous solution of metal ions (Ag^+, Cu^{2+}) and $N_2H_4{\cdot}H_2O$ into the 0.2 M AOT/cyclohexane solution. Cu or Ag/Cu bimetallic nanoparticles were prepared by dropwise addition microemulsion containing the reducing agent (hydrazine) into the microemulsion containing metal precursor in water cores as was shown in Fig. 1. The molar ratio of hydrazine and silver nitrate or copper nitrate was held constant at a value of 3. Water content was controlled by fixing the molar ratio of water to surfactant (w_o) at 2.

Then TiO_2 precursor titanium tetraisopropoxide (0.2M TIP) was added into the

microemulsion containing metal nanoparticles. The concentration of metal precursors, which varied from 0.1 to 6.5 mol% was related to the concentration of TIP in the microemulsion system. During the precipitation nitrogen was bubbled continuously through the solution. The Ag/Cu-TiO_2 particles precipitated were separated, washed with ethanol and deionized water several times to remove the organic contaminants and surfactant. The particles were dried at 80°C for 48 h and were then calcinated at 450°C for 2h.

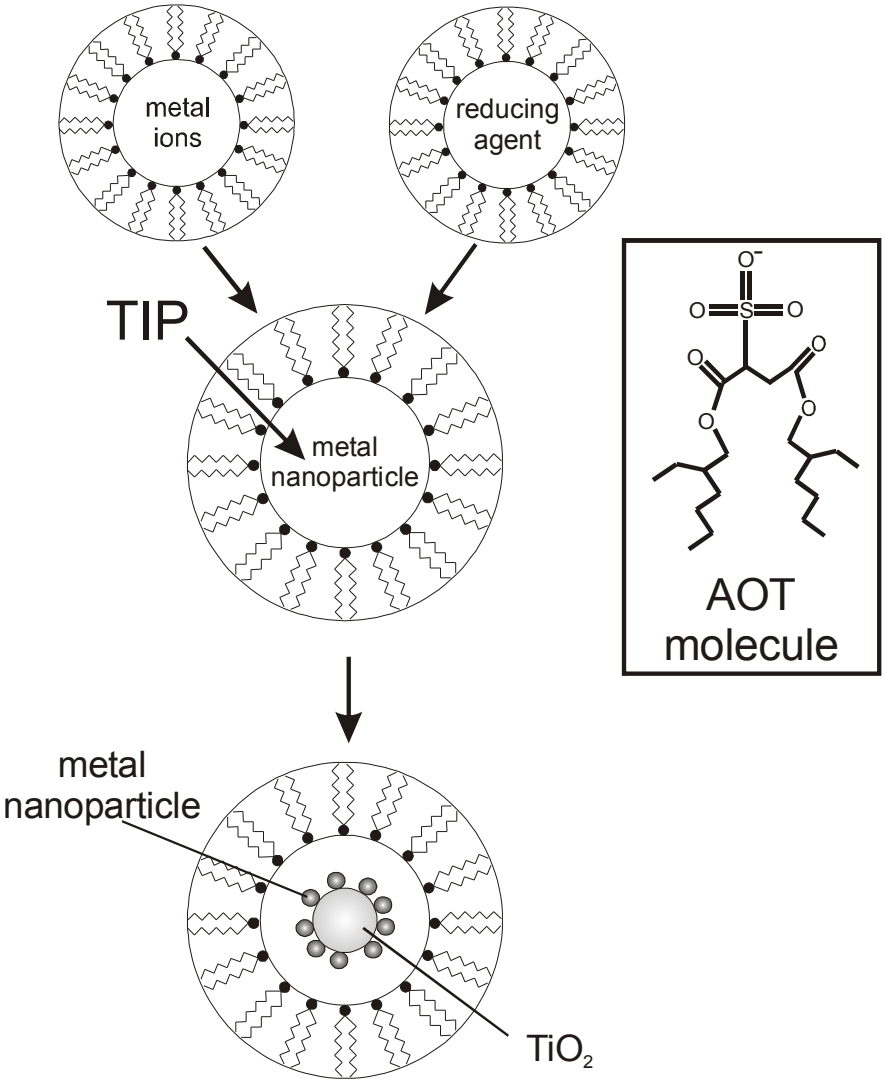

Fig. 1. Mechanism of the preparation method of Ag/Cu-doped titanium (IV) oxide nanoparticles in reverse micelles.

2.4. Measurements of photocatalytic activity

The photocatalytic activity of Ag/Cu-TiO_2 powders under visible light was estimated by measuring the decomposition rate of phenol (0.21 mmol/dm^3) in an aqueous solution. Photocatalytic degradation runs were preceded by blind tests in the absence of a photocatalyst or illumination. Phenol was selected as a model pollutant because it is a non-volatile and common contaminant present in industrial wastewaters. The mechanism of phenol decomposition is also well established. 25ml of phenol solution at concentration of $2.1 \cdot 10^{-4}$ M containing suspended photocatalyst (125 mg) was stirred using a magnetic stirrer and aerated (5 dm^3/h) prior and during the photocatalytic process. Aliquots of 1.0 cm^3 of the aqueous suspension were collected at regular time periods during irradiation and filtered through syringe filters (Ø = 0.2 μm) to remove photocatalyst particles. Phenol concentration was estimated by colorimetric method using UV–vis spectrophotometer (DU-7, Beckman). The suspension was irradiated using 1000 W Xenon lamp (6271H, Oriel), which emits both UV and vis light. The optical path included water filter and glass filters (GG400 or UG1, Schott AG) to cut off IR and VIS or UV irradiation, respectively. GG glass filter transmitted light of wavelength greater than 400 nm. The temperature during the experiments was maintained at 10°C.

2.5. Measurements of bioactivity (antibacterial and antifungal)

Bioactivity was measured as a minimal inhibitory concentration (MIC). Antibacterial and antifungal activity was determined by the serial twofold dilution microtiter plate method, in Tryptic Soy Broth medium (TSB, GibcoBRL), for antibacterial activity determination or in YNBG medium (Yeast Nitrogen Base-glucose minimal medium, containing 0,67 % YNB without amino acids and ammonium sulphate with addition of 2 % glucose and 5 g/l of ammonium sulphate, supplemented with uracil at 30 μg/l) for antifungal activity determination. Wells containing serially diluted examined compounds (suspended Ag/Cu-TiO_2) and compound-free controls were inoculated with overnight cultures of tested strains to the final concentration of 10^4 cfu/ml (colony forming units per ml). The plates were then incubated for 24 h at 37°C (antibacterial activity determination) or at 30°C (antifungal activity determination). The microbial growth was quantified in each well by the measurement of an optical density at λ = 531nm using the microplate reader (Victor^{3}V, PerkinElmer, Centre of Excellence ChemBioFarm, Faculty of Chemistry, Gdansk University of Technology). MIC (minimal inhibitory concentration) was defined as drug concentration at which at least 80 % decrease in turbidity, relative to that of the compound-free growth control well was found. The antimicrobial activity of Ag/Cu-doped titanium (IV) oxide nanocomposites was estimated using *Escherichia coli* ATCC 10536, *Staphylococcus aureus* ATCC 6538, *Candida albicans* ATCC 10231,

Candida glabrata DSM 11226, *Candida tropicalis* KKP 334, *Saccharomyces cerevisiae* ATCC 9763, *S. cerevisiae* JG and JG CDR1.

3. RESULTS AND DISCUSSION

3.1. XRD analysis

The selected XRD pattern of Ag/Cu-doped TiO_2 powders loaded with different amount of silver are shown in Fig. 2. The average size of anatase crystallites for Ag/Cu-TiO_2 nanoparticles determined from the XRD pattern based on the Scherrer formula was from 8 to 9 nm. Peaks marked "A" and "B" correspond to anatase and brookite phases, respectively. The Ag/Cu-TiO_2_1 and Ag/Cu-TiO_2_3 samples contained anatase and small amount of brookite. The higher silver amount (6.5 mol% of Ag for sample Ag/Cu-TiO_2_4) promote the formation of the pure anatase in preference to anatase/brookite photocatalysts. For the Ag/Cu-TiO_2 powder containing 6.5 mol% of Ag and 0.5 mol% of Cu doped, the peak corresponding to metallic silver at $2\Theta = 38.1$ was observed. On the contrary for lower dopant amount no additional XRD peaks corresponding to Ag or Cu present can be revealed. This may be attributed to the well dispersion of nanocrystalline metal nanoparticles in the TiO_2 matrix.

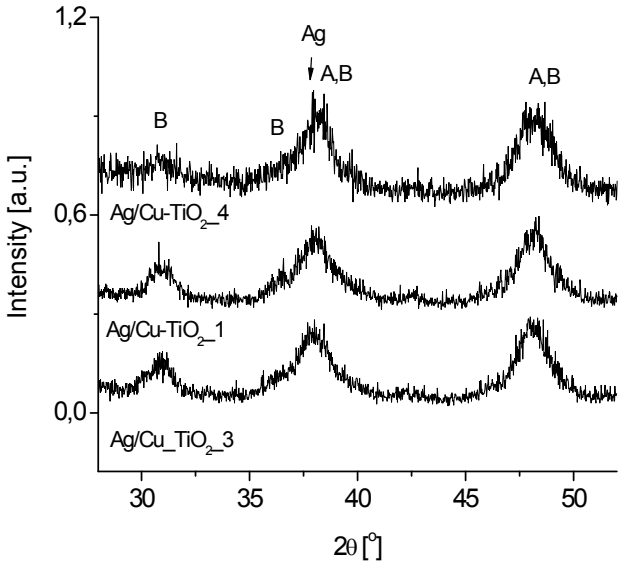

Fig. 2. XRD patterns of Ag/Cu-doped TiO_2 nanoparticles calcinated for 2 hours at 450ºC

3.2. BET surface area and microscopy analysis

Table 1 presents the characterization results for the silver and copper doped TiO_2 nanoparticles. The Cu-TiO_2 photocatalyst modified with 4.5 mol.% of Cu has the lowest BET surface area of about 161 m^2/g, which was comparable to pure TiO_2 obtained in the same microemulsion system.

Table 1. Characteristics of Ag/Cu- doped TiO_2 prepared in w/o microemulsion

Sample label	Amount of metal precursor [mol %]		Surfactant	Sample color	BET [m^2/g]	Phenol degradation rate [μmol/min] under Vis light ($\lambda > 400nm$)
	Cu	Ag				
TiO_2	0	0	AOT	white	160	0,29
Cu-TiO_2_1	0.1	0	AOT	green	195	0.62
Cu-TiO_2_2	0.5	0	AOT	green	206	0.94
Cu-TiO_2_3	2.5	0	AOT	green	202	0.53
Cu-TiO_2_4	4.5	0	AOT	green	161	0.43
Ag/Cu-TiO_2_1	0.5	1.5	AOT	yellow	190	2.41
Ag/Cu-TiO_2_2	1.5	0.5	AOT	green	209	0.74
Ag/Cu-TiO_2_3	0.5	0.5	AOT	yellow	194	1.36
Ag/Cu-TiO_2_4	0.5	6.5	AOT	yellow	187	1.22
Ag/Cu-TiO_2_5	4.5	0.5	AOT	green	223	0.50
Ag/Cu-TiO_2_6	0.5	4.5	AOT	yellow	180	2.25
Ag/Cu-TiO_2_7	0.5	2.5	AOT	yellow	186	2.07

For other Cu-TiO_2 and Ag/Cu-TiO_2 samples containing from 0.1 to 4.5 mol.% of Cu and 0.5 to 6.5 mol.% of Ag the surface areas varied from 180 to 223 m^2/g. It was observed that metal dopant affects the surface area of TiO_2 powder samples obtained by microemulsion system. The BET areas decrease for increasing Ag concentration more than for increasing Cu amount in the sample. Sample modified with 4.5 mol% of Ag and 0.5 mol% of Cu has the BET surface area of about 180 m^2/g.

For sample Ag/Cu-TiO_2_1 containing 1.5 mol.% of Ag and 0.5 mol.% of Cu specific surface area average 190 m^2/g and was lower than for Ag/Cu-TiO_2_2 containing 0.5 mol.% of Ag and 1.5 mol.% of Cu with BET surface area average 209 m^2/g. However, it is known from the literature that for visible irradiation, the surface area is not as crucial as the size of noble metal, as was already shown for Ag-TiO_2 composites [12]. The obtained results indicated that rather other parameters, such as silver or copper presence, cause their enhancement in photoactivity than the surface area.

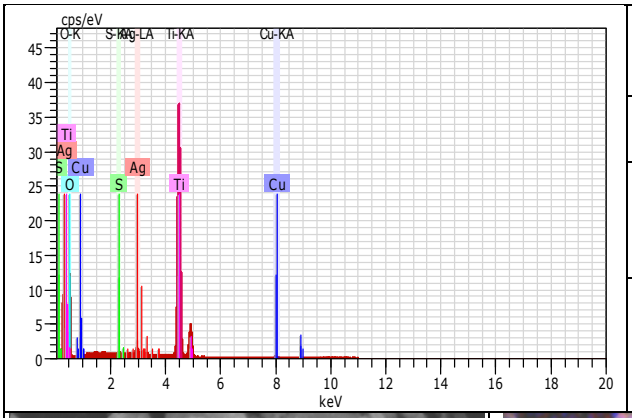

Ag/Cu-TiO_2_1 sample Components (mass percent)			
O [%]	Ti [%]	Ag [%]	Cu [%]
36.41	59.39	1.40	1.55
37.23	57.09	1.45	1.41

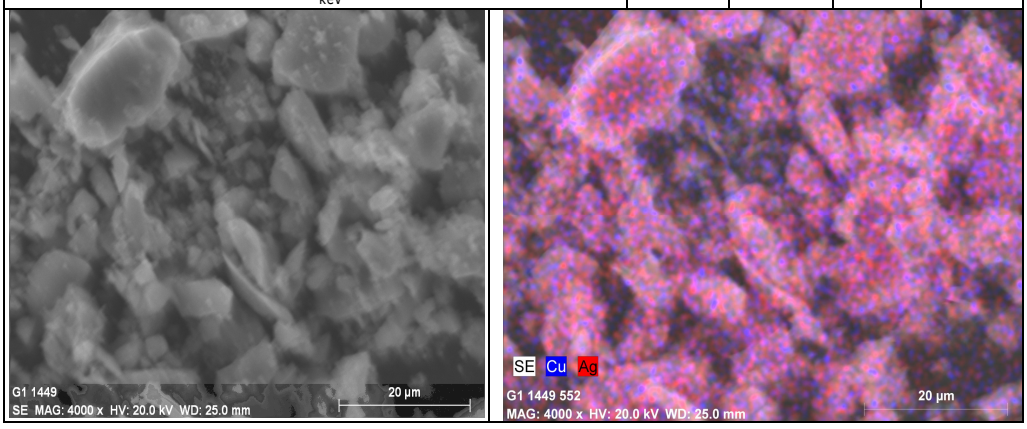

Fig. 3. SEM image and elemental mapping of Ag/Cu-TiO_2_1 nanoparticles prepared by microemulsion method

Microstructures of the obtained nanocomposites and their surface morphologies were studied by SEM equipped with EDS. SEM images and EDS mappings of silver-copper composite material in the TiO_2 matrix for sample Ag/Cu-TiO_2_1 (containing 1.5 mol% of silver and 0.5 mol% of copper) and Ag/Cu-TiO_2_4 (containing 6.5 mol% of silver and 0.5 mol% of copper) are given in Fig. 3. and Fig. 4, respectively. From elemental mapping mode highly and uniformly dispersed Ag/Cu nanoparticles on the TiO_2 support were observed. This implied good interaction between dopant and support in microemulsion preparation method. Since the EDS mapping were scanned from the surface, composition of elements correspond to the surface composition of the structure.

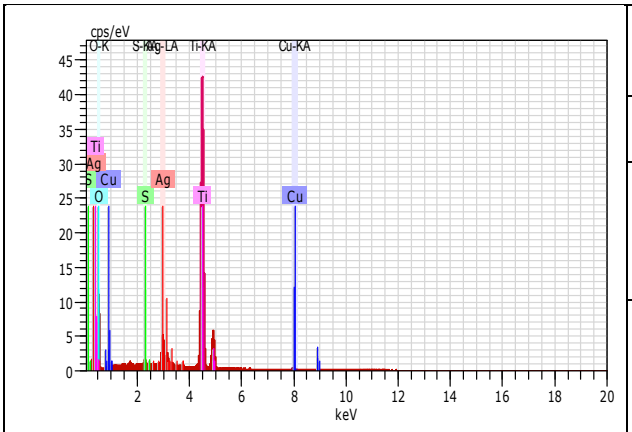

Ag/Cu-TiO_2_1 sample Components (mass percent)			
O [%]	Ti [%]	Ag [%]	Cu [%]
37.56	53.96	5.34	1.40
38.91	51.18	5.36	1.31

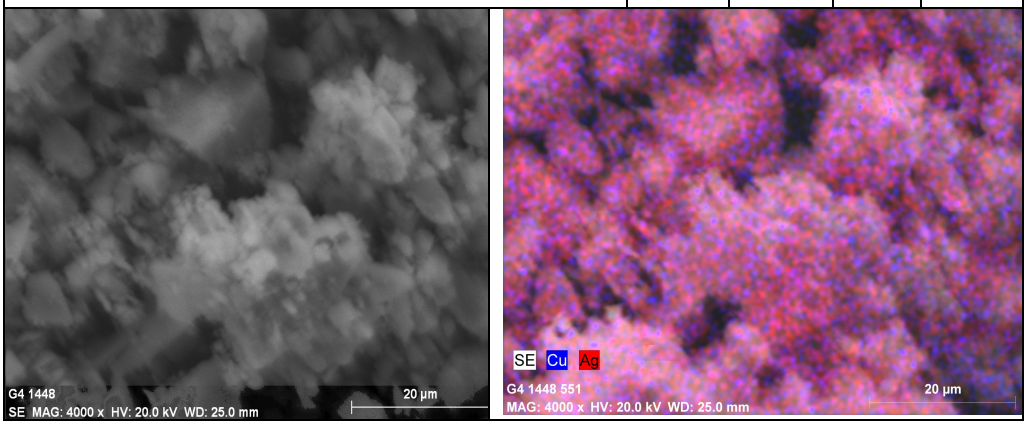

Fig. 4. SEM image and elemental mapping of Ag/Cu-TiO_2_4 nanoparticles prepared by microemulsion method

Since molar ratio of Ag to Cu used during synthesis equaled to 13 and 3 for sample Ag/Cu-TiO_2_4 and Ag/Cu-TiO_2_1, respectively, the higher surface concentration of silver was observed for the sample Ag/Cu-TiO_2_4.

3.3. Photocatalytic activity of Cu-TiO_2 and Ag/Cu-doped TiO_2 under visible light

The photocatalytic activity of the metal-doped TiO_2 nanoparticles was evaluated by measuring the decomposition of phenol. No phenol was degraded in the absence of illumination indicating that there was no dark reaction at the surface of Cu-TiO_2. Also the reference test in the absence of photocatalysts under visible light showed the lack of phenol degradation. The efficiency of phenol degradation after 80 min. illumination by visible light in the presence of Cu-TiO_2 nanoparticles are presented in Table 1. The rate of phenol degradation as a function of mol% of Cu is presented in Fig. 5. The photodegradation efficiency under visible light increased with the increase in the copper loading up to 0.5 mol % and then decreased. The rate of phenol decomposition measured in the presence of the sample Cu-TiO_2_2 after 60 min. of irradiation average 0.94 μmol/min. Thus, it was observed that optimum Cu loading for this preparation method was between 0.5 and 1.0 mol.%. Our results are in good agreement with others. Xin. et al. observed that over 0.06 mol% Cu-TiO_2, the degradation of RhB ratio is the highest. The Cu-TiO_2 photocatalyst containing about 0.06 mol% of Cu possess abundant electronic trap, which effectively inhibits the recombination of photoinduced charge carriers, improving the photocatalytic activity of TiO_2 [13].

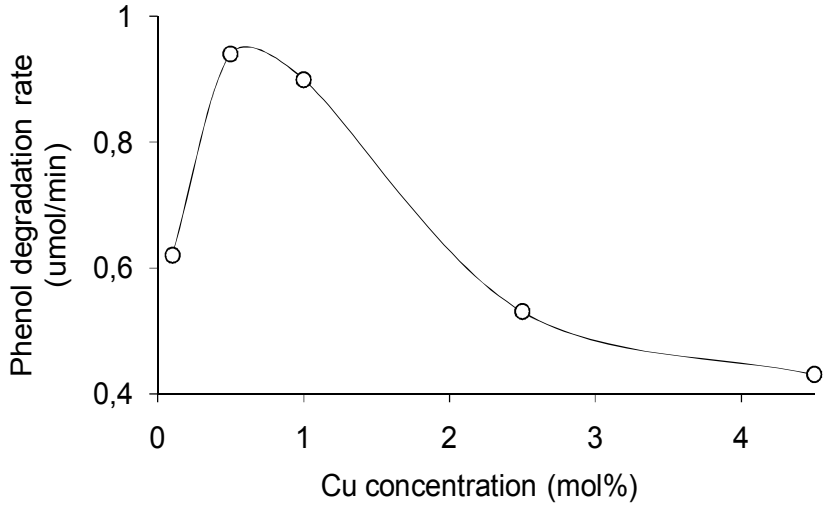

Fig. 5. Degradation rate for phenol v.s. mol% of Cu/TiO_2

For the purpose of increasing the efficiency of phenol degradation under visible light the bimetallic Ag/Cu and Au/Cu nanoparticles were prepared for modification of TiO_2 surface. Previously we have also obtained Ag/Au-modified TiO_2 nanoparticles which exhibited higher photodegradation rate in visible region than both Ag-TiO_2 and Au-TiO_2 photocatalysts. Therefore the synergistic effect of gold and silver nanoparticles on photocatalytic activity of Cu-TiO_2 nanoparticles in visible light was also expected. The efficiency of phenol degradation in the presence of pure TiO_2 and Ag/Cu-doped TiO_2 nanoparticles are presented in Table 1 and Fig. 6.

The maximum in the photocatalytic activity under visible light was observed for sample containing 0.5 mol % of Cu and 1.5 mol% of Ag. The rate of phenol decomposition average 2.41 μmol/min and was higher than for Ag/Cu-TiO_2_2 containing 1.5 mol% of Cu and 0.5 mol% of Ag. It indicates that silver present was more beneficial for visible light activation of TiO_2 doped photocatalysts than higher copper amount.

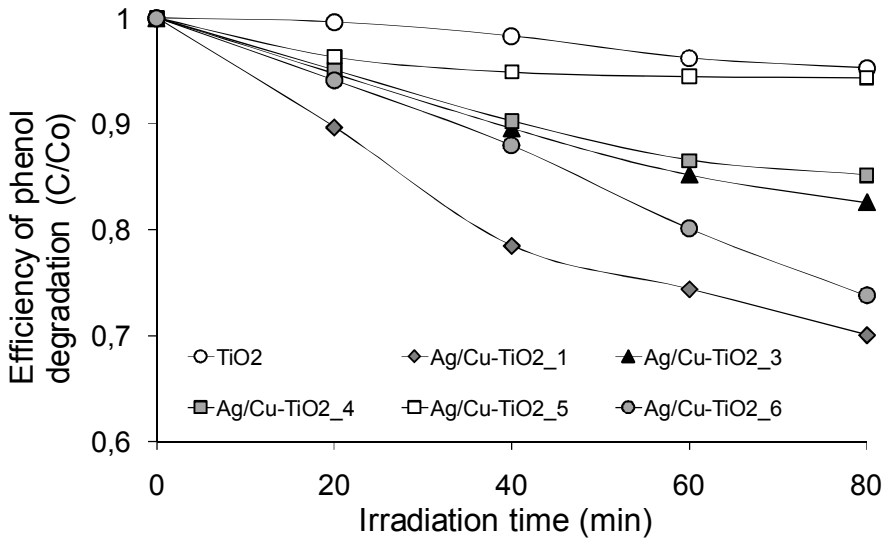

Figure 6. Efficiency of phenol photodegradation in the presence of Ag/Cu-doped TiO_2 under visible light (λ>400 nm). Experimental conditions: Co=0.21 mM, m (TiO_2)=125 mg, T=10˚C, Qair=5 l/h

Compared to Ag/Cu-TiO_2_1 photocatalyst the degradation rate decreased to 2.25 μmol/min, 1.36 μmol/min and 1.22 μmol/min for the Ag/Cu-TiO_2 containing 4.5 mol%, 0.5 mol% and 6.5 mol% of silver, respectively. The Au/Cu-TiO_2 nanoparticles revealed lower photocatalytic activity compared to Ag/Cu-TiO_2 photocatalysts containing the same metal amount loading on TiO_2 surface (see Table 1 samples Ag/Cu-TiO_2_3 and Au/Cu-TiO_2_1).

3.4. Antimicrobial susceptibility testing method (MIC)

It has been well known that silver and copper possesses strong antibacterial activities both as metal nanoparticles and ions. Determining the MIC values of antibacterial agents is a valuable means for comparing the antibacterial effectiveness of the agents. The MIC values were the lowest concentration of Cu-TiO_2 and Ag/Cu-TiO_2 in aqueous solution that inhibited visual growth after 24 h of incubation. Thus, lower MIC value means higher bioactivity.

Table 2. Minimum inhibitory concentration (MIC) of Ag/Cu-doped TiO_2 nanoparticles

Type of micro organism	Microbial Strains	MIC for Ag/Cu-TiO_2 [μg/ml]						MIC for Cu-TiO_2 [μg/ml]				TiO_2
		1	2	3	4	5	6	1	2	3	4	
Yeast	*Candida albicans* ATCC 10231	250	500	500	125	1000	250	>1000	>1000	>1000	>1000	>1000
	Candida glabrata DSM 11226	250	500	500	125	1000	250	>1000	>1000	>1000	>1000	>1000
	Candida tropicalis KKP 334	250	500	500	62	500	125	>1000	>1000	>1000	>1000	>1000
	Saccharomyces cerevisiae ATCC 9763	62	250	250	31	500	125	1000	500	>1000	>1000	>1000
	Saccharomyces cerevisiae JG	62	125	125	16	250	125	1000	>1000	>1000	>1000	>1000
Bacteria	*Escherichia coli* ATCC 10536	250	500	500	62	1000	250	>1000	>1000	>1000	>1000	>1000
	Staphylococcus aureus ATCC 6538	250	500	500	62	1000	250	>1000	>1000	>1000	>1000	>1000

The minimal inhibitory concentration of microorganism growth for as-prepared Ag/Cu-TiO_2 nanocomposites was estimated using bacteria *Escherichia coli* and *Staphylococcus aureus*, yeast *Saccharomyces cerevisiae* and pathogenic fungi belonging to *Candida* family. The effect of silver and copper loading on MIC value is presented in Table 2. For Cu-TiO_2_5 loaded with 4.5 mol.% of Cu, the inhibition in microorganisms growth was not observed even for photocatalyst concentration below 500 μg/ml. The minimal inhibition concentration differed from 62 to 1000 μg/ml, depending on microbial strain and metal concentration. The photocatalysts doped with

silver revealed higher antimicrobial activity than pure TiO_2 obtained in microemulsion system or samples containing only copper nanoparticles deposited on TiO_2 surface. It indicated that silver possess higher antimicrobial activity than copper nanoparticles prepared in microemulsion system. The best antimicrobial activity revealed Ag/Cu-TiO_2_4 with highest silver amount average 6.5 mol% and sample Ag/Cu-TiO_2_1 containing 1.5 mol% of Ag and 0.5 mol% of Cu, which exhibited also the highest efficiency of phenol degradation under visible light as shown in Table 1 and Fig. 6.

4. CONCLUSIONS

The Cu-TiO_2 and Ag/Cu-TiO_2 nanoparticles have been prepared using a water-in-oil microemulsion system of water/AOT/cyclohexane. It was found that obtained nanocomposites contained highly and uniformly dispersed Ag/Cu nanoparticles on the TiO_2 surface. XRD and the BET measurements corroborate that these doped materials are made up of the anatase crystalline phase and have high surface areas fluctuating from 161 to 223 m^2/g depending on metal loading on TiO_2 surface. The photodegradation efficiency under visible light increased with the increase in the copper loading up to 0.5 mol % and then decreased. The maximum in the photocatalytic activity under visible light was observed for sample containing 0.5 mol % of Cu and 1.5 mol% of Ag. The rate of phenol decomposition average 2.41 μmol/min. The antimicrobial susceptibility was tested using bacteria *Escherichia coli* and *Staphylococcus aureus*, yeast *Saccharomyces cerevisiae* and pathogenic fungi belonging to *Candida* family. The photocatalysts doped with silver revealed higher antimicrobial activity than samples containing only copper nanoparticles deposited on TiO_2 surface. It indicated that silver posses higher antimicrobial activity than copper nanoparticles prepared in the same microemulsion system. This study suggested that Ag/Cu-TiO_2 nanoparticles can be used as effective antimicrobial agent for reduction the spread of infections in commercial facilities.

ACKNOWLEDGMENTS

This research was financially supported by Polish Ministry of Science and Higher Education grant No. N N507 272136, by the European Union in the framework of the European Social Fund. The system project of the Pomorskie Voivodeship "InnoDoktorant - Scholarships for PhD students, II edition.

REFERENCES

[1] K. KAWAHARA, K. SUZUKI, Y. OHKO, T. TATSUMA, Phys . Chem. Chem. Phys . 7 (2005) 3851 – 3855.
[2] KOWALSKA E., ABE R., OHTANI B., Chem. Commun., 2 (2009), 241-43
[3] ISHIBAI Y., SATO J., NISHIKAWA T., MIYAGISH S., Appl. Catalal. B: Environmental, 79 2 (2008) 117-121
[4] COLÓN G., MAICU M., HIDALGO M.C., NAVIÓ J.A., Appl. Catal. B: Environmental 67 (2006) 41–51
[5] SONAWANE R.S., KALE B.B., DONGARE M.K., Materials Chemistry and Physics 85 (2004) 52–57
[6] IKEDA S., SUGIYAMA N., PAL B., MARCI G., PALMISANO G., NOGUCHI H., UOSAKI K., OHTANI B., Phys . Chem. Chem. Phys., 3 (2001) 267-273
[7] ZALESKA A., SOBCZAK J.W., GAZDA M., GRABOWSKA E., HUPKA J, Appl. Catal. B 469-475
[8] GÓRSKA P., ZALESKA A., HUPKA J., Sep Purif. Technol. 68 (2009) 90· 96
[9] BAMWENDA G.R., TSUBOTA S., NAKAMURA T., HARUTA M., J. Photochem. and Photobio. A: Chem., 89 (1995) 177
[10] HAMAL D. B., K. J. KLABUNDE, J. Colloid Interf. Sci. 311 (2007) 514–522.
[11] KELEHER J., BASHANT J., HELDT N., JOHNSON L. and LI Y., World J. Microbiol. Biotechnol. 18 (2002) 133–139.
[12] ZIELIŃSKA A., KOWALSKA E.,, SOBCZAK J.W., ŁĄCKA I., GAZDA M., OHTANI B., HUPKA J., ZALESKA A., Sep. Purif Technol. (2010) doi 10.1016/j.seppur.2010.03.002
[13] XIN B., WANG P., DING D., LIU J., REN Z., FU H., Appl Surf Sci, 254 (2008) 2569–2574.

Physicochem. Probl. Miner. Process. 45(2010) 127-140

journal homepage
www.minproc.pwr.wroc.pl/journal/

Physicochemical Problems of Mineral Processing

Index No. 32213X ISSN 1643-1049

Justyna ZIEMIAŃSKA *, Ewa ADAMEK *, Andrzej SOBCZAK *,
Ilona LIPSKA *, Andrzej MAKOWSKI *, Wojciech BARAN *

THE STUDY OF PHOTOCATALYTIC DEGRADATION OF SULFONAMIDES APPLIED TO MUNICIPAL WASTEWATER

Received March 16, 2010; reviewed; accepted May 4, 2010

A photocatalytic process of degradation of the selected sulfonamides (sulfathiazole, sulfamethoxazole and sulfadiazine) added to real wastewater was studied in this work. The process was initiated by UV-a irradiation and TiO_2-P25, $FeCl_3$ and mixtures of TiO_2-P25 with $FeCl_3$ were used as photocatalysts. The effect of pre-treatment of wastewater and the influence of process parameters on the efficiency of sulfonamides removal were also determined. It was found that the highest efficiency of degradation was achieved in the process carried out in the presence of TiO_2-P25/$FeCl_3$ mixture, in full scale effluent wastewater treatment plant..

keywords: sulfonamides, photocatalysis, wastewater treatment, TiO_2, $FeCl_3$

1. INTRODUCTION

Recently, there has been an increasing concern, particularly in highly developed countries, about penetration of pharmaceuticals into the environment and related risks [1-6]. This penetration is caused, among others, by a very high consumption of drugs by societies in these countries and by the growing, unfavourable results of

* Medical University of Silesia, Faculty of Pharmacy Chemistry, 4 Jagiellońska Str.,41-200 Sosnowiec, bw-xxl@wp.pl (W. Baran)

pharmaceuticals' presence in the environment [2]. It is estimated that there are approx. 200 000 pharmaceuticals on the world market, and the quantity of available preparations in individual countries can even achieve the number of 10 000 [7]. At present, the world consumption of pharmaceuticals in medicine and veterinary medicine is estimated at 100 000 t annually [8]. According to other sources, only the antibiotics use ranges from 100 000 to 200 000 t annually in the world, of which 50 to 75% is used in the veterinary prophylaxis and/or as growth promoters in animal breeding [6]. Sarmah et al. [9] have reported that in different countries, sulfonamides (SNs) represent from 2% (USA) to 22% (UK, Kenya) of used veterinary antibiotics. Particular concern is growing from the fact that residues of these pharmaceuticals can easy penetrate to the environment, which has been proved by the data derived from systematic monitoring [2,3,6,7,9]. Almost 100% of samples taken recently from various parts of the hydrosphere contained trace concentrations (mostly below 1 $\mu g\ l^{-1}$) of sulfonamides [6]. Antibiotics, including sulfonamides, in the concentrations below the lethal level are a serious risk to health and to the environment due to the generation of drug-resistance of pathogenic bacteria and bacterial resistance to disinfection products [10].

The reasons described above caused that the methods for elimination of antibiotics from sewage have been intensively sought for several years. The effectiveness of traditional methods (biodegradation, coagulation, sedimentation) is often low or very low [2,3,5,11]. Simultaneously, Turkdogan and Yetilmezsoy [12] have found that the removal efficiency of antibacterial drugs from biosphere during the routine, biological processes was estimated a little above 20%. Scientists have great hopes for the techniques of advanced oxidation processes (AOP) particularly in oznonation [2,13,14] and photocatalytic degradation [13-20]. The use of this technique for treatment of municipal or farm sewage allows to decompose organic substances and medicines present in this type of waste, as a result of oxygenation using hydroxyl radicals ($HO^{\bullet}$) generated in the reaction environment. Many researches have described a mechanism and a kinetics of sulfonamides degradation in the presence of hydroxyl radicals [16,17,20]. It was found that during the initial step of photocatalytic process a decrease in toxicity and a significant increase in biodegradability of solutions containing sulfonamides were observed [21]. Since intermediates of photocatalytic process are chemically and biologically less stable than the initial substrates, the increase of COD and BOD_5 is often observed in the irradiated solutions [22]. The photocatalytic process can lead to the total mineralization of organic substances however it is unfounded from the economic point of view. The further biodegradation of the residual organic products seems to be more correct and well founded. A combination of both processes, namely photocatalysis and biodegradation, should lead to a decrease in the toxicity, the microbial activity as well as to a decrease of COD and BOD_5 in wastewater containing antibiotics [21]. The above mentioned results were obtained in the experiments using sulfonamides solutions in distilled water.

Many of the cited papers have presented the results of experiments concerning the photocatalytic degradation of sulfonamides in the presence of commercial TiO_2-P25 as a catalyst. However, our previous results showed that the efficiency of sulfonamides photodegradation can be considerably higher using Fe(III) salts as a photocatalyst (e.g. $FeCl_3$ [19,20]) than in the presence of TiO_2 alone In these solutions, Fe(III) ions are partly hydrolyzed and in the result, the photoactive $Fe(OH)^{2+}$ ions are formed. After absorption of UVa light by these ions, hydroxyl radicals are generated in solutions [20,23]. The high photocatalytic activity of Fe(III) salts was confirmed in the experiments reported by other researchers [24,25]. According to Mestankova et al. [26] the simultaneous use of TiO_2 and $FeCl_3$ mixture probably cause an increase in efficiency of the photocatalytic system due to the synergic effect. This fact was confirmed experimentally during the photocatalytic decoloration of real tannery wastewater [22].

The aim of the work was determination of the possibility of using photocatalytic process to degradation of selected sulfonamides added to real wastewater and this method optimization.

2. MATERIALS AND METHODS

2.1. Reagents

The characteristics of the investigated sulfonamides are presented in Table 1.

Table 1. The characteristics of investigated SNs

Sulfonamides	Abbr. in text	Structure	pKa_1 [a]	pKa_2 [a]	k_{OH} [b] ($l\ mol^{-1}\ s^{-1}$)	C_o [c] ($mmol\ l^{-1}$)	t_R [d] (min)	LOD [e] ($mmol\ l^{-1}$)
Sulfamethoxazole	SMX	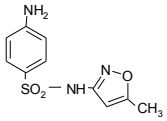	1.60	5.81	$(5.8 \pm 0.2) \cdot 10^9$	0.050	7.49	$1.7 \cdot 10^{-5}$
Sulfadiazine (natrium salt)	SDZ	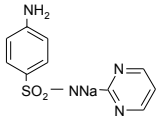	2.00	6.48	$3.7 \cdot 10^9$	0.025	3.48	$1.1 \cdot 10^{-5}$
Sulfathiazole (natrium salt)	STZ	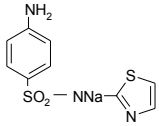	2.36	7.23	$(7.1 \pm 0.2) \cdot 10^9$	0.025	12.66	$2.0 \cdot 10^{-5}$

[a] $SNsH_2^+ \xleftarrow{Ka_1} SNsH \xleftarrow{Ka_2} SNs^-$ [b] reaction rate constant for SNs with $HO^\bullet$ [27,28]

[c] initial concentration of SNs in experiments [d] retention time for mobile phase flow 1.0 ml min^{-1}

[e] limit of detection for injection samples at volume 50 µl

All SNs used throughout this study were of analytical grade and were manufactured by Sigma. Just before experiments, weighed amounts of each sulfonamide were added to wastewater or distilled water and samples were intensively mixed. The theoretically initial concentrations of sulfonamides in samples are shown in Table 1. Titanium(IV) dioxide (TiO_2-P25) obtained from Evonic Degussa GmbH and iron(III) chloride ($FeCl_3$) purchased from POCH were used as photocatalysts. These compounds were selected based on preliminary experiments concerning the photocatalytic degradation of sulfonamides in aqueous solutions [20,21]. Hydrochloric acid (HCl) was added to wastewater samples in order to adjust the pH at a desire value. In our earlier studies, we did not observe significant changes in the sulfonamides concentration in solutions irradiated in the presence of HCl.

2.2. Wastewater samples

The wastewater samples were taken from sewer system that conveys domestic and urban waste to wastewater treatment plant (WWTP) Zagórze in Sosnowiec (Poland). Samples were stored at temperature below -18°C. The characteristics of used wastewaters are presented in Table 2. The synthetic wastewater was prepared on the base ISO 9887:1992(E) (Table 3) [29].

Table 2. The characteristics of used wastewater samples

	Influent	Effluent
pH	7.58-7.92	7.10-7.66
COD (mg O_2 l^{-1})	611-902	137-774
BOD_5 (mg O_2 l^{-1})	152-199	60-89
Conductivity (mS cm^{-1})	0.508-1.789	1.204-1.722
Turbidity (FTU)	40-145	4-50
$Abs_{254\ nm}$	0.380-0.752	0.196-0.346

Table 3. Chemical composition of the synthetic municipal wastewater

Chemicals	Concentration (mg l^{-1})
Peptone	160
Meat extract	110
Urea	30
K_2HPO_4	28
NaCl	7
$CaCl_2 \cdot 2H_2O$	4
$Mg_2SO_4 \cdot 7H_2O$	2

Before beginning the experiments, the samples were stored at room temperature for 1 day. The investigated SNs were not detected in wastewater in the concentration above the detection limit (LOD).

2.3. Conditioning of wastewater samples

The wastewater samples (before SNs addition) were stored in glass adsorption bulbs (250 ml) enabling barbotage for 7 days at 20.4±0.9°C. During the whole experiments, samples were aerated by a continuous airflow (0.41± 0.14 ml s^{-1}). The concentration of oxygen dissolved in wastewater was about ~ 100%.

2.4. Microfiltration of wastewater samples

The wastewater samples (without SNs) were vacuum-filtered using vacuum filtration system (J.T.Baker) with z Milipore HVPL membrane filter (0.45µm, 47 mm) and vacuum pump AgaLabor PL2. The mean speed of filtration was 2.8 ml s^{-1} and the maximum partial vacuum was 0.09 MPa.

2.5. Coagulation of wastewater samples

The coagulation of wastewater samples (before SNs addition) was carried out in beakers (250 ml). Aliquots (4 ml) of the coagulant ($FeCl_3$ stock solution at concentration of 1 mol l^{-1}) were added to 200 ml of wastewaters and mixtures were mixed using compressed air. After the addition of the coagulant, pH of samples was 6.26. After 5 min, the mixing was finished and samples were left in order to settle the sediments. Aliquots of solution were collected from above the sediment and were used in further experiments

2.6. Irradiation

Before irradiation a solid TiO_2 and/or $FeCl_3$ stock solution was added to wastewater or distilled samples containing sulfonamides (Tab. 1). The pH of the irradiated samples was adjusted with concentrated HCl or NaOH solutions (<1 ml). Next, mixtures were homogenized in dark for 30 min by means of magnetic stirrers. The catalyst concentrations are presented in Table 4. In all experiments, open glass crystallizers (volume: 500 ml, exposed surface: 102 cm^2) containing 100 ml of samples were irradiated by four UV lamps (Philips TL-40 W/05 at λ_{max} 366 nm). The intensity of radiation, determined by Parker's actinometer was $5.25 \cdot 10^{-7}$ Einstein $min^{-1}cm^{-2}$ [30]. During the irradiation, mixtures were magnetically stirred and had free contact with air. The temperature of samples was 21-24°C.

2.7. Analytical methodology

After the appropriate irradiation time samples were centrifuged (30 min, 4000 RPM). Before and after irradiation, the concentration of sulfonamides in mixtures was determined using HPLC (column Supelcosil Suplex pKB-100 LC-18, 5 mm, 250 mm x 4.6 mm, detectors Waters TAD 486, λ = 254 nm) and mobile phase K_2HPO_4 (pH 8.2)/CH_3CN in the ratio 95:5. The retention time and LOD value of SNs are shown in Table 1. The pH and concentration of oxygen dissolved in irradiated samples were measured by multimeter HD22569.2 (Delta OHM).

2.8. Analysis of results

Removal of individual SNs was calculated according to the equation:

$$Y_i = 100 \cdot (1 - \frac{C_i}{C_o})$$

where: Y_i is the removal of SDZ, SMX or STZ (%), C_o is the initial concentration of SDZ, SMX or STZ (in standard solution), C_i is the final concentration of SDZ, SMX or STZ (in samples). Removal of SNs sum was calculated as follows:

$$Y_{SNs} = \sum x_i Y_i$$

where x_i is the mole fraction of investigated sulfonamides. The reaction rate constant *(k)* values were determined as a slope of linear relationship:

$$\ln \frac{C_i}{C_o} = -k^I t + b \text{ (the first-order reaction kinetics)}$$

$$\frac{1}{C_i} = k^{II} t + b \text{ (the second-order reaction kinetics)}$$

where t is the irradiation time, b is a free term of the equation. The initial reaction rate (r_o) values were calculated using the formula:

$$r_o^{\ I} = k^I C_o \text{ (the first-order kinetics)}$$

$$r_o^{\ II} = k^{II} C_o^{\ 2} \text{ (the second-order kinetics).}$$

3. RESULTS AND DISCUSSIONS

3.1. The comparison of photocatalytic activities of selected photocatalytic systems (TiO_2, TiO_2/HCl, $FeCl_3$/HCl, and TiO_2/$FeCl_3$/HCl)

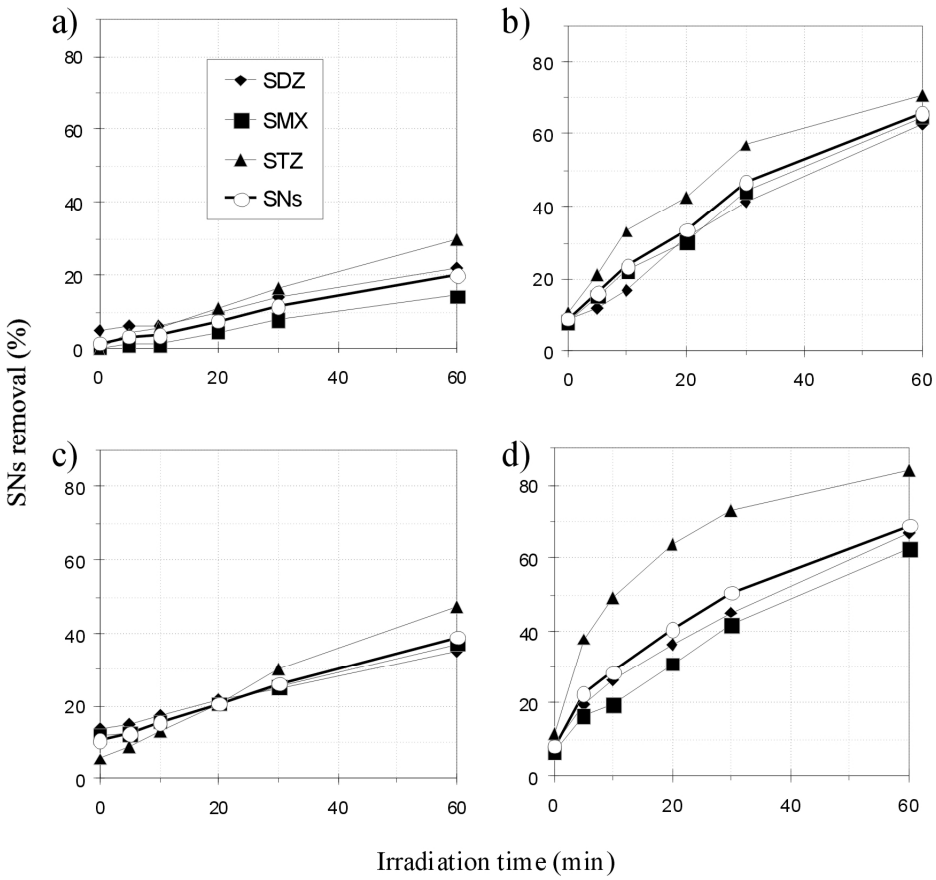

Fig. 1. The dynamics of photocatalytic degradation of SNs added to influent samples during irradiation with TiO_2 (a); TiO_2/HCl (b); $FeCl_3$/HCl (c); and TiO_2/$FeCl_3$/HCl (d)

The dynamics of photodegradation of SNs in the spiced samples of influent in the presence of TiO_2, TiO_2/HCl, $FeCl_3$/HCl and TiO_2/$FeCl_3$/HCl were also studied. The results are showed in Fig. 1. Table 4 shows the reagent concentrations, pH and the initial reaction rate.

HCl was added in order to adjust the optimal pH value for the photoactivity of Fe-salts (based on the literature data [20,23]). No significant changes in the sulfonamides

concentration were observed after irradiation of samples with HCl only.

The decrease in sulfonamides concentration by about 10% was observed in all samples at pH~ 3 (Fig. 1b,c,d), before the beginning of irradiation. Since the influent samples were centrifuged before analysis, the decrease in their concentration was caused by the adsorption of SNs on the suspension particles.

Table 4. The results of initial photocatalytic degradation rate of sulfonamides in spiced influent

Concentration			pH	Initial photocatalytic degradation rate (mmol $l^{-1}min^{-1}$)			
TiO_2 ($g\ l^{-1}$)	$FeCl_3$ (mmol l^{-1})	HCl[a] (mmol l^{-1})		SDZ	SMX	STZ	SNs
0.5	-	-	7.86	$(0.83\pm0.10)\cdot10^{-4}$	$(1.35\pm0.15)\cdot10^{-4}$	$(1.45\pm0.15)\cdot10^{-4}$	$(3.63\pm0.40)\cdot10^{-4}$
0.5	-	5-20	3.00	$(3.83\pm0.38)\cdot10^{-4}$	$(8.05\pm0.80)\cdot10^{-4}$	$(1.18\pm0.10)\cdot10^{-3}$	$(2.36\pm0.21)\cdot10^{-3}$
-	1.0	2-14	3.01	$(1.18\pm0.05)\cdot10^{-4}$	$(2.90\pm0.20)\cdot10^{-4}$	$(5.00\pm0.25)\cdot10^{-4}$	$(9.08\pm0.50)\cdot10^{-4}$
0.5	1.0	2-13	2.98	$(4.10\pm0.30)\cdot10^{-4}$	$(7.60\pm0.40)\cdot10^{-4}$	$(2.13\pm0.07)\cdot10^{-3}$ [b]	$(3.30\pm0.10)\cdot10^{-3}$
2.5	1.0	2-12	3.00	$(4.56\pm0.33)\cdot10^{-4}$	$(7.12\pm0.79)\cdot10^{-4}$	$(7.15\pm0.29)\cdot10^{-3}$ [b]	$(8.32\pm0.40)\cdot10^{-3}$
0.5	3.0	~5[c]	3.00	$(2.21\pm0.15)\cdot10^{-4}$	$(2.40\pm0.10)\cdot10^{-4}$	$(1.83\pm0.11)\cdot10^{-3}$ [b]	$(2.29\pm0.14)\cdot10^{-3}$

[a] HCl was added in order to adjust pH values in samples
[b] calculated based on the second-order kinetics equation
[c] one sample of wastewater was examined only

Further decrease in the SNs concentration occurred during the longer irradiation time. In this case it is most probably caused by the degradation of SNs only. It was found that the photodegradation of SNs in the presence of TiO_2/HCl (Fig. 1b) and TiO_2/$FeCl_3$/HCl (Fig. 1d) was the most effective. Second of the catalytic system is characterized by the high initial rate of STZ photodegradation that follows the second-order kinetics. In the cases of SDZ and SMX, the photocatalytic process is described by first-order reaction kinetics. Similar results were obtained during studies concerning the photocatalytic degradation of SNs in aqueous solutions [20]. The comparison of the propagation rate with the use of SNs and $HO^{\bullet}$ radicals (Table 1) does not explain these differences. Most probably, the photodegradation of STZ in the presence of TiO_2/$FeCl_3$/HCl differs from the degradation of SDZ and SMX with the use of the same catalyst during the initiation step. However, unequivocal explanation of this effect

requires further studies. The described above change in the reaction order causes that the comparison of the photocatalytic process based on the estimation of the initial reaction rate only may be incorrect. During irradiation, the second-order reaction rate slows down more than the first-order one. At the beginning of irradiation the STZ photodegradation was about 6 times faster in the presence of $TiO_2/FeCl_3/HCl$ than with TiO_2/HCl. However, after 60 min of irradiation the change in the removal degree of STZ from wastewater was 13% only (Figs. 1b and 1d). It is worth to mention that the high degradation level of all SNs will be very possible after long-lasting irradiation time. Based on the theoretical calculations and determined experimentally the reaction rate constants it was estimated that the irradiation time necessary to degrade SDZ, SMX and STZ on the level of 90% in influent irradiated with $TiO_2/FeCl_3/HCl$ under the used conditions may be 133, 146 and 105 min, respectively. Moreover, based on the comparison of the initial rate of SNs degradation (Table 4) and the time necessary to obtain the high degradation level, $TiO_2/FeCl_3/HCl$ was selected as the optimum photocatalytic systems for this photodegradation process. It is also important that this catalyst system can be easy separated from the reaction medium [31].

An increase of TiO_2 concentration in $TiO_2/FeCl_3/HCl$ mixture caused a significantly increase in the degradation rate of STZ but it did not observe a large effect on the r_o values for SDZ and SMX. This phenomenon is thoroughly explained in the next section. On the other hand, the increase of $FeCl_3$ concentration (to 3.0 mmol l^{-1}) in $TiO_2/FeCl_3/HCl$ mixture caused only decrease in the reaction rates of all selected SNs. In the case of SMX the r_o value decreased almost 3 times (Table 4) but at present no clear explanation to observed dependence may be given. .

3.2. Influence of pH on the photocatalytic degradation rate of SNs

In photocatalytic processes carried out under heterogeneous conditions, the pH of irradiated mixtures has an influence on the surface charge of the catalyst. Moreover, this value decides about products of $FeCl_3$ hydrolysis and the charge of sulfonamides. Potentially, the best results for heterogeneous catalysis can be achieved in process in which substrates and the photocatalyst surface have opposite charges. Figure 2 shows the influence of pH on the photodegradation of SNs in the presence of TiO_2 or $TiO_2/FeCl_3$ in wastewater influent. The pH values were corrected by the addition of concentrated solutions of HCl or NaOH.

The results for wastewater influent samples are significantly different from results for distilled water [20]. In experiments with the use of distilled water, a decrease in pH caused a decrease in the photodegradation rate of sulfonamide in the presence of TiO_2 while in the presence of $TiO_2/FeCl_3$ it was showed the apparent maximum rate at pH about 3. On the other hand in wastewater the r_o values increased with the increase of acidification of irradiated samples. The decrease in pH had a strong effect on the

degradation rate of STZ and only slight influence on the r_o value for SDZ. In turn, in the presence of TiO_2 the photodegradation of SMX proceeded with the constant rate in the pH range of 3-5.5 but in the presence of $TiO_2/FeCl_3$ a high degradation rate was observed only at pH about 3.

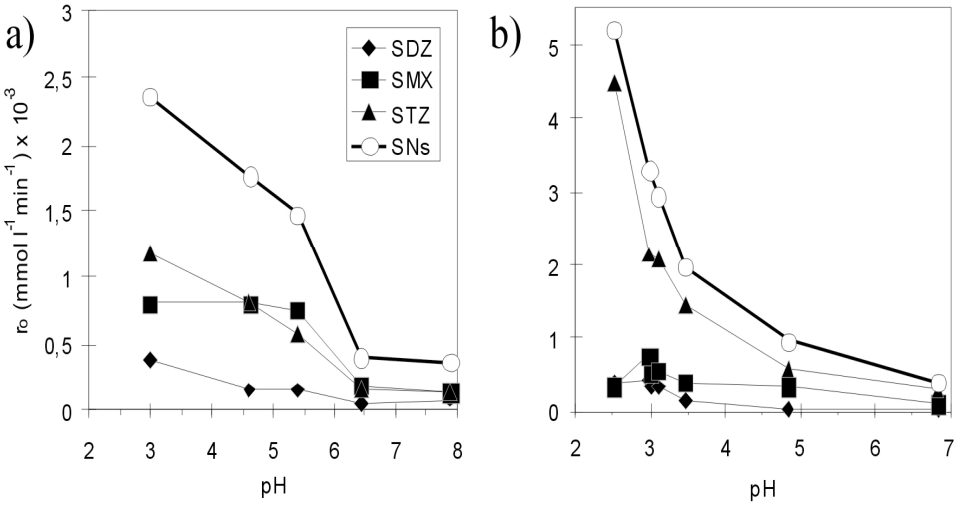

Fig. 2. The effect of pH on the photocatalytic degradation of SNs added to influent samples during irradiation with TiO_2 (a) and $TiO_2/FeCl_3$ (b)

The results described above imply that mainly H^+ ions effect on the degradation rate of STZ. Based on the comparison of pKa_1 for the selected SNs (Table 1) it is clear that the concentration of $SNsH^+$ ions in the acidic medium increases from SMZ to STZ. Moreover, it is possible that $STZH^+$ ions after adsorption onto TiO_2 surface take part in a direct photocatalytic process as acceptors of excited electrons. Fujishima et al. have reported that cations can undergo the sorption onto TiO_2 surface [32]. It confirms our results (Table 4) concerning the increase in the degradation rate of SMX after the increase in TiO_2 concentration. However, this hypothesis should be confirmed by further experiments, including identification and quantitative determination of products of SMX degradation. Results obtained for SMZ and SDZ photodegradation in the presence of $TiO_2/FeCl_3$ implies that $Fe(OH)^{2+}$ ions have a significant effect on their degradation. STZ, as distinct from SMX and SDZ, is relatively easy to biodegrade. Thus from the practical viewpoint, the more important is the choice of suitable conditions for the effective removal of SMX and SDZ. Therefore, the following process conditions were selected as the optimum ones for the degradation of SNs: TiO_2 (0.5 g l^{-1}), $FeCl_3$ (1.0 mmol l^{-1}), pH ~ 3. The economic disadvantage is high consumption of HCl necessary for acidification of samples (Table 4). This effect is caused by high

buffer capacity of wastewater. In experiments with the use of distilled water, the appropriate pH value (about 3) was obtained without the addition of HCl but as a result of $FeCl_3$ hydrolysis. From this reason the search for other methods of modification of the investigated process in order to reduce the consumption of HCl, without the decrease in the photodegradation efficiency, seems to be well founded.

3.3. Effect of preliminary wastewater treatment on the efficiency of photodegradation of sulfonamides

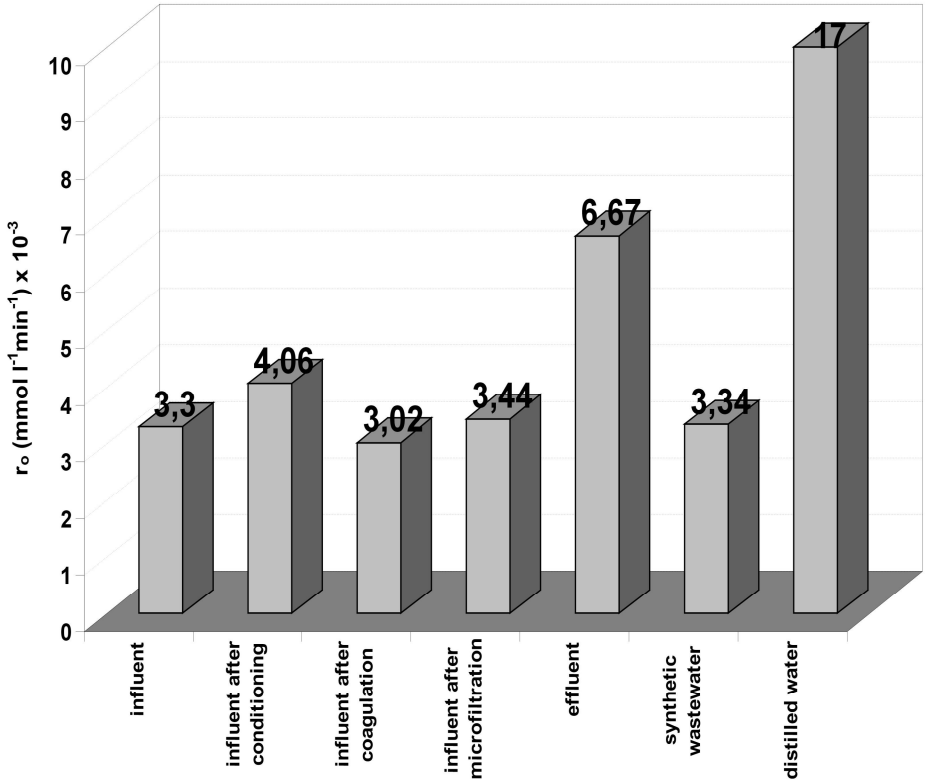

Fig. 3. The assessment of the initial reactions rate (r_o) of SNs photodegradation in spiced real wastewater, before and after pretreatment, in synthetic wastewater and in distilled water with SNs (for the column corresponding to the r_o value for distilled water the scale is not preserved)

In order to decrease of the buffer capacity, wastewater samples were preliminary treated before the photocatalytic process. Then, SNs were added to treated wastewaters and samples were irradiated with $TiO_2/FeCl_3/HCl$ at pH 2.98±0.5. The results obtained, namely the sum of r_o values, are showed in Figure 3.

According to expectations, the photodegradation rate of SNs was in each case

significantly lower in wastewater than in distilled water. Similar results were obtained using the model wastewater.

Microfiltration and coagulation are effective methods in the removal of suspended master and colloids from the aquatic environment. It was observed that the investigated process efficiency did not change in influent samples after microfiltration and coagulation processes (Fig. 3). Probably it is means that small amounts of suspended matter and colloids have no influence on the photodegradation process of SNs. The effectiveness of the elimination of substances forming non ideal solutions during coagulation and microfiltration was low. After these processes the concentration of dissolved organic substances in samples did not decrease considerably. Therefore, the photodegradation rate of SNs is decreased by organic, dissolved in water compounds (e.g. sugars, low-molecular peptides, organic acids and mainly detergents). Due to their significant concentration in wastewater these compounds can compete with SNs for hydroxyl radicals and active centers of catalyst. Negative effect on the SNs photodegradation may also have some inorganic ions with the reduction properties that are presented in insufficient oxygenated wastewater. The concentration of these ions can be decreased using the biodegradation and oxygenation processes proceeded during long-lasting conditioning (simultaneously with wastewater oxygenation) or their treatment w in full scale WWTP. In wastewater samples that were previously conditioned, a slight increase in the photodegradation rate of SNs was observed. By this reason a significant higher photodegradation rate of SNs was in effluent obtained after full scale WWTP (Table 2) than in influent. After 60 min of irradiation of spiced effluent, the degradation degree of SDZ, SMX and STZ was 85.6, 76.9 and 92.7%, respectively whereas the degradation degree of SDZ, SMX and STZ in influent was 67.0, 62.5 and 83.9%, respectively. The observed phenomena can be the confirmation of the above-described thesis. The decrease in the concentration of dissolved organic compounds considerably effects on an decrease in the buffer capacity. In consequence, the amount of HCl used to adjust pH value to 3 is significantly lower in effluent than in influent (Table 2).

4. CONCLUSIONS

Sulfonamides, including difficult biodegradable sulfa-drugs, can be removed from wastewater using the photodegradation process. The optimal catalytic system for the photodegradation of SNs in wastewater is the mixture containing TiO_2 (0.5 g l^{-1}), $FeCl_3$ (1 mmol l^{-1}) and HCl (in order to acidify the samples to pH 3). Under the used conditions the initial rate of the removal of SNs (spiced to municipal wastewater) is almost 15 times higher than for TiO_2 alone.

In wastewater, the rate of SNs photodegradation can be also accelerated by their

pretreated in biological-mechanical processes. Preliminary filtration and coagulation did not effect on the course of investigated photocatalytic process.

REFERENCES

[1] KÜMMERER K. ed., Pharmaceuticals in the environment. Sources, fate, effects and risks. Heidelberg: Springer-Verlag 2001.

[2] TERNES T.A. (project co-ordinator), JANEX-HABIBI M.L., KNACKER T., KREUZINGER N., SIEGRIST H., 2004, *Assesment of Technologies for the Removal of Pharmaceuticals and Personal Care Products in Sewage and Drinking Water Facilities to Improve the Indirect Potable Water Reuse*. Project *POSEIDON,* Contract No. EVK1-CT-2000-00047,

[3] Eintrag von Arzneimitteln und deren Verhalten und Verbleib in der Umwelt Literaturstudie Fachbericht 2, Landesamt für Natur, Umwelt und Verbraucherschutz Nordrhein-Westfalen, Recklinghausen 2007.

[4] Environmentally Classified Pharmaceuticals 2009, Stockholm County Council, http://www.janusinfo.org/imcms/servlet/GetDoc?meta_id=10205

[5] SUKUL P., SPITTELER M., 2006, *Sulfonamides in the environment as veterinary drugs*, Environ. Contam. Toxicol., 187, 67-101.

[6] KÜMMERER K., 2009, *Antibiotics in the aquatic environment* – A review – Part I, Chemosphere,75, 417-434.

[7] KOT-WASIK A., DĘBSKA A., NAMIEŚNIK J., *Przemiany, stężenia i oznaczanie pozostałości środków farmaceutycznych w środowisku*: Nowe horyzonty i wyzwania w analityce i monitoringu środowiskowym (34), Gdańsk: CEEAM 2003.

[8] Knowledge and Need Assessment on Pharmaceutical Products in Environmental Waters, 2007, Project acronym: KNAPPE, Proposal N° 036864.

[9] SARMAH A.K., MEYER M.T., BOXALL A.B.A., 2006, *A global perspective on the use, sales, exposure pathways, occurrence, fate and effects of veterinary antibiotics (Vas) in the environment*, Chemosphere, 65, 725–759.

[10] KEMPER N., 2008, *Veterinary antibiotics in the aquatic and terrestrial environment*, Ecol. Ind., 8, 1–13.

[11] BATT A.L., KIM S., AGA D.S., 2007, *Comparison of the occurrence of antibiotics in four full-scale wastewater treatment plants with varying designs and operations*, Chemosphere, 68, 428-435.

[12] TURKDOGAN F.I., YETILMEZSOY K., 2009, *Appraisal of potential environmental risks associated with human antibiotic consumption in Turkey*, J. Hazard. Mater., 166, 297–308.

[13] KLAVARIOTI M., MANTZAVINOS D., KASSINOS D., 2009, *Removal of residual pharmaceuticals from aqueous systems by advanced oxidation processes*. Environ. Int. 35, 402–417.

[14] BELTRAN F.J., AGUINACO A., GARCIA-ARAYA J.F., OROPESA A., 2009, *Ozone and photocatalytic processes to remove the antibiotic sulfamethoxazole from water*, Water Res., 43, 1359-1369.

[15] KANIOU S., PITARAKIS K., BARLAGIANNI I., POULIOS I., 2005, *Photocatalytic oxidation of sulfamethazine*, Chemosphere, 60, 372–380.

[16] HU L., FLANDERS P.M., MILLER P.L., STRATHMANN T.J., 2007, *Oxidation of Sulfamethoxazole and Related Antimicrobial Agents by TiO_2 Photocatalysis*., Water Res., 41, 2612 – 2626.

[17] CALZA P., MEDANA C., M. PAZZI, BAIOCCHI C., PELIZZETTI E., 2004, *Photocatalytic transformation of sulphonamides on titanium dioxide*, App. Catal. B-Environ., 53, 63-69.
[18] ABELLAN M.N., GIMENEZ J., ESPLUGAS S., 2009, *Photocatalytic degradation of antibiotics: The case of sulfamethoxazole and trimethoprim*, Catal. Today 144, 131–136.
[19] BARAN W., ADAMEK E., SOBCZAK A., SOCHACKA J., 2009, *The comparison of photocatalytic activity of Fe-salts, TiO_2 and $TiO_2/FeCl_3$ during the sulfanilamide degradation process*. Catal. Comm., 10, 811-814.
[20] BARAN W., ADAMEK E., SOBCZAK A., MAKOWSKI A., 2009, *Photocatalytic degradation of sulfa drugs with TiO_2, Fe salts and $TiO_2/FeCl_3$ in aquatic environment—Kinetics and degradation pathway*, Appl. Catal. B: Environ., 90, 516-525.
[21] BARAN W., SOCHACKA J., WARDAS W., 2006, *Toxicity and biodegradability of sulfonamides and products of their photocatalytic degradation in aqueous solutions*, Chemosphere, 65, 1295-1299.
[22] ADAMEK E., BARAN W., SOBCZAK A., MAKOWSKI A., 2009, *The photocatalytic decoloration of wastewater containing azo-dyes*. – Pol. J. Environ. Stud., 18-2B, 80-82.
[23] WU F., DENG N., 2000, *Photochemistry of hydrolytic iron (III) species and photoinduced degradation of organic compounds*. A minireview, Chemosphere 40, 389-394.
[24] CATASTINI C., SARAKHA M., MAILHOT G., BOLTE M., 2002, *Iron (III) aquacomplexes as effective photocatalysts for the degradation of pesticides in homogeneous aqueous solutions*, Sci. Total Environ., 298, 219-228.
[25] ANDREOZZI R., CANTERINO M., MAROTTA R., 2006, *Fe(III) homogeneous photocatalysis for the removal of 1,2-dichlorobenzene in aqueous solution by means UV lamp and solar light*, Water Res., 40, 3785 – 3792.
[26] MESTANKOVA H., MAILHOT G., JIRKOVSKY J., KRYSA J., BOLTE M., 2005, *Mechanistic approach of the combined (iron–TiO_2) photocatalytic system for the degradation of pollutants in aqueous solution: an attempt of rationalisation*, Appl. Catal. B Environ., 57, 257–265.
[27] BOREEN A.L., ARNOLD W.A., MC NEILL K., 2004, *Photochemical fate of sulfa drugs in the aquatic environment: sulfa drugs containing five-membered heterocyclic groups*, Environ. Sci. Technol., 38, 3933-3940.
[28] BOREEN A.L., ARNOLD W.A., MC NEILL K., 2005, *Triplet-sensitized photodegradation of sulfa-drugs containing six-membered heterocyclic groups: Identification of an SO_2 extrusion photoproduct*, Environ. Sci. Technol., 39, 3630-3638.
[29] ISO 9887:1992(E) Water quality - Evaluation of the aerobic biodegradability of organic compounds in an aqueous medium -Semi-continuous activated sludge method (SCAS)
[30] HATCHARD C., PARKER C., 1956, *A new sensitive chemical actinometer. II. Potassium ferrioxalate as a standard chemical actinometer*, Proc. Roy. Soc. A 235, 518-36.
[31] BARAN W., MAKOWSKI A., WARDAS W., 2005, *The separation of catalyst after photocatalytic reaction conducted in the presence of $TiO_2/FeCl_3/UV$*, Chemosphere 59, 853-859.
[32] FUJISHIMA A., ZANG X., TRYK D.A., 2008, *TiO_2 photocatalysis and related surface phenomena*, Surf. Sci. Rep., 63, 515-582.

Physicochem. Probl. Miner. Process. 45(2010) 141-151

journal homepage
www.minproc.pwr.wroc.pl/journal/

Physicochemical Problems of Mineral Processing

Index No. 32213X ISSN 1643-1049

Wojciech ZMUDZIŃSKI *

PRELIMINARY RESULTS OF GLUCOSE OXIDATION BY PHOTOCATALYSIS ON TITANIUM DIOXIDE - PRIMARY INTERMEDIATES

Received March 16, 2010; reviewed; accepted May 7, 2010

In the presented paper preliminary results of glucose oxidation on illuminated titania are reported. For comparison, results of direct glucose photolysis are also included. At high glucose concentration, up to 1.4 g/dm^3, the yield of 3 hour reaction, determined by COD measurements, was small and amounted to about 5.8%. Additionally, pH measurements show, that oxidation of glucose leads to formation of acidic compounds – after 3 hours the pH lowered from 6.5-6.8, depending on glucose concentration, to about 4.5. Attempt has been undertaken to identify some of the intermediates of the photocatalytic reaction using GC-MS analysis of specially treated samples of the reactor slurry. The analysis showed the existence of intermediates which were formed both as a result of intramolecular changes and of oxidation reactions. Five acidic derivatives were found among the intermediate compounds.

keywords: photocatalysis, TiO_2, glucose, primary intermediates

1. INTRODUCTION

Food industry constitutes one of the most important parts of the world economy. It gives also huge amount of solid and liquid wastes which have to be utilized. The

* Faculty of Commodity Science, University of Economics, Al. Niepodległości 10, 61-875 Poznań, Poland, w.zmudzinski@ue.poznan.pl

wastes, usually not toxic both for humans and animals, have been broadly utilized as animal food or they serve as raw materials in many fields of food and other industries. However, even these not toxic wastes become very harmful for natural environment if their concentration in waters exceeds certain level. Sewage from food industry are highly loaded with various organics possessing reductive character, and raising strongly because of that water COD and BOD indexes. The sewage contain also other pollutants, as for example purifying agents (e.g. detergents), lubricants etc. [1]. The sewage from food industry contain first of all water-soluble carbohydrates, the main ingredient of plants and plant food. On the one hand the mono- and oligosaccharides can serve as food for any microorganisms widely utilized in biological sewage-treatment plants [2]. On the other, these usually highly reductive compounds pose, unfortunately, a serious threat for any aqueous livings, both for water plants and animals.

Until now the sewage from food industry are purified using mainly biological methods. The processes base on special metabolisms of some of bacteria, transforming organics containing in water into mineral compounds. At present the methods of sludge digesters (producing methane) become popular, especially in the case of highly loaded sewage. Also small, home sludge digesters have appeared in some farms [2,3].

Since more than twenty years a research has been undertaken on practical application of Advanced Oxidation Processes for purification of industry sewage, including food industry. AOP`s methods utilise highly reactive $OH^{\bullet}$ radicals generated *in situ* in various ways. Organic matter is usually fully mineralised, i.e. to CO_2 and H_2O [4-7]. The processes such as photocatalysis on semiconductors, H_2O_2 action, ozonation, Fenton and photo-Fenton reactions, electrochemical oxidation, and also their combinations, are good examples of the Advanced Oxidation Processes. Among the AOP's photocatalysis on semiconductors seems to be the most promising. The process needs only a photoactive semiconductor and appropriate light - UV part of solar spectrum is sufficient for excitation of semiconductor electrons. Titanium dioxide serves mainly as the semiconductor: the compound, besides its high photoactivity, is very stable chemically and photochemically, non-toxic and relatively cheap [3,5,8]. Many compounds such as carboxylic acids, organic dyes, phenols, pesticides, surfactants, some of inorganic compounds, and many others are fully mineralized by photocatalysis on TiO_2 [9,10]. One should remember, however, that the photocatalytic processes are efficient only at low concentration of water contaminants. Therefore, they can be regarded as the so called tertiary methods of water purification.

Illumination of a semiconductor with a light of an appropriate energy ($h\upsilon \geq E_g$, E_g – width of a semiconductor forbidden band) causes formation of free electrons (electrons in semiconductor conduction band) and holes in semiconductor valence band. If their lifetime is sufficiently long they can react with some molecules reducing (electrons) or oxidising (holes) them. Full set of initiated by the light reactions has been reported in

literature [11-13]. The excited electrons reduce oxygen molecules dissolved in water. The holes react mainly with water molecules or with OH^-, generating highly reactive $OH^\bullet$ radicals, which in turn attack any organic matter oxidizing it. At higher concentration of organic water pollutants direct oxidation of them by holes is also possible [14-16].

It can be added here that the process is conducted under normal (room-like) temperature and pressure conditions, the photocatalyst is wholly recovered after the process and its active surface is able to run the reactions again [17,18]. In contrast to other water purification methods, in the case of water contaminants containing only C, H and O atoms the heterogeneous photocatalytic processes do not introduce to the environment any additional impurities except CO_2 and H_2O.

The presented studies focus on identification of primary intermediates of glucose photooxidation on titania. However, first part of the paper is devoted to the possibility of glucose oxidation on illuminated TiO_2 – these studies were conducted in order to find the conditions, in which the degree of glucose degradation was small allowing thus determination of only partly oxidized products. The studies are a part of a broader research on purification of dairy sewage conducted since several years.

2. MATERIALS AND METHODS

Photochemical studies were conducted using solutions having various concentration of glucose. Depending on experiment, the concentrations of glucose-D(+) (99.5%, Aldrich) were as follows: 0.28, 0.40, 0.60, 0.80, 1.0 or 1.4 $g \cdot dm^3$. In the all photocatalytic experiments 230 cm^3 of an appropriate solution of glucose was mixed with 0.05 g TiO_2 (99.9%, Aldrich, anatase) and sonicated for 5 minutes. Then the homogenized slurry was transported to an air lift loop photoreactor (Pyrex made, 250 cm^3 volume) described elsewhere [19,20]. The photoreactor contents were mixed by an air lift (50 $cm^3 \cdot min^{-1}$) controlled by a narrow draft tube placed in the centre of the tube reactor. The conical bottom of the reactor was equipped with a septum through which the air stream was fed to the reactor with a needle, the loop of which reached the bottom of the draft tube. The reactor was illuminated from the side wall with two 300W xenon lamps (OSRAM). The bulbs were placed in a distance of 50 cm from the reactor, the distance between them was also 50 cm. Pyrex walls of the reactor determined lower limit of entering light (about 300 nm cutoff filter). The photoreactor was cooled by an air stream, the temperature was maintained at 30 ^{0}C.

Photocatalytic experiments were performed in a non-continuous mode (batch reactor); before each experiment the reaction slurry was aerated for 15 minutes. The photoreactions were conducted 3 hours, pH of illuminated solutions were measured at 30 minute intervals. After the illumination had been stopped, several cm^3 of the reaction

slurry (depending on initial glucose concentration) was analysed for COD using a dichromate method [21]. Each photocatalytic experiment was repeated at least twice, also each reaction solution (reaction slurry) was analysed for COD at least twice prior and after illumination. Direct glucose photolysis was also studied using the same reactor and light source.

Intermediates of the process of glucose photocatalytic degradation were identified using gas chromatography – mass spectroscopy techniques. Analyses were performed on a Varian GC/MS 4000 apparatus equipped with a capillary column VF – 5MS (30m·0.25mm·0.39mm). After three hour illumination the reaction slurry was filtered using Millipore Millex GV_3 filters and liquid phase was evaporated on a rotary evaporator to dryness. The residue was silanized 60 min at 70^{o}C using TMSI – N-trimethylsilylimidazole : pyridine = 1 : 4 (Sylon^{TM}TP, Supelco).

The water used for photocatalytic studies was doubly distilled in a quartz still. Prior to distillation the water was de-ionised on a special column. All chemicals were of p.a. purity. Anatase titania (99.9%, Aldrich) used as a photocatalyst had a BET specific surface area of 11.9 $m^2 \cdot g^{-1}$ as measured on a Micromeritics apparatus. It showed a typical anatase spectrum with the adsorption onset at about 400 nm (taken on a Specord M-40 spectrophotometer). An average particle size of the TiO_2 powder was about 0.1 μm (89% of the particles were in the range 0.07 – 0.2 μm), as measured on a Malvern Instruments Ltd. (UK) granulometer using water as a liquid medium.

3. RESULTS AND DISCUSSION

As it was mentioned above, the goal of this study was to identify primary intermediates of glucose photocatalytic oxidation. However, prior to identification studies the conditions suitable for production of possibly large amount of primary products of the reaction of hydroxyl radicals, generated by illuminated titania, with glucose molecules were established. In these studies glucose oxidation was followed by determination of COD (Chemical Oxygen Demand) prior and after illumination of the solutions. Although time consuming, the COD dichromate method seemed to be the only one suitable for these studies - it was possible to determine at the same time the compounds present in water and adsorbed on titania grains (the slurry was not filtered). It was checked in blank experiments that the presence of small titania admixture did not influence the results of COD measurements. The results of previous studies conducted in this laboratory [22] were the base for setting of the reaction conditions: 230 cm^3 of the reaction solution, 0.05 g TiO_2, air stream rate 50 $cm^3 \cdot min^{-1}$. There were two reasons for the choice of glucose concentration: (1^0) possibility of production of only partly oxidized glucose derivatives, and (2^0) the fact, that at too high concentrations of organics in water the photoreaction rate could be substantially reduced or even totally

inhibited.

The results of three-hour illumination of diluted solutions, having various concentration of glucose, in the presence of TiO_2 photocatalyst are shown in Table 1.

Table 1. Degradation of glucose during three hour illumination of 230 cm^3 of the solution in the presence of TiO_2

Glucose initial concentration					Decrease of COD	
[g/dm^3]	[mmole/dm^3]	[Glucose contained in 230mL]			[%]	[mmole O_2]**
		[g]	[mmole]	[mmole O_2]*		
0.28	1.5	0.064	0.35	2.10	6.19	0.13
0.40	2.2	0.092	0.51	3.06	5.84	0.18
0.60	3.3	0.138	0.77	4.62	5.84	0.27
0.80	4.4	0.184	1.02	6.12	5.67	0.35
1.00	5.5	0.230	1.28	7.68	5.72	0.44
1.40	7.8	0.322	1.79	10.74	5.63	0.60

* amount of oxygen necessary for full oxidation of glucose contained on the photoreactor

** decrease of oxygen demand after three-hour illumination; the values correspond to the extent of oxidation reactions procceding in the reactor during illuminatiom

It follows from the data shown in Table 1 that three-hour illumination of glucose solutions with TiO_2 admixtures causes slow oxidation of the substrate. Moreover, quantitatively decrease of COD is directly proportional to its initial value, in other words – to initial concentration of glucose. Therefore, it can be assumed roughly, that the photocatalytic reaction fulfils universally applied Langmuir-Hinshelwood equation [14]. At too high concentrations of the degraded substrates, however, the kinetics of the process can change to zero order, because the reaction rate is limited by the rate of generation of $OH^{\bullet}$ radicals on the surface of illuminated titania, which is constant under constant illumination. In order to find real influence of the catalytic effect of illuminated TiO_2 it was of interest to study also direct glucose photolysis.

Table 2. Glucose degradation under illumination of glucose solution with and without TiO_2 admixture

Glucose concentration	Decrease of COD			
	With TiO_2 admixture		Without TiO_2 admixture	
[g/dm^3]	[%]	[mmole O_2]*	[%]	[mmole O_2]*
0.28	6.19	0.13	1.06	0.022
0.60	5.84	0.27	0.57	0.026
1.40	5.63	0.60	0.33	0.035

* see footnote below Table 1

The results are shown in Table 2; for comparison, the results obtained in the presence of TiO_2 are also inserted in Table 2.

One can see from Table 2 that the yield of direct glucose photolysis, which leads to oxidation, ranges from 6 to 17 % of that in the presence of TiO_2. The amount of oxidized glucose is somewhat higher at higher substrate concentration, although the increase is much smaller than that in the presence of TiO_2.

It was mentioned in *Experimental* that during the photocatalytic reactions, pH of the slurry was measured at 30 minute intervals. In the case of all photocatalytic reactions, lowering of pH was observed with the time of illumination. For reactions conducted in the presence of illuminated TiO_2 the pH values lowered during three-hour reaction from initial pH 6.5 - 6.8, depending on glucose concentration, to 4.5 - 4.8. As an example Fig.1 shows the changes of 1.0 $g \cdot dm^{-3}$ glucose solution in the presence of TiO_2.

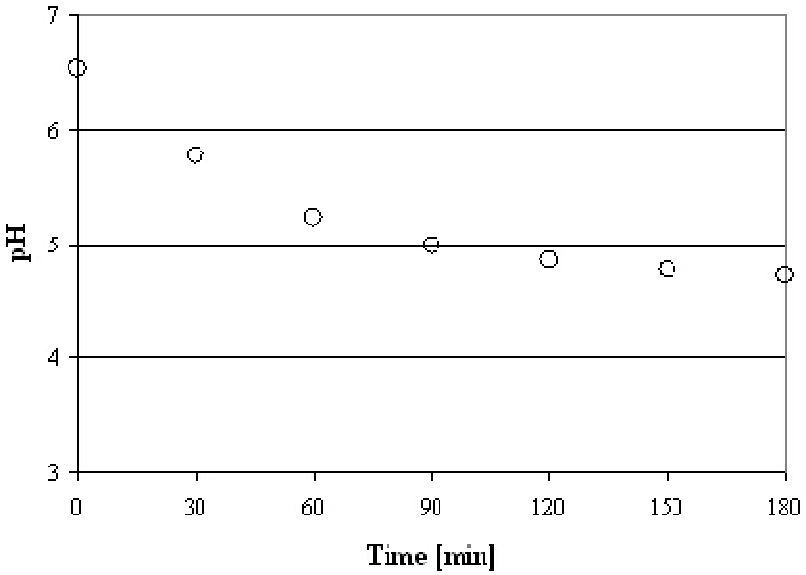

Fig. 1. pH changes during 3-hour illumination of 1.0 g dm^{-3} glucose solution in the presence of TiO_2.

The formation of acidic intermediates is not surprising. According to literature, oxidation of water contaminants in the presence of illuminated titania proceeds *via* formation of $OH^{\bullet}$ radicals, direct oxidation by electron holes can take place in the cases of highly concentrated water solutions. Also strong adsorption of the compound on TiO_2 facilitates its direct oxidation by the holes [15,16]. The attack of $OH^{\bullet}$ radicals on hydroxylated carbon atom in sugar leads firstly to formation of a new carbonyl group.

The reaction of $OH^{\bullet}$ with the carbonyl group (the already existing or the new formed) causes formation of a carboxyl group. If the CO group is non-terminal, the brake of a carbon chain and formation of two new compounds are observed. Therefore, although the oxidation in the presence of illuminated TiO_2 leads finally to CO_2 and H_2O, a lot of various intermediates are formed in the one-electron processes caused by $OH^{\bullet}$ radicals. And reactions of formation of acidic compounds and their next decarboxylation are necessary in the whole process of mineralization of organic compounds.

pH changes illustrated in Fig.1 show, that the photoreaction still proceeds during the whole period of illumination. However, the pH decrease, fast during first 90 minutes, becomes slower and slower in the next period, *i.e.* when pH of the slurry decreases below 5.

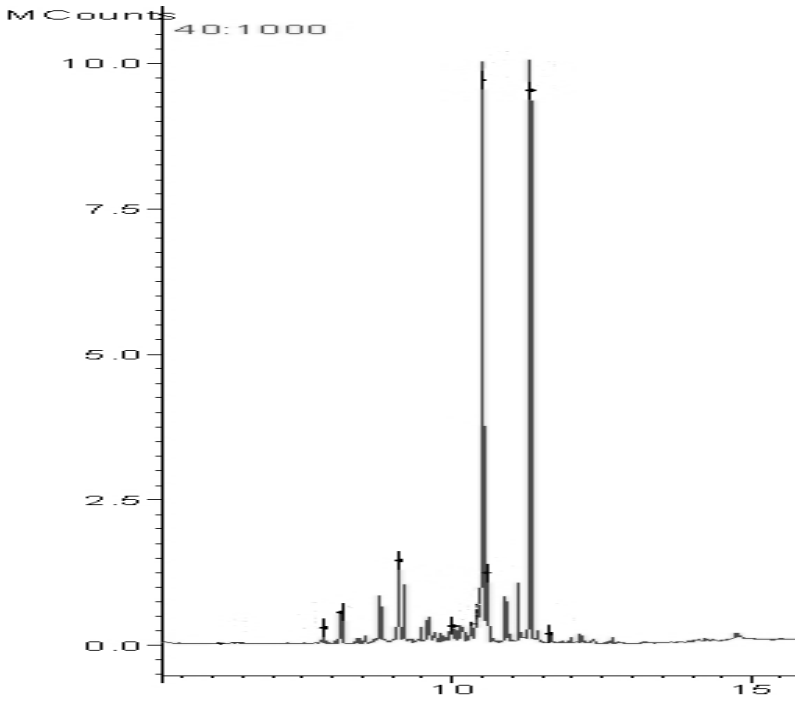

Fig. 2. GC-MS chromatogram of an after reaction mixture. Glucose concentration, 0.4 $g \cdot dm^{-3}$, time of illumination, 3 hours; amount of titania, 0.05 g.

Intermediates of glucose oxidation on illuminated titania were determined using GC-MS technique. Prior to analysis 0.4 $g \cdot dm^{-3}$ aqueous glucose solution was illuminated 3 hours in the presence of TiO_2, filtered, dried, and dry residue was silanized (see *Experimental*). Typical GC-MS chromatogram is shown in Fig.2.

MS analysis of the after-reaction mixture ingredients showed the existence of many intermediate compounds, which were formed both as a result of intramolecular changes and oxidation reactions. Formulas of the derived compounds (their silanized derivatives) are collected below, see Fig.3.

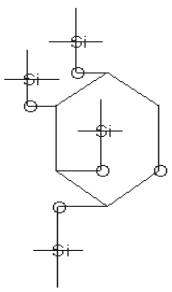

D-Arabinose

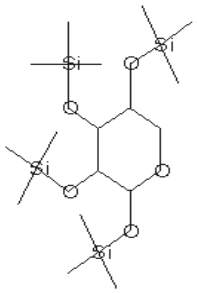

Beta-L-Arabinopyranose

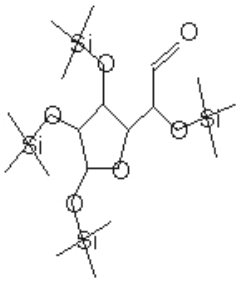

2-Furanacetaldehyde

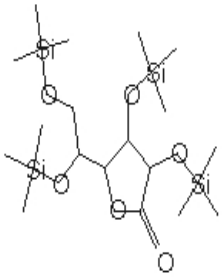

Allonic acid

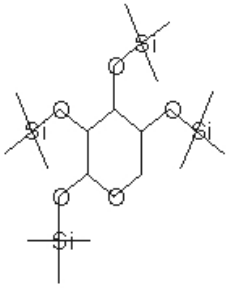

Alpha-D-Xylopyranose

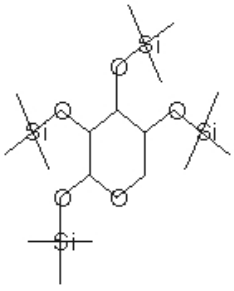

D-Xylopyranose

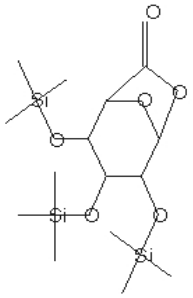

Glucuronolactone

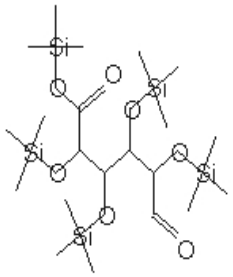

D-Glucuronic acid

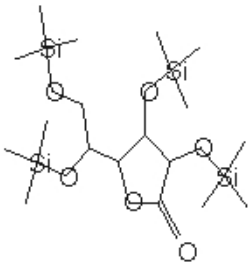

Gluconic acid

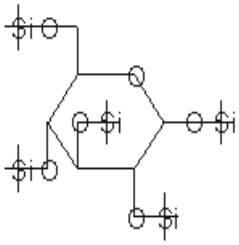

Glucopyranose

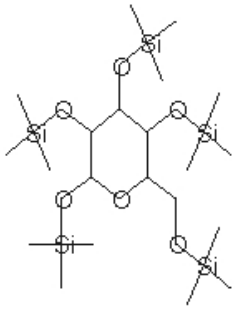

Alpha-D-Glucopyranose

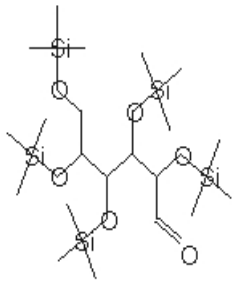

D-Glucose

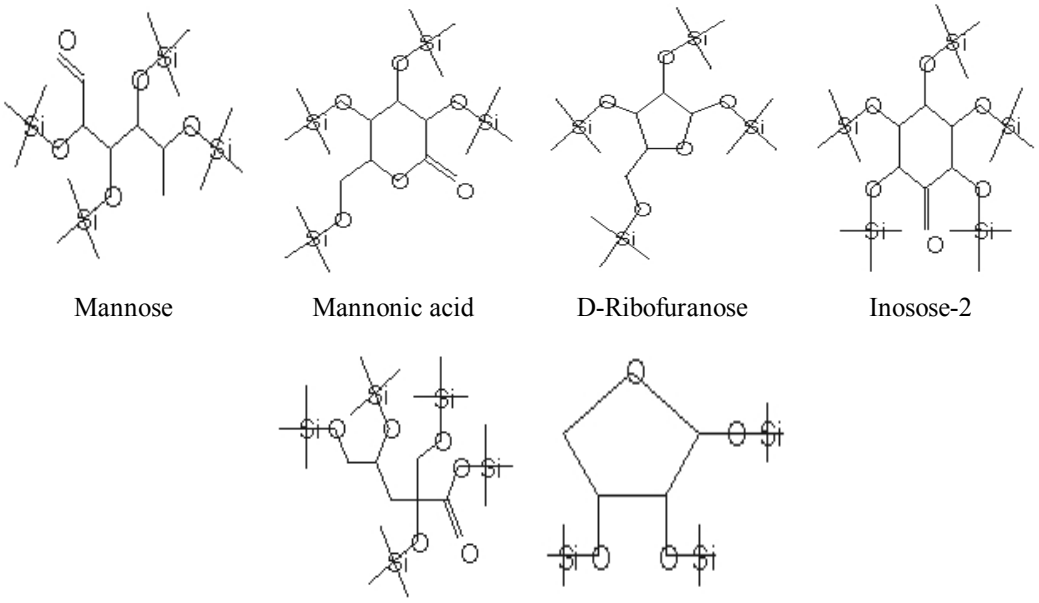

Fig. 3. Formulas of silanized derivatives of the compounds determined by GC-MS.

The highest peaks in Fig.2 correspond to the next compounds in the order: glucopyranose>glucose>gluconic acid>2-furanacetaldehyde>allonic acid. Note, that acidic derivatives were indeed formed during the photocatalytic reaction confirming thus the results of pH measurements. And two of the acids, *i.e.* the gluconic and allonic ones, gave the most intensive peaks among the oxidized intermediates. The formation of glucose derivatives in the way of intramolecular transformation can be a result of both pH changes and catalytic action of titania surface, acidic in principle. The research is in progress in order to establish the main direction of glucose oxidation by the photogenerated $OH^{\bullet}$ radicals and to determine also the shorter chain intermediates.

4. CONCLUSIONS

Illumination of glucose diluted solutions in the presence of TiO_2 leads to oxidation of the substrate. In the range of concentration 0.20-1.40 $g \cdot dm^{-3}$ the yield of glucose degradation, measured as a decrease of COD, was small and amounted to 5.8%. It was assumed, that the reaction shows 1st order behaviour. During illumination pH of the reaction solutions lowered showing thus formation of acidic intermediates. GC-MS analysis, conducted after silanization of the reaction products, showed the existence of

many intermediate compounds, both these formed in result of intramolecular changes, and these formed by glucose oxidation. Acidic compounds such as: gluconic acid, D-glucuronic acid, mannonic acid, erytho-pentonic acid and the allonic one were found as reaction intermediates. Two of the acids, i.e. gluconic and allonic ones, gave the most intensive peaks among the intermediates.

REFERENCES

[1] URBANIEC, K. (2004). *Waste and wastewater management in food production*, Przemysł Spożywczy, 11, 54-55 [In Polish]

[2] ZAWIRSKA, A., SZAMAŃSKI, L. *Water-sewage management in food industry*. Editory of Agricultural Academy, Wrocław 2002 [In Polish].

[3] BARTKIEWICZ, B. Purification of industrial sewage. PWN Warszawa 2006 [In Polish].

[4] KAVITHA, V., PALANIVELU, K. (2004). *The role of ferrus ion in Fenton and photo-Fenton processes for the degradation of phenol*, Chemosphere 55, 1235-1243

[5] ZIELIŃSKA, B., GRZECHULSKA, J., KALEŃCZUK, R., MORAWSKI, A. (2003). *The pH influence on photocatalytic decomposition of organic dyes over A11 and P25 titanium dioxide*, Appl.Catal.B: Environm. 45, 293-300

[6] DOBOSZ, A., SOBCZYŃSKI, A. (2003). *The influence of silver additives on titania photoactivity in the photooxidation of phenol*, Water Res. 37, 1489-1496

[7] KAVITHA, V., PALANIVELU, K. (2005). *Degradation of nitrophenols by Fenton and photo-Fenton processes*, J. Photochem Photobiol. A: Chem 170, 83-95

[8] COLPINI, L., ALVES, H., SANTOS, O., COSTA, C. (2008). *Discoloration and degradation of textile dye aqueous solutions with titanium oxide catalysts obtained by the sol–gel method*. Dyes Pigm. 76, 525-529

[9] GRZECHULSKA-DAMSZEL, J., TOMASZEWSKA, M.U. (2008). *Purification of water in the reactor having replaceable photoactive insert.* Przemysł Chemiczny (Chemical Industry) 87/5, 460-462 [In Polish]

[10] ROBERT, D., MALATO, S. (2002). *Solar photocatalysis: a clean process for water detoxification*. Sci. Total Environ. 291, 85-97

[11] HATIPOGLU, A., SAN, N., CINAR, Z. (2004). *An experimental and theoretical investigation of the photocatalytic degradation of meta-cresol in TiO_2 suspensions: a model for the product distribution*, J. Photochem. Photobiol. A: Chem. 165, 119-129

[12] CARPIO, E., ZUNIGA, P., PONCE, S., SOLIS, J., RODRIGUEZ, J., ESTRADA, W. (2005). *Photocatalytic degradation of phenol using TiO_2 nanocrystals supported on activated carbon*, J. Mol. Catal. A: Chem. 228, 293-298

[13] TARIQ, M., FAISAL, M., SAQUIB, M., MUNEER, M. (2008). *Heterogeneous photocatalytic degradation of an anthraquinone and a triphenylmethane dye derivative in aqueous suspensions of semiconductor*, Dyes Pigm. 76, 358-365

[14] SOBCZYŃSKI, A., DOBOSZ, A. (2001). *Water Purification by Photocatalysis on Semiconductors*, Pol. J. Environ. Stud. 10, 195-205

[15] LAWLESS, D., SERPONE, N., MEISEL D. (1991). *Role of $OH^{\bullet}$ radicals and trapped holes in photocatalysis. A pulse radiolysis study*, J. Phys. Chem. 95, 5166-5170

[16] STAFFORD, U., GRAY, K.A., KAMAT, P.V. (1994). *Radiolytic and TiO_2-assisted photocatalytic degradation of 4-chlorophenol. A comparative study*, J. Phys. Chem. 98, 6343-6351

[17] SUN, L., LU, H., ZHOU, J. (2008). *Degradation of H-acid by combined photocatalysis and ozonation processes*, Dyes Pigm. 76, 604-609

[18] MANSILLA, H., MORA, A., PINCHEIRA, C., MONDACA, M., MARCATO, P., DURAN, N., FREER, J. (2007). *New photocatalytic reactor with TiO_2 coating on sintered glass cylinders*, Appl. Catal. B: Environm. 76, 57-63

[19] SOBCZYŃSKI, A., JIMENES, J., CERVERA – MARCH, S. (1997). *Photodecomposition of phenol in a flow reactor: adsorption and kinetics*, Monatsch.Chem.128, 1109-1118

[20] SOBCZYŃSKI, A., DUCZMAL, Ł., ZMUDZIŃSKI, W. (2004). *Phenol destruction by photocatalysis on TiO_2: an attempt to solve the reaction mechanism*, J. Mol. Catal. A: Chem. 213, 225-230

[21] PN (Polish Standards) - ISO 6060:2006. Water Quality. Determination of Chemical Oxygen Demand [In Polish]

[22] ZMUDZIŃSKI, W. (2009). *Preliminary results of purification of dairy sewage by photocatalysis on titania*, Pol. J. Environm. Stud. 18, 1225-1228